An investigation into the contribution of c-Myc induced changes to nuclear architecture towards early stage oncogenesis

Koshiro Kiso

Supervisor: Prof. Rob de Bruin

Co-supervisor: Dr. Cosetta Bertoli

UCL

Doctor of Philosophy

I, Koshiro Kiso, confirm that the work presented in this thesis is my own. Where information has been derived from other sources, I confirm that this has been indicated in the thesis.

Abstract

Abnormal nuclear morphologies (nuclear atypia) are a common and widespread feature of cancer cells and are robust enough to be used as diagnostic markers for tumour tissue. However, the mechanisms leading to the generation of these morphologies, as well as their potential contribution towards the tumourigenic and tumour evolution process are two aspects that have not received much study until recently. In this project, I focus on the contribution of oncogene induced alterations to nuclear morphology and architecture towards early stage oncogenesis. Using an oncogene inducible cell line as a model system, I show that c-Myc activity causes acute and significant changes to nuclear morphology and that it leads to both a reduction and a mislocalisation of components of the nuclear lamina (lamins A and B1). Following on from this, I provide evidence suggesting that this c-Myc induced downregulation of lamin A in particular is partially mediated by its induction of the micro-RNA molecule miR-9. I also show that c-Myc induced nuclear morphology defects and lamin A mislocalisations are partially cell cycle and mitosis dependent. Finally, I show that c-Myc induction causes nuclei to undergo an increased frequency of nuclear envelope rupture (NER) events, that could then contribute towards oncogenesis by leading to increasing levels of DNA damage and genomic instability (GIN). Taken together, my work highlights a novel potential pathway of oncogenesis which involves the direct dysregulation of components maintaining nuclear morphology in untreated cells that then leads to increases in downstream genome instability. This work has interesting implications for the understanding of cancer cell evolution as it suggests that dysregulation of nuclear morphology is a phenomenon that occurs very early in the oncogenic process and that it is an important driver of subsequent tumour cell evolution.

Impact Statement

For at least a century, diagnostic pathologists have been using the morphological defects present in a wide variety of cancer cells to distinguish between benign and malignant cells. Whilst our knowledge of the genetic alterations that result in cancer cell transformation has rapidly advanced, the mechanisms that underlie these nuclear morphological defects remains poorly understood. For instance, there is no known direct link between a defined mutation and a set of nuclear morphology defects. This is likely because the nuclear atypia seen within tumour tissue is a complex combination of dysregulation of cell signaling, aneuploidy and alterations to nuclear envelope proteins, chromatin and cytoskeletal dynamics.

To address this phenomenon, an alternative approach may be required. This would be the investigation of nuclear atypia in the context of early tumour cell transformation, and not within mature tumour tissue. This would mean an investigation into the likely conserved and necessary events that occur in the very early stages of oncogenesis. By addressing the phenomenon of nuclear atypia from this end of the transformation process, it is possible to uncover potential conserved and necessary early pathways that lead to nuclear morphological defects that are present in all subsequent cancer cells, which would explain why they are such a conserved feature in cancer.

My work focuses on nuclear morphology defects within this context of early cell oncogenesis. I find that oncogene activity leads to acute and significant changes in the levels of nuclear morphology regulators (components of the nuclear lamina and cytoskeleton), that then have downstream impacts that contribute towards oncogenesis. Importantly, this suggests that defects in the regulators of nuclear morphology are themselves contributors towards oncogenesis and provide valuable insights into a general process of cancer evolution. This has two applications. Firstly, the refining of existing diagnostic techniques that identify and stratify cancers based on specific morphological defects. Secondly, the development of novel strategies to target cancer cells with morphology defects for either selective elimination, or for rescue. The lack current studies that focus on the targeting of nuclear morphology abnormalities in cancer means that this is fertile ground for both basic and clinical research.

Acknowledgements

I would like to extend my heartfelt thanks to my supervisor Professor Rob de Bruin for his steadfast support and encouragement throughout my project. Though it started off as an open-ended question his advice helped to shape the work and give it a sense of direction. Through the upheavals of COVID and the hectic schedule of my final year his guidance both within and without my project helped me mature both as a scientist and as a professional and for that I will be forever grateful. The positive, friendly and encouraging lab ethos he has helped to create was an especial pleasure to work in and I consider myself incredibly fortunate I could carry out my PhD within that group.

I would also like to thank my co-supervisor Dr. Cosetta Bertoli, who was incredibly helpful and supportive throughout my work, though especially in the initial stages when I had just started picking up all the lab techniques I was to employ within my work. On that note, many thanks to fellow lab members, past and present: Elena, Biswa, Silvia, Sophie, Gemma, Joe, Karla, Leticia and Milk for providing such a lovely environment to work in and for putting up with my no doubt frequent questions on all things lab related.

I would also like to thank the MRC LMCB graduate programme for providing the funding for my PhD. Whilst it has now ended, I am incredibly fortunate to have been able to complete the majority of my research in a department as vibrant and nurturing as the LMCB and I wish it all the best in its future research directions.

I thank the other students on my programme for their continued support as both friends and fellow scientists. Regular trips to the pub with Ffion, Giulia (Baum) and Rici, coffees with Tasha and Giulia (Lloyd) helped break up what could occasionally be long solitary stints at the microscope.

Finally, I thank my non-scientist friends and family, who helped provide me with a reality check whenever an experiment did not go well or progress was slow. Though a PhD is nominally an individual enterprise, I would not have been able to see it through without the support I was given from the people around me. Whilst I have left the realm of academia, the four and a half years between my graduation and the start of my current position will be a time I will cherish for many years to come.

Contents

List of Figures

List of Tables

1. Introduction

1.1 The cancer nucleus.

The differences in overall cell morphology between tumours and healthy cells was first discovered 150 years ago by Sir Lionel Beale (Fischer, 2020). Salient features first seen include changes to cell shape volume and nuclear size. It is now clear that cancer nuclei differ in morphology and architecture from normal nuclei (termed 'nuclear atypia). These differences are so robust that they are still employed as diagnostic markers of tumour tissue. An example still employed today is the Pap smear, used in the screening of cervical cancer (Pap), which involved the visual inspection of cells for any abnormalities in their appearance, such as increased nuclear size or abnormal chromatin distribution. Other examples include cells collected using fine needle aspiration biopsies. The reliability of such metrics as diagnostic tools is reflected in the fact that even in this current age of computer-assisted semi-automated screening, the parameters investigated still rely heavily on traditional abnormal nuclear morphologies. Trained pathologists can identify features such as NE smoothness, chromatin localization and the presence of NE invaginations as markers for cancerous cells (Figure 1.1). Importantly, altered nuclear morphology has been shown to correlate with tumour grade and prognosis (Bussolati et al., 2014)

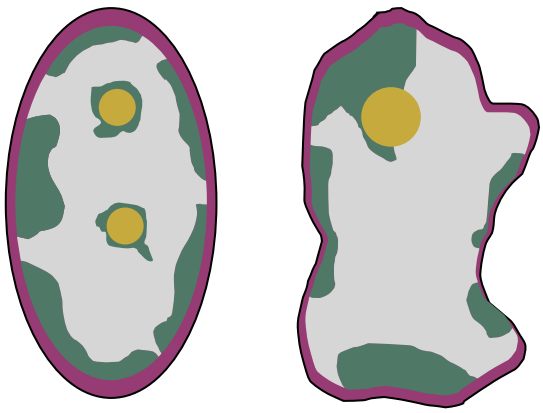

Figure 1.1: Key features of nuclear atypia. Left: regular nucleus. The underlying lamina (purple) shows regular distribution and association with chromatin (green) and 1-2 nucleoli (yellow) per nucleus. Right: cancerous nucleus, showing several common features often seen in tumour cells. These include an irregular shape, folds in the NE surface, enlarged nucleoli and uneven distribution of the lamina, as well as uneven association of the lamina with underlying chromatin. These features depend on the tumour type and not all are present in every cancer nucleus. (Figure adapted from Zink et al., 2004).

Another piece of evidence highlighting the centrality of nuclear morphology in cancer pathophysiology is the fact that despite the wide variety of source tissues and the range of mechanisms of tumorigenesis, nuclear abnormalities are relatively common

in all cancers. This suggests that structural alterations to the nucleus are highly relevant and conserved in carcinogenesis, meaning that changes to nuclear morphology are linked to the transformation process. Despite this, the factors that cause these alterations and their associated downstream consequences remain poorly understood. There is a need to elucidate the precise causal relationships between certain changes to nuclear architecture and stages of tumourigenesis. Some previous work has suggested that such alterations could be a direct consequence of oncogene activation or loss of tumour suppressor activity (Boyd et al., 1991, Fischer et al., 2014). Taken together, this suggests that changes to nuclear morphology and architecture may occur early in transformation and constitutes a key feature of tumourigenesis.

1.1.1 Features of cancer nuclei.

Nuclear enlargement is a common change seen and represents a deregulation of nuclear size. Under physiological conditions, nuclear size and cell size are tightly linked and ploidy has been shown to be one determinant of the former; with cells with larger genomes tending to have larger nuclei and cells. Lamins and components of the LINC complex have been linked to the regulation of nuclear size and are abnormally expressed in many studies (Jevtic and Levy, 2014). The mechanistic details behind nuclear enlargement however remain unclear, and their contribution to the tumorigenic process is unknown. It is likely that nuclear enlargement does not occur in isolation and represents a consequence of alterations to nuclear architecture and chromatin organisation that occur during oncogenesis.

Irregular nuclear shape is another commonly seen feature in cancer nuclei. The nuclei of epithelial, lymphoid and stromal cells range from spherical to ovoid (elliptical) and have regular outlines. Malignant tumours contain nuclei however with irregular nuclear contours, such as folds and grooves within the NE. A study has shown that oncogene activity alone was sufficient to induce the formation of these irregularities.

This study used the RET-PTC oncogene, which is a rearranged and constitutively active fusion protein containing part of the *RET* proto-oncogene. *RET* itself is located on chromosome 10q and encodes a receptor tyrosine kinase that, under normal circumstances, responds to the glial-cell-derived neurotropic factor (GDNF) ligand family; in turn activating diverse downstream pathways such as the PI3-K/Akt and MAPK signaling pathways (Prescott and Zeiger, 2015). In oncogenic RET-PTCs (thus termed since they first discovered in papillary thyroid carcinoma (PTC)), the C-terminal kinase domain has become fused in frame to the N-terminal end of an

unrelated gene through chromosomal rearrangement, producing a hybrid fusion protein that is constitutively active and oncogenic. There are at least thirteen known different RET/PTC fusion proteins (termed RET/PTC1-9) that have been discovered, with the most common being RET/PTC1-3; the remaining being incredibly rare. These proteins are formed through different forms of chromosomal rearrangement, with paracentric intrachromosomal inversion of chromosome 10q accounting for RET/PTC1 and RET/PTC3 and chromosomal translocation (between chromosomes 10 and 17) accounting for the formation of RET/PTC2 (Ciampi et al., 2007).

The study in question showed that injection of this RET-PTC oncogene into normal thyroid epithelial cells led to irregularities within as short as 8 hours, intriguingly without the cells requiring entry and exit from mitosis (Fischer et al., 2003). However, despite this elegant proof-of-concept, the mechanistic and molecular details underpinning the generation of these NE alterations remain unknown.

A third feature is the misregulation of chromatin distribution; the differences here are so prominent that they are easily visible under the microscope. The terminology used to describe such changes is less than precise however, with malignant nuclei labelled as hyperchromatic with coarse or clumped chromatin distribution and in some cases as vesicular or open' (Fischer., 2020). The striking degree of differences represents gross alterations in chromatin organisation, function and subsequent gene expression. It is hypothesized these changes are caused by condensation or decondensation of chromatin domains (Zink et al., 2004). Again, precise molecular pathways leading to this are unknown.

To conclude, features of cancer nuclei are well documented and correlate well with tumour grade and prognosis. The real challenge is linking these changes to any specific upstream molecular pathways. For instance, there is currently no known direct relationship between mutational profile and nuclear membrane irregularities. Causes are therefore likely complex, context dependent and multi-factorial.

1.2 Nuclear architecture.

Before discussing the mechanisms of aberrant nuclear morphology in a cancer context, it is important to first establish the concept of nuclear architecture under normal conditions. The eukaryotic nucleus is a highly specialized sub-cellular organelle that stores, preserves, reads and duplicates a cell's genome (Crosetto and

Bienko, 2020). It is surrounded by a nuclear envelope (NE) that consists of three distinct parts with the inner nuclear membrane (INM), outer nuclear membrane (ONM) and the intervening perinuclear space. The two membranes are separated by this space that ranges from 30-50 nm in human cells. Both membranes are traversed by nuclear pore complexes (NPCs) that are involved in the transport of substances into and out of the nucleus itself (Callan et al., 1950, Tapley and Starr, 2013, Suntharalingam and Wente, 2003).

1.2.1 The nuclear lamina.

In metazoan organisms, there is a scaffolding network of proteins that span throughout the nuclear periphery known as the nuclear lamina, located just beneath the INM (Figure 1.2). This lamina has a primary role in providing structural support to the nucleus and protecting chromatin (Isermann and Lammerding, 2013). The lamina itself consists of the main component of lamin proteins and their complement of binding partners. Lamins are c. 70 kDa proteins classed as type V intermediate filaments based on their sequence. It is estimated that there are around 3 million copies of lamins in a single mammalian nucleus (Gerace and Burke, 1988)

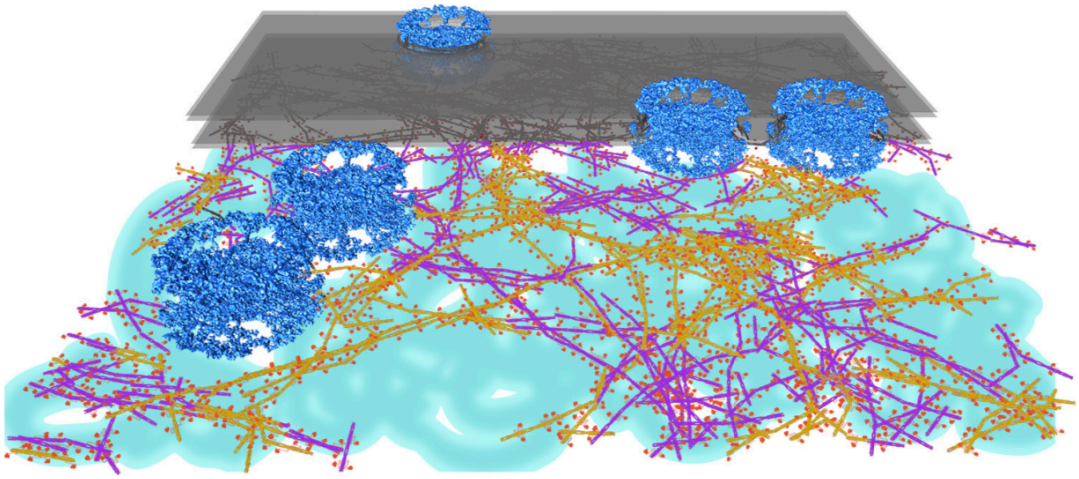

Figure 1.2: The nuclear lamina. Lamins form a network of proteins beneath the INM (grey) and interact directly with chromatin (cyan). Lamins are either A-type (orange) or B-type (purple), which form separate networks and are connected to NPCs (blue). (Figure from de Leeuw et al., 2018)

1.2.2 Lamins.

In mammalian cells there are four lamin proteins expressed. A-type lamins (lamins A and C) are generated from the alternative splicing of the *LMNA* gene. Lamin C protein is the mature product of direct *LMNA* mRNA translation. The mechanism to produce lamin A protein is less straightforward (Figure 1.3). It is initially made as a pre-lamin

A precursor that is then subjected to further post-translational processing to produce mature lamin A. Pre-lamin A is first farnesylated at a C-terminal cysteine residue that is part of a -CAAX motif. This motif is then cleaved by the zinc metalloprotease Zmpste24. This removes three residues of the -CAAX motif that exposes a site for carboxymethylation on the farnesylated cysteine, after which a second cleavage event by the same Zmpste24 enzyme removes a further 15 residues from the C-terminus, producing mature lamin A protein without an attached C-terminal farnesyl group (Schreiber and Kennedy, 2013).

B-type lamins (lamins B1 and B2) on the other hand are encoded by two separate *LMNB1* and *LMNB2* genes found on separate chromosomes. *LMNB2* also encodes a minor isoform lamin B3 that is germ cell-specific via alternative splicing (Burke and Stewart, 2013). Both lamins B1 and B2 undergo processing as pre-lamins with C-terminal -CAAX motifs. The cysteins in the -CAAX motifs are also farnesylated, with subsequent -AAX cleavage and carboxymethylation of the remaining C-terminal farnesylated cysteine (Evangelisti et al., 2022).

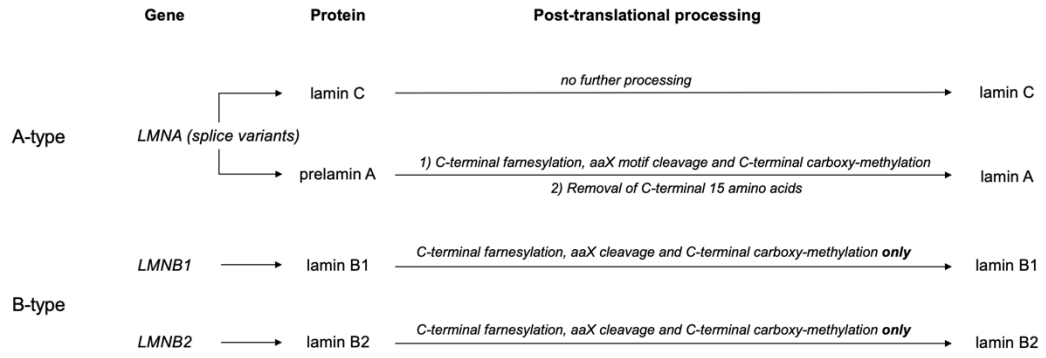

Figure 1.3: A summary of the major A and B-type lamins in mammals. (Figure adapted from Reddy and Comai, 2016). A and B-type lamins undergo separate processing pathways after translation; *LMNA,* encoding A-type lamins produce two proteins via alternative splicing. Lamin C lacks a C-terminal CaaX motif and undergoes no further post-translational processing. Lamin A and lamins B1 and B2 contain a C-terminal CaaX motif that undergoes farnesylation on the terminal cysteine residue, subsequent cleavage of the aaX motif and carboxy-methylation of the same C-terminal cysteine. Processing for B-type lamins ends here, while A-type lamins undergo an additional processing step, involving cleavage of 15 amino acids at the C-terminus (including the farnesylated and carboxymethylated cysteine) to produce the mature lamin A form that does not contain the C-terminal farnesyl group.

Lamins share similarities in their domains to other IF proteins such as keratin (type I/II) and vimentin (type IV) (Gruenbaum and Aebi, 2014). They consist of an N-terminal head domain, a central coiled-coil rod domain and a C-terminal tail that contains an immunoglobulin-like domain (Ho and Lammerding, 2012). Lamins are

also subject to a number of post-translational modifications including phosphorylation, SUMOylation and glycosylation, which will be discussed later. Given their non-globular conformation, no full-length structure of lamins have been reported. Lamins also polymerise under high concentrations, which prevents crystallization. Like other IFs, lamins form filaments in a hierarchical process. Single proteins form homodimers via coiled-coil interactions, that themselves self-assemble head-to-tail into polymers. These then interact laterally to form tetrameric proto-filaments that assemble into non-polar filaments (Gruenbaum and Medalia 2015).

The structural and functional differences between A and B-type lamins, and of the relative contributions of each individual isoform have been a topic of emerging interest. In terms of localization, A-type lamins are mostly present in the lamina but can also be found in the nucleoplasm as a pool of freely diffusible molecules (Moir et al., 2000). B-type lamins on the other hand are permanently farnesylated and localized to the nuclear membrane with a proportionately smaller and more static pool found in the nucleoplasm (Dechat et al., 2009, Shimi et al., 2015, Nmezi et al., 2019). Each isoform (A, C, B1 and B2) also forms distinct but overlapping meshworks as seen from 3D-structured illumination microscopy (3D-SIM) and direct stochastic optical reconstruction microscopy (dSTORM) (Shimi et al., 2015, Xie et al., 2016). Interestingly, the loss of one isoform has shown to affect the structural organisation of the other isoform networks, indicating a level of inter-isoform interaction within the lamina. However, the functional differences between each meshwork, as well as the mechanisms of their interactions remain unclear.

These two types also differ in their expression patterns. A-type lamin expression is tightly developmentally regulated, being absent in embryonic stem cells and only measurable after differentiation (Dechat et al. 2010). B-type lamins are expressed in most cell types regardless of differentiation state. They have roles in normal tissue development, particularly the central nervous system (Coffinier et al., 2011), though are non-essential in other areas such as the epidermis (Yang et al., 2011).

Laminopathies. Mutations in the *LMNA* gene are linked to a range of diseases, termed laminopathies, many of which are autosomal dominant. Currently, over 600 disease-causing mutations have been mapped to *LMNA* gene, making it one of the most frequently mutated, disease-associated genes known to date (Willaume et al., 2021). These include ageing disorders of which Hutchinson-Gilford progeria syndrome (HGPS) is the most well-characterised. Others include peripheral

neuropathy and lipodystrophies (Worman and Bonne, 2007). Diseases linked to B-type lamins are more rare and consequently less well studied.

Laminopathies as a whole are a highly useful case study for studying the mechanisms of lamin function and pose many questions that can be applied to other disease contexts. For instance, different mutations throughout the *LMNA* gene can cause the same type of disorder; penetrance can vary between individuals from the same mutation; most intriguingly, each laminopathy typically involves defects in a few tissues, despite the ubiquitous nature of lamin expression. Several models have been put forward to explain these discrepancies. The 'mechanical model' states that lamin mutations affect the ability of a nucleus to withstand mechanical stresses, leading to nuclear dysfunction specifically in tissues that experience these forces, such as muscle. The 'gene expression model' states instead that lamin mutations impair chromatin organisation and affect the expression of developmental genes that manifest in specific tissues. It is likely that both models have varying validity in different contexts, highlighting the fact that the relationships between genotypes and phenotypes are far from straightforward. (Graziano et al., 2018).

1.2.3 The LINC complex.

A key interactor to the nuclear lamina is the linker of cytoskeleton-nucleoskeleton (LINC) complex that provides a physical link between the two (Figure 1.4). The complex itself consists of two main families of proteins which are the INM-anchored Sad1/UNC-84 (SUN) and ONM-anchored Klarsicht/ANC-1/SYNE homology (KASH) proteins. The conserved luminal KASH domain binds the SUN domain linking the two together. In mammalian cells on either end, the cytoplasmic domains of the KASH proteins (nesprins 1-4) binds to various parts of the cytoskeleton whilst the nucleoplasmic domains of the SUN proteins (SUN1 and 2) bind to various parts of the nucleoskeleton. The complex plays a key role in nuclear positioning and movement by physically connecting it to the cytoskeleton (Lee and Burke, 2018). Furthermore, they are the main mode of force transmission to the nucleus from the cytoskeleton or extracellular environment, that in turn regulates chromatin organisation and gene expression (Bouzid et al., 2019, Wong et al., 2021).

Lamin proteins form the main interactors with SUN proteins on the laminar side of the nucleus, with evidence suggesting that SUN proteins interact with A-type lamins but not with B-type lamins, following co-immunoprecipitation and pulldown of SUN1 with GFP-tagged lamin A (Haque et al., 2006).

On the outside of the nucleus, specific nesprin types form distinct networks with different cytoskeletal elements. There are four main types of nesprins (nesprin-1-4), each encoded by separate genes (*SYNE1-4,* respectively). Nesprin-1 and nesprin-2 are both found as the full-length isoforms (known as nesprin-1 giant and nesprin-2 giant forms), as well as shorter variants and are ubiquitously expressed, with especially high levels found in skeletal and cardiac muscle cells (Janin and Gache, 2018). Nesprin-3 is similarly ubiquitously expressed, whereas nesprin-4 is found exclusively in secretory epithelial and mechanosensory cochlear hair cells (Roux et al., 2009, Horn et al., 2013). Mutations in *SYNE1-2* have been linked with Autosomal Dominant Emery-Dreifuss Muscular Dystropshy (AD-EDMD) and dilated cardiomyopathy (DCM). Nesprins-3 and 4 are less well studied, though a truncating mutation with nesprin-4 was linked with progressive high frequency hearing loss (Horn et al., 2013). There is currently very little evidence linking nesprins in regulating the cell cycle, though an association has been seen between nesprin-2 and the smc2 complex throughout the cell cycle, with association particularly strong in S-phase. However, the precise function of this interaction was not studied (Xing et al., 2017). In terms of interacting partners, nesprins-1 and 2 and can directly bind F-actin via their N-terminal calponin-homology (CH) domains. Nesprins-1,2 and 4 can also bind kinesin and dynein motor proteins and nesprin-3 can link with intermediate filaments via plectin.

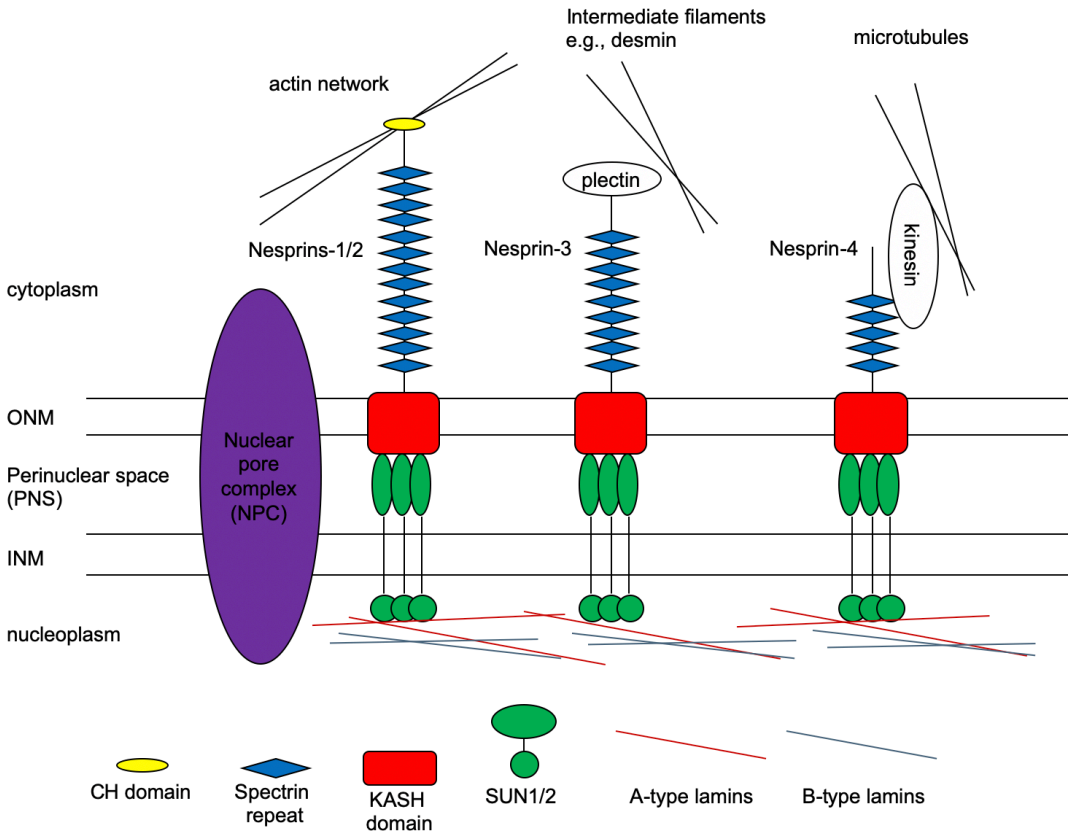

Figure 1.4: The organisation of proteins at the NE. The LINC complex spans the NE and interact with cytoskeletal elements through nesprins and the lamina through SUN proteins. Nesprins-1 and 2 can bind directly to the actin network via thir N-terminal calponin-homology (CH domains). Nesprin-3 contains a plectin-binding domain (PBD) that can bind plectin and interacts indirectly with intermediate filaments (e.g., desmin). Nesprin-4 can interact with microtubules via kinesin, while nesprins-1 and 2 can also interact with microtubules via dynein. All four nesprins contain C-terminal KASH domains that span the ONM and bind with the SUN domains of SUN1/2 in the PNS. Each nesprin interacts with a SUN1/2 homotrimer that itself spans the INM, linking with A-type lamins in the nucleoplasm, forming a direct physical link between the inside and outside of the nucleus. (Figure adapted from Mellad et al., 2011).

1.2.4. Lamin binding proteins.

Lamins interact with hundreds of protein binding partners, which are mostly INM and nuclear peripheral proteins (de Leeuw et al., 2018). These collectively contribute towards the maintenance of nuclear architecture, nuclear mechanics, chromatin organisation, cell cycle regulation and cell signaling. A prominent family of lamin binding partners are the LEM group, which includes emerin and are characterized by the presence of a LEM protein domain motif that binds to the DNA and chromatin binding protein barrier to autointegration factor (BAF) (Jamin and Wiebe, 2015). The LEM proteins, alongside lamins, interact with heterochromatin and anchor it to the lamina both directly and through BAF. Some of these LEM proteins mediate lamin's regulation of cell signaling. For instance, emerin regulates Wnt signaling by binding

β-catenin (Tilgner et al., 2009); MAN1 with the TGF-β pathway (Pan et al., 2005) and mammalian LAP2 isoforms with HDACs, alongside emerin (Holaska and Wilson, 2007). Other binding partners include lamin B receptor (LBR), involved in tethering peripheral chromatin to the lamina and gene silencing (Solovei et al., 2013) and LAP1.

1.2.5. Functions of lamins.

As the main component to the nuclear lamina, lamin proteins have key roles in maintaining nuclear structure and function. Their roles can be broadly divided into two categories, though there is much overlap between the two. These categories are those to do with nuclear mechanics (providing mechanical strength to the nucleus and contributing towards nuclear mechano-sensing) and those to do with controlling genome organisation and stability (through the regulation of chromatin organisation, gene expression and processes such as DNA replication and repair). Many other functions have also been described, such as autophagy, apoptosis, management of oxidative stress and differentiation, though these will not be covered here.

Lamins in structural integrity. Lamins provide the main source of structural stability to the nucleus. A-type lamins in particular help to increase nuclear stiffness whilst maintaining elasticity, that helps the nucleus maintain its morphology in response to mechanical stresses (Osmanagic-Myers et al., 2015). An *in vitro* study investigating lamin A assembly dynamics found that lamin A filaments are highly elastic due to their central rod domains and weak intra-tetrameric interactions that allow them to experience mechanical stresses without becoming disassembled (Makarov et al., 2019). Furthermore, the nuclei of *LMNA*-null mice fibroblasts were found to be more fragile and deformable than wild type (Lammerding et al., 2004). Work on nuclei of cells with HGPS, caused by a point mutation in the *LMNA* gene that produces a truncated lamin A protein, have revealed nuclei with irregular morphologies, thickened sections of nuclear lamina, NE blebbing and loss of peripheral heterochromatin (Goldman et al., 2004). These studies thus provided early evidence that lamins are necessary in maintaining nuclear morphology and nuclear architecture.

Lamins in mechano-sensing and mechano-signaling. Linked to its roles in structural stability, lamin A/C is also involved in active mechano-sensing and signalling. The precise contributions of lamins towards nuclear mechanics and mechano-regulation will be discussed in later sections.

Lamins in chromatin organisation. EM studies first revealed a dense layer of chromatin next to the lamina (Fawcett, 1966). As mentioned, lamins form direct and indirect links with chromatin. The lamina that interacts directly with the underlying chromatin does so via regions known as lamina-associated domains (LADs). Global chromatin association profiles have shown that 40% of the human genome is organized into around 1300 of these LADs, that span from kb to 10 Mb in length (Meuleman et al., 2013, Bickmore et al., 2013). These mostly consist of heterochromatin with repressive marks such as H3K9me2 and H3K9me3 (Guelen et al., 2008, Wen et al., 2009), have low gene density and are usually transcriptionally repressed, as well as being flanked by CTCF binding sites. Some LAD boundaries have also been shown to be enriched in in the facultative heterochromatin mark H3K27me3 (Guelen et al., 2008, Harr et al., 2015). Additional work has shown that there are hundreds of further genomic regions termed 'facultative LADs' that change association with lamins during differentiation (van Steensel et al., 2017). These links serve important roles in maintaining chromatin organisation and regulating gene expression. Downregulation of lamin A/C leads to chromatin reorganization, with a striking 'inversion in architecture' with peripheral heterochromatin localizing to the nuclear centre, leading to dysregulated differentiation and development of muscle tissue (Solovei et al., 2013). Another study has found that lamin A/C can modulate gene expression through interaction with adjustable sites on gene promoters, and that downregulation lead to dissociation of lamin A/C from said promoter regions, remodeling histone modifications and enhancing transcriptional activity (Lund et al., 2013). Conversely, experimentally induced tethering of genomic regions to the lamina lead to downregulation of their associated genes, mediated by the activity of local histone deacetylases (Finlan et al., 2008, Lee et al., 2009, Reddy et al., 2008). This shows how the lamina's effect on gene expression is an active and regulated process.

Lamins and differentiation. Linked to the above, A-type lamins have key roles in cell differentiation. Initial studies working on mouse development found a correlation between lamin A/C levels and stem cell differentiation. Embryonic stem cells (ESCs) completely lack lamin A/C, and lamin A/C deficient mice undergo normal embryonic development (Stewart and Burke, 1987, Sullivan et al., 1999). In later stages however, A-type lamin levels have been seen to increase with differentiation (Rober et al., 1989). In adult mice, cell types that have more proliferative and stem cell-like properties exhibit lower lamin A/C levels compared to other somatic cells (Broers et al., 1997, Rober et al., 1989, Swift et al., 2013). Somatic cells with high levels of lamin A show a predicted low efficiency in ease of reprogramming to induced pluripotent stem cells

(iPSCs), but alterations to increase or decrease lamin A levels can lead to a reduced or increased efficiency in iPSC induction (Zuo et al., 2012). Mechanistically, this role is partly due to its interaction with chromatin and its regulation of nuclear organisation. Such interactions are highly flexible and play a role in lineage determination (Lund et al., 2013). Loss of lamin A/C is accompanied by a corresponding loss of heterochromatin markers, meaning increased lamin A/C levels can therefore physically constrain tissue-specific patterns of heterochromatin localization and contribute towards locking in a cell state.

Lamins in maintaining genome stability. Lamins have roles in acting as 'caretakers of the genome' (Graziano et al., 2018) and preventing genome instability through its actions in DNA repair, telomere maintenance and DNA replication.

DNA repair is a critical process to maintaining genome stability. Out of the different types of DNA damage, double-strand breaks (DSBs) are the most harmful to a cell, since their inaccurate repair can then lead to gene mutations or chromosomal translocations (Li et al., 2016). DSBs are dealt with by a cell through activation of the DNA damage response pathway (DDR) that induces cell cycle arrest, providing time for repair to take place (Jackson, 2002). If the damage is too significant or the repair machinery is insufficient, senescence or cell death is triggered. Two systems of non-homologous end joining (NHEJ) and homology directed repair (HDR) are involved in DSB repair.

LMNA-KO mouse embryonic fibroblasts (MEFs) show accumulation of high levels of DNA damage (measured through marker γH2AX), increased chromosome and chromatid breaks and impaired NHEJ, due to the loss of p53-binding protein 1 (53BP1), a factor involved in DNA repair (Gonzalez-Suarez et al., 2011). The same study showed that this was due to the upregulation of protease cathepsin-L (CTSL) in lamin A/C deficient cells that is responsible for the degradation 53BP1, as well as the tumour suppressor proteins pRB and p107. Lamin A/C depletion also leads to downregulated transcription of DNA repair protein BRCA1 and impaired HDR (Redwood et al., 2011).

Since the discovery of HGPS as an ageing disorder, there has been much work looking into the link between lamins and telomere maintenance. The association of lamin A/C with telomeres is important for their localization and mobility within the nucleus, as well as for the maintenance of their length (Bronstein et al., 2009, de Vos

et al., 2010). *LMNA*-deficient mice display decreased telomere length and an increased number of chromosomes lacking telomeric signals (Gonzales-Suarez et al., 2009), and telomere shortening has been reported in nuclei of cells with HGPS (248, 324, 325). Lamin A/C also interacts with TRF2, a component of the protective shelterin complex found at telomeres that is essential for genome stability (Wood et al., 2014). Again, the link between B-type lamins and telomere stability has been less well studied.

Finally, there has been emerging evidence linking the importance of lamin A/C in DNA replication (Willaume et al., 2021). Initial work showed a co-localisation of both A and B-type lamins with PCNA, a key factor in the elongation phase of DNA replication, hinting that lamins may be involved in the spatiotemporal organisation of DNA replication within the nucleus (Goldman et al., 2002). Lamin A/C also has roles in managing replication stress through the recruitment of DNA repair and stalled fork protection factors. Studies have shown that lamin A/C is required for the restart of stalled replication forks (Singh et al., 2013). Lamin A depletion leads to cells with increased sensitivity to treatments preventing fork progression, such as replication stress inducing agents (hydroxyurea: HU) and crosslinkers (cisplatin, mitomycin C). Another study found that pre-lamin A expression leads to PCNA mono-ubiquitination and Pol η induction, both associated with replication fork stalling (Cobb et al., 2013). Work using the mutant lamin A protein progerin suggests that they may sequester PCNA away from the replication fork to induce replication stress, defined as the slowing or stalling of active replication forks. However, the mechanistic details of how lamins facilitate DNA replication are still unknown. They could either be through direct binding to the replisome and facilitating fork progression or through the indirect regulation of the stability of necessary replication factors. What is clear however, is that lamin A deregulation impairs the management of replication stress.

1.3 Chromatin organisation

Within the nucleus in mammalian cells, the average length of genomic DNA once stretched out is over two meters, which represents over 200000 times the diameter of the nucleus in which it is housed (Travers and Muskhelishvili, 2015). To fill this limited space, DNA is therefore tightly and sequentially packaged, with each step under extensive regulation (Figure 1.5).

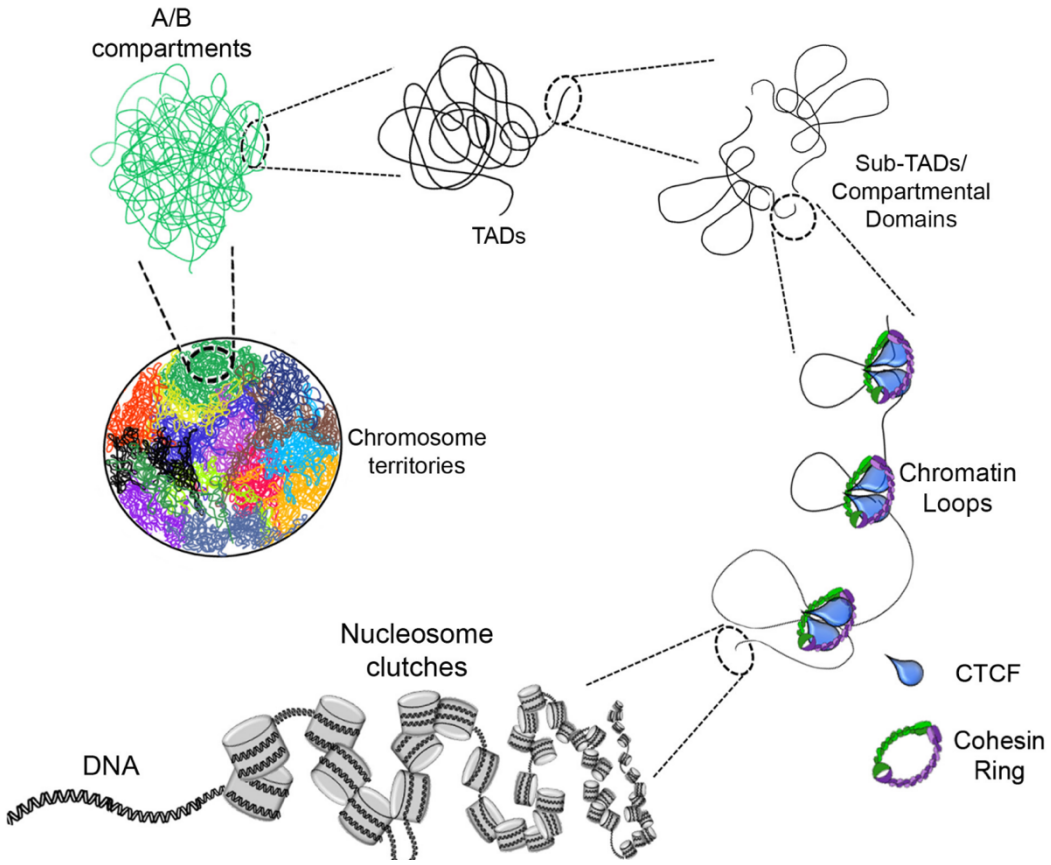

Figure 1.5: The hierachical nature of eukaryotic chromatin organisation. Eukaryotic DNA first interacts with octameric histones, forming nucleosomes that then aggregate into clutches of several nucleosomes that are close in physical space. These clutches condense to then form chromatin fibres that are then formed into loops via loop extrusion and stabilised with CTCF and cohesins. These chromatin loops are then organized into distinct TADs (areas of distinct domains of DNA replication). TADs themselves are then organised into A/B compartments that differ in their transcriptional activity (genes found in the A compartment being more active and genes in the B compartment generally more silent). Finally, these compartments themselves are part of a specific chromosome, which occupies a specific territory within the nucleus. (Figure from Magaña-Acosta and Graham, 2020)

1.3.1 Levels of chromatin organisation.

At the lowest level, DNA is wrapped around octameric histone proteins that serve as scaffolds, forming repeating units of 6.5 nm known as nucleosomes. Nucleosomes consist of 147 base pairs of DNA, core histone subunits and tails that are sites of post-

translational modifications such as methylation, acetylation and phosphorylation (Luger et al., 1997). A study using super-resolution (SR) microscopy has shown that nucleosomes can organize into discrete groups termed ‘nucleosome clutches’ that lack an organized structure (Ricci et al., 2015).

The next level of packaging consists of chromatin loops. These are on the order of kilobases (kb) and are formed from nucleosomes that themselves coil into chromatin strands. They represent an important level of regulation as it allows for the formation of physical contacts between sections of the genome that are distant, such as enhancers and promoters. Changes to these inter-loop contacts can lead to differences in gene regulation and expression (Greenwald et al., 2019).

In vertebrates, these chromatin loops are formed and stabilized by the protein CCCTC-binding factor (CTCF) and the cohesin complex. CTCF localizes to specific binding motifs in DNA via their zinc fingers (Filippova et al., 1996) and recruit cohesin to target loci (Wendt et al., 2008). Depletion of CTCF or cohesin leads to the disruption of chromatin loops whilst depletion of cohesin release factor Wapl promotes their stability (Wutz et al., 2017). In terms of loop formation, the ‘loop extrusion model’ has been proposed that suggests the DNA is pulled by the cohesin complex until the cohesin ring (consisting of the Smc proteins and Rad21) becomes stuck with the bound CTCF (Fudenberg et al., 2016).

At the next level come the topologically associated domains (TADs). These are on the Mb scale and correspond to domains of DNA replication (Pope et al., 2014). Sections within a TAD display strong interactions with others within the same TAD but weak interactions across different TADs (Beagan and Phillips-Cremins, 2020). To further complicate the picture, high resolution Hi-C studies have shown the presence of smaller domains termed sub-TADs that average 200 kb that differ between each other by transcriptional activity (Rao et al., 2014, Rowley et al., 2017). Almost all TADs contain CTCF and cohesin complexes on their boundaries, which suggest that TADs, like chromatin loops, were formed by the loop extrusion mechanism.

The next discrete level of organisation come with chromatin compartments, termed A and B (Lieberman-Aiden et al., 2009). Sections within the A compartment generally contain active histone modifications (eg. H3K9ac, H3K27ac) and transcriptionally active genes, whereas the B compartment contains silenced genes with histone modifications associated with a repressed state, such as H3K9me2 and H3K9me3

(Guelen et al., 2008). These compartments have non-random localization within the nucleus and this corresponds to their transcriptional profiles. A compartments are found in the nuclear centre and close to nuclear pore complexes (NPCs), whilst B compartments are found on the nuclear periphery, interacting with parts of the nuclear lamina, a protein network found beneath the inner nuclear membrane (INM). The sections where B compartments interact directly with the nuclear lamina are termed lamina-associated domains (LADs) and comprise approximately 10% of all the genes and a third of the total genome in mammalian cells (Peric-Hupkes and van Steensel 2010, Kind et al., 2015).

Lastly, we reach chromosomes themselves, which formed from the cumulative coiling of chromatin strands into discrete units within the nucleus. They represent the 'fundamental structural unit of the genome' (Kim et al., 2019) and each occupies a space in the interphase nucleus, termed a chromosome territory (CT). Studies using 3D fluorescent *in situ* hybridization (3D FISH) have shown that the distribution of CTs within a nucleus is non-random (Cremer et al., 2001). Chromosomes with higher gene density have CTs near the nuclear centre where they are more transcriptionally active than those with lower gene density at the nuclear periphery (Bolzer et al., 2005). CTs have been shown to be dynamic, with chromosomes relocalising across the nucleus during differentiation.

1.3.2 Chromatin remodeling.

Chromatin structure is highly dynamic and frequently oscillates between open, active euchromatin and closed, silenced heterochromatin to fine-tune transcription of specific sections of the genome. Chromatin can be remodeled in three ways. Firstly, the N-termini of histones are subject to extensive post-translational modifications, mediated by histone methyltransferases, kinases and acetyltransferases, with different marks associated with altered transcriptional states of the target genes. For instance, H3K9 and H3K14 acetylation corresponds to an active state, whereas H3K4me2 leads to gene silencing. Other less well studied examples of modifications include ubiquitylation and crotonylation.

Secondly, remodeling can be promoted by histone variants. These contain different residues, domains or expression patterns to canonical histones and can in turn influence the properties of the nucleosomes that they form. For instance, histone H3.3 is found specifically at telomeres and has been suggested to enhance chromatin accessibility (Lewis et al., 2010).

Thirdly, chromatin remodeling complexes (CRCs) can remove or deposit nucleosomes or histones and modify chromatin accessibility at different and specific regions to regulate transcriptional activation. These can impact chromatin structural properties on multiple levels, from nucleosome to chromatin loop and higher order compartments.

1.4 Nuclear mechanics.

The nucleus is both the largest and stiffest organelle within a cell and is therefore subjected to a wide range of forces from both within and outside the cell (Isermann and Lammerding, 2013). The appearance and response of a given nucleus in terms of its mechanics is governed by a balance between its inherent mechanical properties (intrinsic factors) and the nature of the forces acting on it, largely exerted through the cytoskeletal network (extrinsic factors).

The nucleus itself has been characterized as a viscoelastic material (such as rubber), that displays both elastic and viscous properties when subjected to external mechanical forces (Guilak et al., 2000), though the precise mechanical response is context dependent. This is perhaps counter-intuitive: elastic materials deform quickly and reversibly under force, such as a spring; viscous materials on the other hand deform slowly and irreversibly, behaving more like flowing liquids. The complexity of this phenomenon is due to the fact that the nucleus itself is a material with coupling between chromatin, lamins and other components that lead to variations in its response depending on the nature of the applied force and the cells studied. A key study revealed this response depended on the scale of the deformations induced. For small changes (<30% of the original nuclear length), the response is dominated by chromatin organisation, whereas at larger deformations resistance is dictated by the expression levels of lamins A/C (Stephens et al., 2017).

1.4.1 Intrinsic determinants of nuclear mechanics.

The nucleus itself has two main elements that determine its mechanical properties: the lamina and the chromatin.

Their importance of the lamina towards maintaining both nuclear stiffness, integrity and morphology is well established. Early work showed dramatic changes in nuclear shape upon depletion of lamin A/C or B1 in MEFs (Sullivan et al., 1999, Vergnes et al., 2004). Later studies suggested differential contributions of A and B-type lamins

towards nuclear mechanics. The current model states that A-types contribute towards nuclear viscosity by behaving as a highly viscous fluid that resists deformation, while B-types regulate elasticity by serving as elastic walls on the nuclear periphery that serve to restore shape following deformation. This is in line with evidence showing that depletion of A-type lamins has been shown to promote defective nuclear morphology, increased nuclear fragility and reduced nuclear stiffness (Lammerding et al., 2004), but also that B-types appear to contribute towards maintain NE integrity, but not nuclear stiffness, as (Lammerding et al., 2006).

A landmark study then showed how levels of lamin A protein in nuclei are upregulated in response to increases in extracellular matrix and cytoskeletal stiffness, indicating both that the nucleus is mechano-sensitive, and that lamin A protein plays a mechano-protective role in nuclei of tissues that experience higher levels of mechanical stress (Swift et al., 2013). The same study found that the stoichiometry between A and B-types regulate nuclear stiffness, and that since levels of B-type lamins remain constant, it is the actively regulated A-type lamins that act to resist deformation. The contributions of A and B-types are still a topic of intense investigation, especially as they are likely to be context dependent. Studies have shown that loss of lamin B1 can increase nuclear fragility (Vargas et al., 2012, Hatch et al., 2013), and that overexpression can increase nuclear rigidity (Ferrera et al., 2014). One possible reconciliation of these findings is the idea that stiffnesses of nuclei are only sensitive in cells with low lamin A but not high lamin A (Stephens et al., 2018).

Aside from lamin levels, the conformation of underlying chromatin is also a major determinant of nuclear mechanical properties. Introducing whole genome alterations to chromatin conformation through the use of histone deacetylase inhibitors (increasing euchromatin) and methyltransferase inhibitors (decreasing heterochromatin) both lead to softer nuclei and a higher frequency of blebbing events, importantly independently of lamin levels (Stephens et al., 2017, Furusawa et al., 2015). There is also evidence that chromatin-associated proteins also provide mechanical support and regulate nuclear morphology. These facilitate chromatin-NE interactions that contribute towards nuclear stiffness by forming a close-knit network (Kalukula et al., 2022).

1.4.2 Extrinsic (cytoskeletal) contributions to nuclear mechanics.

There is growing evidence suggesting the interplay between the nucleus and perinuclear cytoskeleton contribute towards nuclear mechanics and stability, quite

aside from the biochemical components of the nucleus itself. This is supported by both computational and experimental work that both show altering cytoskeletal dynamics have direct consequences towards nuclear morphology and stiffness (Alisafaei et al., 2019). For instance, disrupting the assembly of microtubules and F-actin using nocodazole and cytochalasin D each produces a reduction in nuclear stiffness (Zhang et al., 2020). These elements of the cytoskeleton exert forces onto the nucleus through the previously described LINC complex, that spans the NE and provides a direct physical link between the cytoskeletal network and nucleoskeletal elements such as the lamina and chromatin. Disruption to elements of the LINC complex have been shown to lead to impaired propagation of forces to the nucleus and aberrant nuclear morphologies (Bouzid et al., 2019).

F-actin fibers can exert compression forces directly onto the NE, which can lead to nuclear deformations and even NE rupture events (Hatch and Hetzer, 2016). This can be rescued by drugs that inhibit F-actin polymerization, such as latrunculin or cytochalasin D, or the inhibition of myosin II using blebbistatin (Hatch and Hetzer, 2016, Denais et al., 2016). In addition, within adherent cells in 2D cell culture, studies have demonstrated the existence of a set of dynamic actin filaments that form a dome-like structure on top of the nucleus connecting its apical side (via the LINC complex) to the basal side of the cell (via focal adhesions) termed the actin cap (Chambliss et al., 2013; Khatau et al., 2009). This cap has been shown to exert contractile forces directly onto the nucleus, with a study using SIM revealing deep indentations on the nuclear surface and underlying lamina when tension is exerted through these filaments (Versaevel et al., 2014). Intriguingly, these indentations have been accompanied by the reversible formation of distinct chromatin domains that themselves may affect gene expression, DNA replication and DNA repair. Later work in mouse embryonic fibroblasts (MEFs) showed both that the actin cap can be formed in response to mechanical stress and serves a protective role that resists deformation and that this formation is mediated by A-type lamins (Kim et al., 2017).

Microtubules can also exert forces onto the nucleus. Their association with kinesin and dynein motor proteins can damage nuclei by mediating aberrant nuclear movements, rather than by exerting direct compression like the abovementioned actomyosin networks (Earle et al., 2020). Dynein generated forces can increase the frequency of transient NE rupture events in nuclei expressing a modified weakened lamin mutant (Penfield et al., 2018), also supporting the idea of lamin having a mechano-protective role in withstand such forces under normal conditions.

1.4.3 Mechanosensing and mechanotransduction.

It has long been known that mechanically induced nuclear deformations have short and long-term consequences on nuclear function. However, there is increasing evidence to suggest that the nucleus itself contributes towards and regulates a cell's perception of its surroundings, acting as a "mechanosensor" and "mechanotransducer" to then translate these mechanical signals into downstream changes in gene expression and cellular function. These can take place by a variety of pathways, though three stand out as the most well studied.

Firstly, the NE itself can stretch under force, leading to an altered conformation of its pores and channels within it. Imaging and EM studies have revealed NPCs are sensitive to nuclear membrane tension (Zimmerli et al., 2021) and can increase their diameter in response to increased tension, allowing the entry of previously cytoplasmic protein such as the mechano-sensitive transcription factors Yap (Elosegui-Artola et al., 2017). In addition, the NE and associated ER membranes contain various stretch-sensitive ion channels that can open in response to increased membrane tension and allow calcium entry into the nucleus, which can lead to increased cell contractility (Lomakin et al., 2020, Venturini et al., 2020) or changes to chromatin organisation.

Secondly, forces on the nucleus can induce conformational changes to proteins within the NE. A good example of this is lamin A/C, which is phosphorylated in response to low cytoskeletal tension, increasing mobility and turnover and leading to a decreased nuclear stiffness (Buxboim et al., 2014, Kochin et al., 2014). Conversely, lamin A/C recruitment to the lamina is promoted when forces are applied onto the nucleus, via Src-mediated emerin phosphorylation (Guilluy et al., 2014). How the changes in mechanical forces are initially sensed by either kinase however is yet unclear.

Thirdly, mechanical forces can induce alterations to chromatin organisation, that then have consequences towards the expression of mechanosensitive genes. Two studies have provided the most direct evidence of this phenomenon. The first found using extracellular stretching applied via RGD-coated magnetic beads that force application led to rapid chromatin stretching as visualized by fluorescently tagged flanking genomic loci, and a rapid increase in transcription of a reporter gene (Tajik et al., 2016). The second showed that this force-mediated upregulation of transcription was associated with specific histone modification (H3K9me3 demethylation), suggesting that chromatin 'stretching' represented partial chromatin unpacking that promoted accessibility to remodeling factors (Nava et al., 2020). This pathway was also

dependent on the lamina and LINC complex, again highlighting the importance of direct nucleo-cytoskeletal coupling in force transmission and mechano-sensing.

1.4.4 Consequences of nuclear deformations.

The nucleus is subject to a wide variety of forces and consequently experiences frequent and dynamic changes to its morphology in the form of deformations, both on the short and long-term scales. These occur both in normal and pathogenic contexts and it is important to have a clear idea of the causes and functional consequences of such events. Given the ubiquity and range of deformation events, there are a range of downstream consequences that occur, such as activation of signalling pathways, altered gene expression, as well as increased NE rupture and DNA damage. Given the context of my project, I have decided to focus here on processes that affect genome stability.

NE rupture. NE rupture refers to a transient loss of NE integrity at local sites, as opposed to a global breakdown that occurs during open mitosis. These events last on the order of minutes and were seen in cells of patients with laminopathies (De Vos et al., 2011) and, importantly, in cancer cells (Vargas et al., 2012). It is now clear that increased physical stresses on the cell and nucleus can direct lead to an increase in transient NE rupture events, especially during the movement of a cell through narrow constrictions, relevant in cell migration, with the frequency of rupture events correlating with the degree of confinement (Raab et al., 2016, Denais et al., 2016).

The accepted model by which NE ruptures occur can be seen in Figure 1.6. A pre-existing gap within the lamina, especially for the lamin B meshwork leads to a local inability of the network to support the nuclear membrane. This leads the membrane to detach from the lamina and form a bleb, that expands under continued mechanical stress from ECM, actin stress fibres or cell contractions until it ruptures, leading to a leakage of nuclear proteins into the cytoplasm and influx of cytoplasmic proteins into the nucleus (Isermann and Lammerding, 2017). Blebs occur in areas of high local membrane curvature and typically lack lamin B and NPCs. Blebs themselves can last from minutes to hours but the rupture event is on the order of minutes. There have been observations of rupture events that occur without gaps within the nuclear lamina; in these cases they can occur when the membrane detaches from the lamina under increased cytoskeletal forces onto the nucleus (Raab et al., 2016, Irianto et al., 2017). Unsurprisingly, NE rupture events have also been associated with loss or depletion of A and B-type lamins (Pfeifer et al., 2019) and increased mechanical stresses onto

the nucleus via a variety of pathways (Hatch et al., 2016, Raab et al., 2016, Denais et al., 2016, Harada et al., 2014, Takaki et al., 2017).

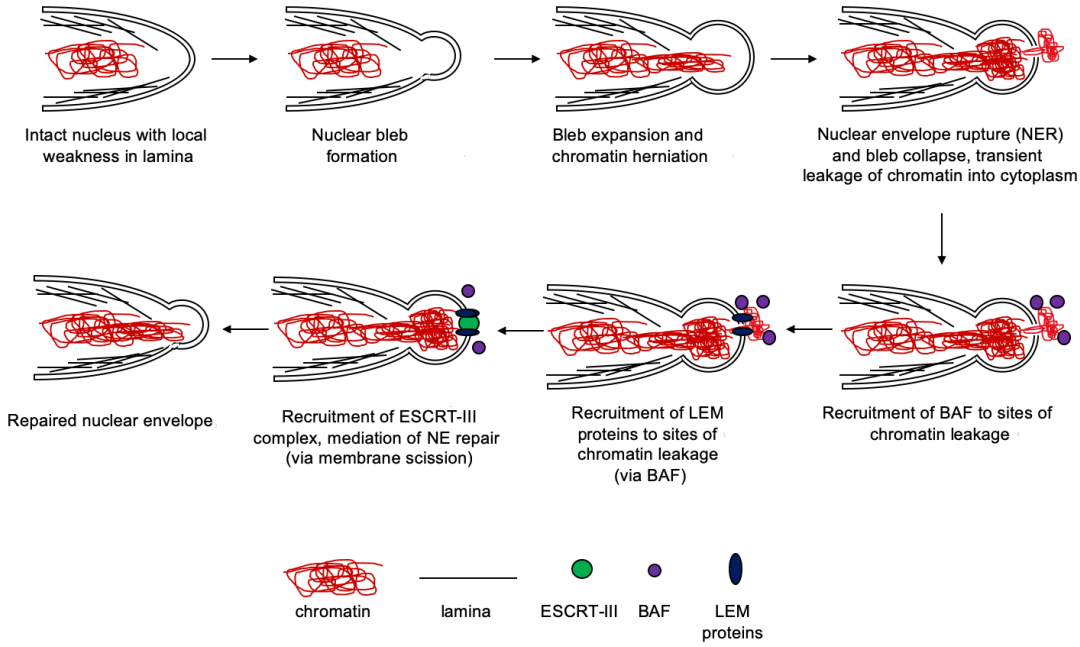

Figure 1.6: The mechanism of NE rupture and repair. NE rupture is initiated by a local weakness in the underlying nuclear lamina, leading to the formation of a nuclear bleb. This expands, eventually leading to NE breakage (rupture) and transient leakage of nuclear contents (e.g., chromatin) into the cytoplasm. Repair of the NE is then initiated by recruitment of BAF to sites of DNA leakage. BAF in turn recruits LEM proteins and ESCRT-III complex proteins, which mediate membrane repair. (Figure adapted from Shah et al., 2017 and Kamikawa et al., 2022).

As these events are typically transient, the cell has a robust pathway to repair NE rupture events. The protein machinery involved with NE rupture repair is similar to those used in NE resealing following mitosis (Figure 1.6). BAF is first recruited to the rupture site by recognizing DNA exposed to the cytoplasm. BAF then targets LEM proteins to these sites. LEM proteins further recruit endosomal sorting complexes required for transport (ESCRT)-III are to complete membrane repair. This process takes 10-15 minutes and is also associated with nucleoplasmic lamin A/C recruitment to reinforce the sites of rupture.

NE rupture and genome stability. NE rupture leads to the exposure of genetic material to the cytoplasm and the loss of integrity of the nucleus as a compartment. This leads to increased DNA damage (seen through an increase in both DSBs and single-stranded (ss)-DNA) and consequent GIN, though the mechanisms by which this occurs can vary. For instance, loss of nuclear integrity allows the entry of cytoplasmic nucleases. This can lead to the generation of DSBs, since interphase chromatin is highly accessible to nucleases and thus vulnerable to their actions. An

example would be the exonuclease TREX1 (Nader et al., 2021). TREX1 is known to localize to DNA bridges following rupture and generate ssDNA via exonucleolytic resection (Xia et al., 2019). Another mechanism could involve the mislocalisation of mitochondria into the nucleus following rupture, that produce reactive oxygen species (ROS) that can add further levels of DNA damage (Vargas et al., 2012). A particularly important mechanism of damage that follows NE rupture occurs during the migration of cells and nuclei through narrow constrictions. Here, a number of studies have shown that such transits cause mislocalisation of soluble complexes that mediate DSB repair (Irianto et al., 2016), limiting local access to the damaged DNA and prolonging the repair process.

There is also evidence to suggest mechanically induced DNA damage in the absence of a NE rupture event (Irianto et al., 2016, Shah et al., 2021). This is unlikely to occur via direct mechanical breakage of DNA from intranuclear forces, but rather through the generation of stalled replication forks and replication stress due to torsional stress on DNA from nuclear deformation. These processes are more relevant in lamin A/C deficient nuclei, which have been documented to be more deformable, more prone to NE rupture and more sensitive to DNA damage and replication stress (Irianto et al., 2016). This type of DNA damage exhibits different kinetics to NER-induced damage, occurring in the S/G2 phases of the cell cycle (during active DNA replication), as opposed to the latter, which occurs throughout interphase. How these two types of DNA damage differ in relevance across cell lines remains unclear.

More generally, the mislocalisation of nuclear factors (including DNA repair but also transcription factors) can deregulate nuclear processes such as transcription, DNA replication and chromatin organisation. The precise contributions of the different mechanisms driving increase DNA damage and GIN following NE rupture are unknown and a subject of increasing interest, especially due to the potential relevance that the DNA damage caused by such rupture events has in facilitating tumour evolution in cancer. NE rupture has been linked to chromothripsis, characterized by thousands of simultaneous chromosome rearrangements through the formation of micronuclei (Hatch et al., 2013). These mis-segregated and rearranged chromosomes can then contribute towards GIN and oncogenesis.

1.5 Lamins and cancer.

An attractive mediator of the generation of altered nuclear morphology first outlined in 1.1 is via altered NE protein expression, which is seen in many cancer nuclei. This is perhaps unsurprising as they represent key determinants of regular nuclear morphology. The features and implications of altered NE protein expression will be discussed in this section.

Altered NE protein expression has been found in a wide range of human cancers and can correlate with prognosis and survival. Amongst the most well studied are A-type lamin expression. Finding vary among different tumour types, and heterogeneity was even found with single tumours. Depending on the context, higher or lower lamin levels was seen as poor prognostic markers. For instance, colorectal and prostate tumours have been shown to associate with increased lamin A/C levels (Kong et al., 2012, Willis et al., 2008). This contrasts with work on colon, gastric, breast, prostate and ovarian cancers (Belt et al., 2011, Gong et al., 2015, Matsumoto et al., 2015, Saarinen et al., 2015, Wu et al., 2009) that show an association between decreased lamin A/C expression and worse prognosis. B-type lamins was reduced in some lung and intenstinal carcinomas but elevated in prostate cancers (Jevtic et al., 2014). Such studies demonstrate an important point that lamins likely have a context-dependent role in cancer, meaning further work is necessary to elucidate the differential roles it plays within cancer progression across different tissue types and stages. In addition, the poor prognosis of lamin expression in either direction highlights its importance in nuclear function and the dependence of many nuclear processes on its precise levels.

1.5.1 Consequences of lamin dysregulation in cancer.

As outlined in section 1.2.5, lamins (particularly A-type lamins) have a range of roles that contribute towards nuclear function. The loss or overexpression of lamin A/C therefore has a corresponding range of consequences, some of which are particularly relevant in promoting oncogenesis and tumour cell evolution. Processes affected include cell signalling, genome stability and cell migration.

Lamins and genome instability. Genomic instability (GIN) is another of the canonical hallmarks of cancer, contributing to tumourigenesis. As such, the maintenance of genome stability is crucial in preventing cancer evolution and is reflected in the roles of tumour suppressors as DNA checkpoint proteins. Lamin A/C deficient models have clear phenotypes of deformed nuclei, increased levels of DNA

damage, decreased capacity for DNA repair and loss of lamin-associated heterochromatin markers (Hutchison 2011, Lammerding et al., 2004). Lamin A/C loss can change the physical localization of telomeres within the nucleus and leads to telomere shortening, increasing GIN (Gonzalez Suarez et al., 2009, Wood et al., 2014).

Deregulated lamin A/C expression can also impair the cell's ability to perform DNA damage repair, that could accelerate tumour initiation and progression. Disruption of lamin A/C can increase activation of p53 signalling (Liu et al., 2005). Lamin A/C expression has also been shown to interact with p53 binding protein-1 (53BP1) that is involved in DNA repair (Ward et al., 2003). Studies in human fibroblasts have shown a reduced 53BP-1 stability in cells with lamin A/C deficiency, leading to defects in DNA repair (Redwood et al., 2011).

Lamins and misregulated cell signaling. As mentioned previously, lamins act as important signaling hubs for a number of pathways. As such, there is a significant degree of interplay between lamins, oncogenes and tumour suppressors that becomes important within a cancer context, where such interactions become deregulated. For instance, lamin A/C and its binding partner LAP2α sequester tumour suppressor Rb away from its target genes.

Depletion of lamin A/C in a human lung cancer cell line led to increases in tumour growth rate (Johnson et al., 2004), through mislocalisation and proteasomal degradation of Rb, which are both restored on reintroduction of lamin A. Lamin A/C has also been linked to the mitogen activated protein kinase (MAPK) pathway that regulates a diverse array of processes including gene expression, mitosis, proliferation and survival. Loss of lamin A/C or emerin can lead to hyperactivation of parts of this pathway (Emerson et al., 2009, Muchir et al., 2007). Other pathways linked to lamin A include Wnt/β-catenin, and TGF-β.

One example of a lamin A-linked protein involves the mechanosensitive transcriptional coactivator megakaryoblastic leukemia protein-1 (MKL1/MRTF) that binds serum response factor (SRF) and plays a role in tumour progression through its promotion of cell migration and metastasis. It is usually found in the cytoplasm bound to G-actin, but translocates to the nucleus on mechanical or mitogenic stimulation, where it activates expression of proteins key to cytoskeletal organisation and dynamics. Loss of lamin A/C or emerin impairs nuclear localization of MKL1, that

can in turn alter cytoskeletal actin dynamics in lamin A/C or emerin deficient cells (Ho et al., 2013). Another involves the similarly mechanosensitive transcription factor Yap1 of the Hippo pathway, also implicated in tumour progression (Moroishi et al., 2015). Recent work has shown that lamin A relocalistion from the lamina to the nucleoplasm represents an essential step in Yap1 nuclear import following nuclear deformation (Koushki et al., 2020). These two proteins demonstrate the tight interconnectedness of nuclear function and mechanics and their dysregulation in cancer.

Lamins in cancer stem cells. Given the centrality of lamin A/C in cell differentiation and pluripotency, its dysregulation in a cancer context is an intriguing line of inquiry. Within a tumour, there can be a subpopulation of tumour cells termed cancer stem cells (CSCs) that exhibit stem-cell like characteristics of self-renewal and phenotypic plasticity. It is predicted such CSCs can cause relapse via their persistence during therapy and subsequent formation of new tumours that can metastasise. Deregulation of lamin A/C expression and subsequent reprogramming of signaling pathways required for stemness could prove crucial in the generation or maintenance of this population of CSCs. One study has already found that depletion of lamin A/C in neuroblastoma cells lead to a distinct subpopulation with increased stem-cell like features (Nardella et al., 2015). The decreases in lamin A/C levels seen in some cancers could be a reflection of a CSC subpopulation that is key for the tumour's proliferation and differentiation.

1.5.2 Lamins and cancer nuclear mechanics.

An emerging line of inquiry of carcinogenesis is the role of the physical tumour microenvironment and tumour mechanics. Cancer cells exhibit a reduction in stiffness, can generate an increase in contractile forces and are affected by the mechanics of their environment. Tumour cells can be distinguished from normal ones by physical parameters, and further sub-divided by their metastatic potential. The relevance of nuclear mechanics specifically in cancer comes from the fact that the nucleus is the largest and stiffest organelle within the cell. It therefore largely dictates the cell's mechanical response in certain mechanical stimuli, such as the squeezing through narrow pores formed by neighbouring cells during migration, as part of the metastatic process of tissue invasion.

Lamins in migration. In this process, cells must move through small spaces in the ECM of their environment that are significantly more narrow than the size of the nucleus (Weigelin et al., 2012). They achieve this by a number of ways. One is the

direct degradation of ECM fibers in their microenvironment via externally secreted matrix metalloproteases (MMPs), that have been shown to be upregulated in many types of cancer and increased levels correlate with a worse prognosis (Coussens et al., 2002). Another is for cells themselves to physically deform in order to squeeze through the constrictions (McGregor et al., 2016). The nucleus and its deformation represents a rate-determining step and many studies have established that nuclear deformability is a function of A-type lamin expression (Lammerding et al., 2004, Pajerowski et al., 2007). As such, studies using transwell plates and microfluidics have shown that consequently, cells that exhibit reduced lamin A/C expression migrate at significantly faster rates through artificially determined narrow constrictions of 3 μm (Davidson and Lammerding, 2014, Harada et al., 2014). Harada et al in particular has extended this to a more *in vivo* setting, showing that cells found in the edges of a xenograft tumour model exhibit both lower lamin A protein levels and greater nuclear deformation, suggesting that such cells are more invasive. Taken together, the work underlines the importance of A-type dependent nuclear deformability in both normal and cancer cell contexts.

Lamins in NER. An important point to note is that while a decrease in lamin A/C expression contributes towards tumorigenesis via its effects on facilitating migration, it can also lead to cells more prone to mechanical stress. Increased nuclear fragility and NE rupture frequency has been seen in lamin A/C deficient models of laminopathies (Broers et al., 2004, Lammerding 2004, Vargas et al., 2012). Such reductions in lamin A/C can lead to chromatin segregation into nuclear blebs, further increasing chromosomal instability (Denais et al., 2016, Hatch et al., 2016).

1.5.3 Regulation of lamin A/C in cancer.

Whilst mutations in *LMNA* are the cause of a range of laminopathies, tumour analysis has shown that they are not as common in human cancers, whereas copy number variations comprise the majority of genomic alterations (Bell and Lammerding, 2016). How these variations affect protein levels remains to be studied, as well as any post-translational modifications that may affect their stability. However, as changes in lamin A/C transcript and protein expression are common in many human cancers, the mechanisms for lamin A regulation is fertile ground for study for further understanding for tumour evolution.

Gene expression of *LMNA*. Transcription of *LMNA* can be regulated by a variety of mechanisms. The first discovered was the retinoic acid (RA) family of transcription factors, where a study noted the presence of a retinoic acid responsive element (L-

RARE) in the *LMNA* promoter region (Okumura et al., 2004). A vitamin A derivative, RA is involved in the development and regeneration process and can either enhance or repress lamin levels depending on the cellular context (Okumura et al., 2004).

Another way is the use of microRNAs, which are short non-coding sections of RNA that decrease target protein levels by binding to target mRNAs. An example of one miR-9, which is deregulated in cancer and is a potential contributor to tumorigenesis (Nowek et al., 2018). mi-R9 has been shown to downregulate lamin A but not C in brain tissue (Jung et al., 2012). Intriguingly, ectopic expression of the *MYC* oncogene in breast cancer cells increases miR-9 expression, that enhances invasion and metastasis through its downregulation of E-cadherin (Ma et al., 2010).

Since lamins A and C represent alternative splice products of the same *LMNA* gene, regulation of the splicing process can modulate the relative expression levels of the two. Alternative splicing leads to large tissue-based variation of lamin A and C levels (Aljada et al., 2016). The same paper found that an elevated lamin C/A ratio could be used as a diagnostic marker in all stages of breast cancer, as well as liver, lung, thyroid, colon, ovary and prostate cancers. Little work has been done on teasing apart the individual functions of lamins A and C, and most commercial antibodies do not distinguish between the two splice variants. There is some evidence however that the two have separate effects on cancer progression. For instance, a study in epithelial ovarian cancer cells revealed that loss of lamin A but not C correlated with increased metastasis and a worse prognosis (Gong et al., 2015). This hint at the potential importance of *LMNA* splicing in modulating nuclear properties in different tissue contexts.

Lamin A/C post translational modifications. The assembly, function and stability of A-type lamins are all controlled by post-translational modifications. The most well studied examples occur during lamina disassembly in mitosis, where Cdk1 and PKC mediate phosphorylation at the key sites of S22, S392, S404 and S406 mediate lamin depolymerization (Simon and Wilson, 2013). Studies have also shown phosphorylation as a regulatory mechanism during interphase. Kochin et al. (2014) found that two of the predominant mitotic phosphorylation sites (S22 and S392) were also involved in the regulation of lamin A organisation, turnover and mobility in interphase. Buxboim et al. (2014) in turn showed that matrix stiffness promotes lamin A/C dephosphorylation at S22, which affects turnover, mechanics and actomyosin expression. This was counteracted by Cdk-dependent increases in lamin A/C S22

phosphorylation, that led to increased turnover, migration to the nucleoplasm and reductions of nuclear stiffness and nuclear tension.

Akt signaling has also been implicated in *LMNA* regulation. Akt (protein kinase B) is a serine/threonine kinase that acts as a master regulator of pathways including growth, survival, metabolism and cell cycle regulation. Akt has been shown to phosphorylate A-type lamins at S301 and S404 (Cenni et al., 2008) under physiological conditions. Further work has revealed Akt regulates *LMNA* transcription through its phosphorylation of S404, that targets prelamin A for degradation, important in epidermal differentiation (Bertacchini et al., 2013). One promising recent study provided the first mechanistic evidence for how oncogenesis can lead directly to altered lamin A/C levels. Bell et al., (2022) showed that oncogenic activation of Akt signalling led to the reduction of lamin A/C protein expression and an increased in nuclear deformability across a panel of breast cancer cell lines. Since the Akt pathway is hyperactivated in 60% of breast cancers (Ortega et al., 2020), this provides one of no doubt several routes that lead to depletion of lamin A/C in tumour nuclei.

Post-translational modifications that don't involve phosphorylation have been less well studied; however, ubiquitination, acetylation and the addition of small ubiquitin-like modifier (SUMO) proteins have been implicated. However, a full mechanistic understanding of these modifications and their functional consequences is yet unclear.

1.5.4 Summary

Overall, work suggests that the relationship between lamin A/C levels and cancer is far from a simple one. Decreased expression can facilitate cell migration and invasion via increased nuclear deformability, whereas increased expression can serve mechano-protective roles that are important in cells experiencing increased interstitial pressure within a tumour. Meanwhile, lamin A/C's additional roles in cytoskeletal organisation and cell polarity suggest that a baseline level of lamin A/C activity is necessary in any context. All of this explains the heterogeneity in lamin A/C expression found across different cancers, as high or low levels likely favour cells differently depending on disease stage and tissue background. The rarity of cancer-associated mutations or deletions in *LMNA* suggests that a base level of expression and functionality is required in order for tumours to adapt to their environment. It is unclear whether lamin A/C levels are merely a reflection of tumours conditions at any given time, or whether they can independently contribute towards oncogenesis.

1.6 Oncogenic c-Myc.

c-Myc is a member of transcription factors (including N-Myc and L-Myc) that regulates the expression of a range of target genes (Stine 2015). The c-Myc protein itself is encoded for by the *MYC* gene and the three Myc proteins combine to regulate at least 15% of the entire genome, a total of several thousand genes (Dang et al., 2006). These targets are involved in a wide variety of processes, such as cell cycle progression, proliferation, protein translation and metabolism (Figure 1.7).

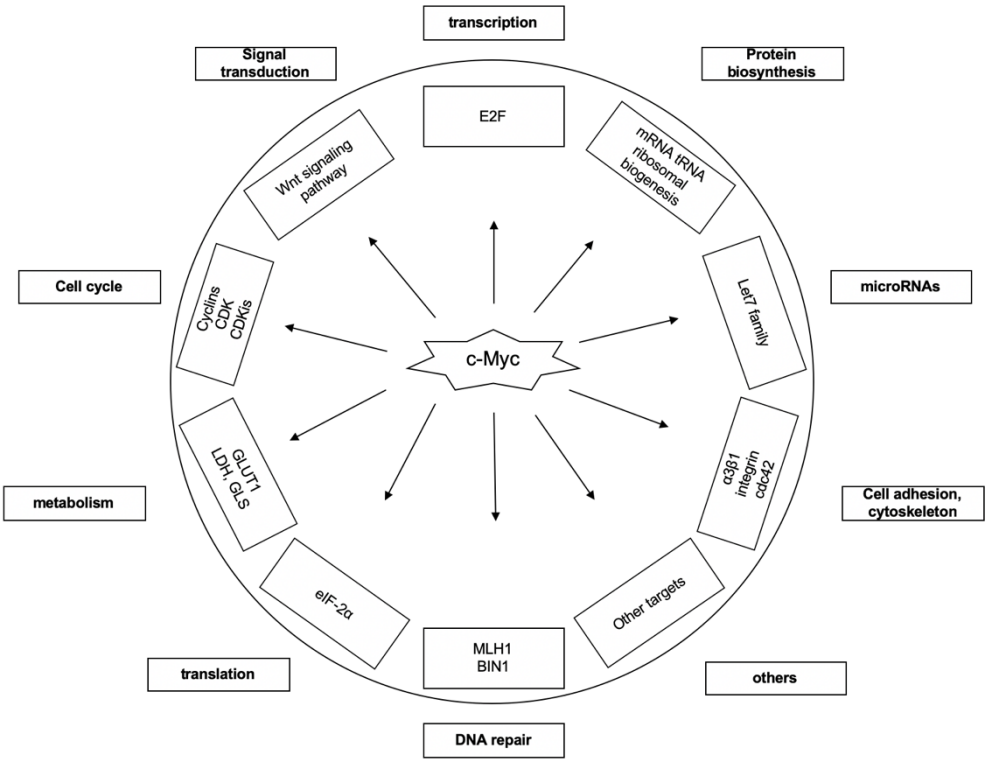

Figure 1.7: the c-Myc regulatory network. (Figure adapted from Chen et al., 2018). c-Myc regulates a wide range of cellular processes, including the cell cycle, protein transcription and translation and DNA repair. Targets that fall into the "other targets" section include regulators of processes such as apoptosis (e.g., Bax), immune response (e.g., PD-L1) and chromatin remodeling (e.g., EZH2).

The three Myc paralogs all have similar functions but can be distinguished based on their tissue distributions and expression dynamics during development. c-Myc is the most widely expressed both in normal development and in different types of tumour. N-Myc is found in neural tissue and deregulated in a number of cancers such as retinoblastoma and neuroblastoma. L-Myc is found in lung tissue and is predominant in small cell lung carcinomas, but is less well studied as it is thought to have a lower potential to induce tumour formation (Masso-Valles et al., 2020).

As a protein with a wide range of downstream targets, Myc is under tight regulation at both the transcription and protein levels in normal cells and is frequently

deregulated in cancer. Estimations place its expression to be deregulated in up to 70% of human cancers (Carabet et al., 2018), especially those that show limited response to currently available treatments. It has been found to be the third most amplified gene in human cancers (Raeder et al., 2013), further underlining the clinical relevance of its study. Increased c-Myc expression can be induced via chromosomal translocation/amplification, mutation of upstream regulatory pathways and retroviral promoter insertion. Studies involving the induction of c-Myc in tissue culture is sufficient to produce many tumour-like properties in healthy cells, such as the induction of cell growth and proliferation in the absence of growth factors. Studies in transgenic mouse tumour models have shown that alterations of Myc levels directly affects tumour incidence and development. Myc depletion abolishes tumorigenesis (Sansom et al., 2007) and conversely, Myc overexpression leads to enhanced tumorigenesis in several tissue models. It has been shown that *in vivo* Myc inhibition leads to tumour regression by the promotion of proliferative arrest, apoptosis and senescence in cancerous tissue. In addition, Myc has been shown to have a key role in allowing tumours to escape immunosurveillance through its upregulation of immune checkpoint proteins and inhibitory cytokines (Han et al., 2019).

1.6.1 Myc structure.

As the most widely expressed of the three paralogs, c-Myc is the most intensively studied. c-Myc is a 439 amino acid protein that contains a C-terminal DNA-binding and N-terminal transactivation domain (TAD). The C-terminus (residues 357-439) contains a basic helix-loop-helix leucine zipper (bHLH-LZ) motif that allows binding with partner Max (Amati et al., 1993). Under physiological conditions, this obligate heterodimer regulates gene expression by binding to a conserved E-box DNA sequence (5'-CACGTG-3') on the transcriptional regulatory region of the target gene. When c-Myc is deregulated, it has also been shown to bind open segments of chromatin containing the more common 5'-CANNTG-3' boxes (Blackwell et al., 1993).

The N-terminus (residues 1-143) contain an intrinsically disordered domain necessary for c-Myc mediated transcription. Recent work suggests that this disordered segment promotes formation of transcriptional condensates at super-enhancer sites that can be exploited by treatment options that preferentially deliver agents to these phase-separated condensates (Boijja et al., 2018). The transcriptional condensate model is one explanation of local transcription, in which phase separation leads to the formation of condensates at sites of active transcription, which contain high concentrations of proteins required for transcription (DNA-binding transcription factors,

transcriptional co-activators and transcription machinery e.g., RNA polymerases). A separate model, known as the “hub model” also exists to explain local transcription. This model shares much in common with the condensate model but does not stipulate formation of a distinct liquid phase at sites of active transcription (Palacio and Taatjes, 2022). Both models are supported by traditional evidence that labeled RNA polymerase II with gold nanoparticles that showed several hundred to thousand sites of active transcription (“transcription factories”) in each human cell nucleus.

The rest of c-Myc’s protein sequence contains several conserved segments known as Myc homology boxes (MB), shared with paralogs N-Myc and L-Myc that mediate protein-protein interactions with binding partners that can modulate Myc’s function as a ‘master regulator’, though the contribution of each individual MB towards Myc activity is highly complex and context-dependent, as well as being partially redundant (Tu et al., 2015).

1.6.2 Targeting c-Myc in cancer.

There has been significant work towards methods of targeting c-Myc, either through direct inhibition of the c-Myc-Max heterodimer or via targeted c-Myc degradation.

The importance of Max as an essential binding partner for c-Myc activity has led to much work dedicated to developing direct small molecule inhibitors targeting the Myc-Max heterodimer. The most promising of these is Omomyc, which is a truncated 90 residue polypeptide containing the C-terminal bHLH-LZ domain that competes with all three Myc paralogs for binding to DNA, effectively acting as a dominant negative protein that both displaces the Myc-Max heterodimers and inhibits target gene transcription (Demma et al., 2019). It is currently in Phase I/II clinical trials for advanced solid tumours such as non-small cell lung and triple negative breast cancer (Demma et al., 2019). The advantage is that direct inhibitors are speculated to lead to a lower incidence of drug resistance, as c-Myc acts as a central regulatory hub of gene expression without any alternative redundancies in available pathways. However, the complex structure of c-Myc, especially its intrinsically disordered domains, provides substantial challenges for the design and optimization of direct small molecule inhibitors. Whilst recent strides have been made in the use of *in silico* predictions of protein structure, the computational power required for such modelling processes is an important practical limitation that remains unaddressed.

Indirect approaches, which rely on targeting binding proteins crucial for c-Myc’s oncogenic activity has also been promising. These broadly rely on targeting c-Myc

post-translational modifiers or chromatin modifiers. In terms of the former, since Myc protein stability is under tight regulation by the Ub-proteasome system under physiological conditions, there are many potential avenues of research with the different proteins implicated. Particularly promising examples include the selective inhibition of Polo-like kinase-1 (PLK1), involved in N-Myc stabilization. The single agent Volasertib is currently in Phase II clinical trials for patients with ovarian cancer. In terms of targeting c-Myc chromatin modifiers, BRD4 inhibitors are by far the most intensively studied. BRD4 is a well-established transcriptional regulator of the *MYC* and *MYC-N* that destabilises them at the protein level through a ternary complex with ERK1 (Devaiah et al., 2020). Many BRD4 inhibitors are currently in Phase I/II clinical trials, though none have received approval so far.

The discovery of novel binding partners creates many new avenues of research, whilst also increasing our fundamental understanding on the mechanisms of c-Myc activity that can in turn shed light on the oncogenic process. The wealth of proven binding partners to c-Myc can however be seen as a double-edged sword, as it has also demonstrated the complexity of its function as well as its context dependence. This means that different targets in indirect c-Myc inhibition will have tumour specific effects, increasing the research required to tease apart the contributions of individual binding partners in different tissues and pathways before moving onto any clinical testing.

1.6.3 The c-Myc-ER inducible system. The ER fusion inducible system, which was characterised by its ability to reversibly switch the activity of a protein of interest on or off, has been used extensively in the study of tumourigenesis. The system relies on the use of a mutant human oestrogen receptor (ER) protein, that preferentially binds 4-hydroxytamoxifen (4-OHT), is insensitive to oestrogen and lacks the inherent transactivation activity seen in the wild type ER protein (Danielian et al., 1993). Fusion of this ER protein to a gene of interest (such as an oncogene) would allow reversible induction of its activity and study of its contribution to downstream phenomena, such as tumorigenesis. Previous models that tried to investigate the effects of specific genes on tumour development were limited in that the gene of interest was placed under a tissue-specific regulatory element that was expressed throughout the organism and tissue's life cycle (Whitfield et al., 2015). In addition, these early transgenic models could not turn the activity of a gene off once it was turned on, meaning it was impossible to determine whether sustained activation of the gene of interest was required to maintain a tumour phenotype.

The first study that combined the versatility of the ER fusion inducible system with c-Myc was published from Gerard Evan's lab; this study targeted the expression and activity of c-Myc to skin epidermis and showed that activation of c-Myc (through addition of 4-OHT) led to the development of rapid proliferation and changes that resembled human precancerous epithelial lesions. These changes were also shown to regress on deactivation of c-Myc (Pelengaris et al., 1999). Further studies using this system have shown that in pancreatic mature β-cells c-Myc activity can lead to simultaneous proliferation and apoptosis, and that c-Myc-triggered tumorigenesis is only achieved on suppression of c-Myc indced apoptosis by co-expression of Bcl-xL (Pelengaris et al., 2002). These early studies suggested that acquisition of additional mutations is needed for further progression of c-Myc driven tumours and that sustained c-Myc activity alone was not enough to fully drive tumour formation (Morton and Sansom, 2013).

Yet more studies have been performed with this system, with the Evan lab publishing several papers. Firstly, Murphy et al. (2004) showed that showing for instance that the Id2 target gene was not necessary for c-Myc's induction of epidermal hyperplasia (Murphy et al., 2003). Further work using the c-Myc-ER system and oligonucleotide arrays identified a set of key c-Myc target genes (involved in processes such as cell cycle regulation, cell adhesion and apoptosis) that are responsible for the maintenance of c-Myc driven tumours (Lawlor et al., 2006). A key paper in the understanding of oncogenesis was one in which a transgenic mouse containing the c-Myc-ER fusion protein was placed under the control of an active *Rosa26* promoter. The weakness but ubiquity of the *Rosa26* promoter allowed the study of low levels of c-Myc activation, which led to a separate phenotype to high levels of induced expression generated in previous work and did not activate the apoptotic pathways usually seen with high sudden c-Myc activation, with increased proliferation seen in most tissues and therefore organs (Murphy et al., 2008). What this showed was that *in vivo* there are separate thresholds of c-Myc activity that alter its downstream phenotypes. When c-Myc activity is deregulated but not overexpressed, oncogenesis and somatic cell proliferation is seen, but overexpression of c-Myc leads to activation of apoptotic and p53 tumour surveillance pathways. In another paper (Finch et al., 2009), overexpression of c-Myc in intestinal epithelial cells was seen to partially recapitulate phenotypic changes seen on Wnt/β-catenin signaling (that also activates c-Myc as a downstream target), indicating that there are phenotypic differences between direct and indirect c-Myc activation (e.g., direct c-Myc overexpression

engaging the ARF/p53/p21 tumour suppressor pathway, whilst indirect c-Myc activation does not).

Outside of the Evan lab, the c-Myc-ER system has been used to study c-Myc's interactions with other suspected oncogenes to further understand the process of tumourigenesis in different contexts. For instance, Kim et al., (2010) found through comparing microarray profiles of c-Myc activated cells with and without Pim1 expression that Pim1 can promote prostate tumourigenesis through its enhancing of c-Myc activity and upregulation of c-Myc target genes. In addition, the c-Myc-ER system has been used to identify synthetic lethal interactions with therapeutic implications. Sato et al., (2021) found that downregulation of DNA repair gene *UVSSA* led to increased ATM/Chk pathway activation and decreased viability in c-Myc expressing cells.

In terms of any direct effects of c-Myc's overexpression on nuclear morphology, none have been directly reported in studies using the c-Myc-ER system. However, there have been reports of c-Myc overexpressing tumours *in vivo* displaying increased nuclear atypia. Stearns et al. (2006) found that c-Myc over-expressing xenograft medulloblastoma tumours reported increases in nuclear atypia and macronucleoli. Merve et al. (2019) found mild nuclear atypia in c-Myc overexpressing choroid plexus cells within mice at three months. Taken together, this suggests that c-Myc activity could directly impact nuclear morphology and the contribution of this towards oncogenesis is a topic of particular interest, especially as it has not been extensively studied before.

1.7 Research Aims.

The aims of this research project were to study both the nature of and mechanisms that lead to changes in nuclear morphology and to then further investigate their contributions towards tumour evolution, specifically in the context of early stage oncogenesis using c-Myc activation as a model. My main research questions are summarized in Figure 1.8.

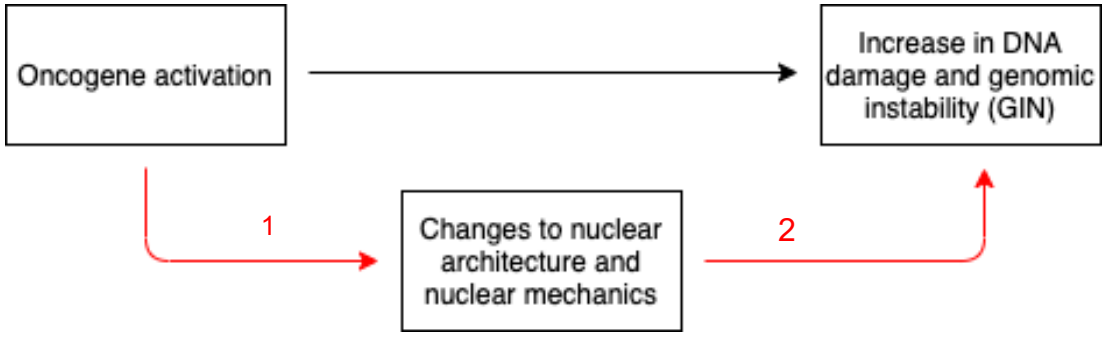

Figure 1.8: Schematic of project questions. Black arrow indicates what is well-known; that oncogene activation can lead to increases in DNA damage and GIN that represent hallmarks of cancer and are key contributors toward tumorigenesis. The two red arrows represent what is currently less well established and my two main research questions. First (1), how oncogene activation affects a cell's nuclear architecture and nuclear mechanics in the short-term. Second (2), how these changes then contribute towards the oncogenic process, by increasing DNA damage and GIN.

As previously stated, irregular nuclear morphologies are a widespread and robust marker for tumour tissue. There is however a lack of knowledge of the mechanistic processes that generate such phenotypes, and thus a gap in our understanding of basic tumour cell evolution. In addition, it is currently unknown at what stage of the tumorigenic process these alterations to nuclear morphologies manifest, and of their relative importance in feeding back to the process and furthering tumour evolution.

There is some recent evidence linking the loss of tumour suppressor and the generation of irregular nuclear shapes. p53 knockdown induced abnormalities in human breast epithelial cells (Tamashunas et al., 2020) and NE rupture and enlargement in human retinal pigment epithelial cells (Yang et al., 2017). In addition, depletion of tumour suppressor p63, a related protein, led to reductions in lamin A/C and B1 in basal keratinocytes and irregular shape in mouse embryos (Rapisarda et al., 2017). Conversely, as mentioned previously the microinjection of the *RET/PTC* oncogene into normal human thyroid epithelial cells induced shape irregularities (Fischer et al., 2003). Taken together, this work provided evidence that nuclear morphology defects can be directly induced by the activation or loss of a single gene and suggested that I would expect a similar phenotype on c-Myc activation in non-

oncogenic cells. However, there was very little available evidence suggesting a direct link between c-Myc activity and alterations to NE protein levels in the current literature.

In chapter 3, I begin by using an *in vitro* system to study the consequences of c-Myc activation on nuclear morphology at the earliest stages of oncogenesis (24 and 48 hours post induction). Encouragingly, I see gross changes to nuclear shape and size, accompanied by altered levels of key NE proteins, such as reductions in both A and B-type lamins.

Of the many NE proteins that c-Myc activation alters, I focus on its effects on lamin A/C, by far the most well studied of the NE proteins both in normal and cancerous cells. This is for three reasons. Firstly, lamin A/C silencing has direct implications for nuclear morphology through a number of ways: determining nuclear stiffness and deformability, altering chromatin organisation and promoting mitotic failure and defective post-mitotic NE reassembly, meaning the contribution of lamin A/C silencing to defective nuclear morphology is likely more significant than alterations to the levelf of other proteins. Secondly, there is clinical relevance to the work as lamin A/C depletion has already been reported in a wide variety of cancer types. Thirdly, altered lamin A/C levels in general have significant therapeutic relevance, as reduced mRNA and protein levels have been correlated with parameters for poor prognosis, such as larger tumour size, invasiveness, metastatic potential and decreased survival rates (Alhudiri et al., 2019, Alijada et al., 2016).

There is currently little known about the mechanistic pathways that generate nuclear morphology defects, or even those that lead to the misregulation of NE protein expression levels. On seeing reductions in A-type lamin levels, I focus in Chapter 4 on investigating a mechanism for c-Myc's apparent silencing of both lamin A/C mRNA and protein by investigating c-Myc's effects on mi-R9, emerin protein and cell cycle dynamics.

As discussed previously, there is much evidence to link NE rupture with the generation of GIN through a variety of mechanisms that increase DNA damage in the short and long-term. To therefore address the second of my questions, I focus on the downstream consequences of c-Myc induced lamin A/C deregulation, with a specific focus on NE rupture in Chapter 5 of my thesis. I also study similar pathways that could be affected by lamin A silencing, such as Yap signalling.

To summarise, my work investigates the ways in which c-Myc activity affect nuclear morphology, the mechanisms by which these changes take place, and the downstream consequences of such an event and their contribution towards oncogenesis.

2. Materials and Methods

2.1 Cell culture.

Retinal pigment epithelium (RPE)-TetON c-Myc ER cells were produced by Cosetta Bertoli according to published protocols (Bertoli et al., 2016). RPE1-hTERT cells were retrovirally transduced with pBABE c-Myc-ER plasmid (Addgene, 19128) containing the c-Myc ER fusion protein. Infected cells were selected in 2 µg/mL puromycin and cell lines were generated by expansion of the surviving polyclonal population. Cells were culture at 37ºC, 5% CO_2 in DMEM/F12 no phenol red media (Gibco, 21041) supplemented with 10% charcoal-treated fetal bovine serum (FBS) (Sigma, F7524), 1% penicillin/streptomycin (Gibco, 15140) and 3.5% sodium bicarbonate (Gibco, 25080). Upon thawing, cells were selected using 2 µg/mL puromycin before using in experiments. Charcoal-treated FBS was prepared by the addition of 0.5 g charcoal and 0.05 g dextran to 500 mL FBS that was then warmed to 37ºC for 2.5 hours and filtered under vacuum through a 0.2 µm filter.

2.2 Drug treatment

RPE1-cMyc ER cells were treated with 100 nM hydroxytamoxifen (4-OHT) (Sigma, H7904) in antibiotic and bicarbonate supplemented media for the timepoints described. Cdk1 inhibitor RO-3306 (Sigma, SML0569) was prepared according to the manufacturer's instructions by dilution in dimethyl sulphoxide (DMSO) (Sigma, D8418) before final concentrations of 9 µM were added to cells. Cdk4/6 inhibitor palbociclib was also prepared in DMSO before adding to cells at a final concentration of 150 nM.

2.3 Transfection

For siRNA treatments, Lipofectamine RNAiMAX (Thermo, 13778075) was diluted in Opti-MEM (Gibco, 51985-026) according to the manufacturer's reverse transfection protocol with a concentration of 20 nM siRNA oligo in every condition. Cells were plated in antibiotic-free media with transfection mixtures and collected 24 or 48 hours post transfection. For the negative control, non-targeting control siRNA (Dharmacon, Horizon Discovery, D-0018180-01-20) was used.

siRNA sequences used

- siLMNA (SMARTpool: ONTARGETplus, LMNA siRNA, Dharmacon, Horizon Discovery, L-004978-00-0005)
- siEMD (SMARTpool: ONTARGETplus, EMD siRNA, Dharmacon, Horizon Discovery, L-011025-00-0005)

For micro-RNA mimic and inhibitor treatments, cells were treated according to the standard RNAiMAX forward transfection protocol as per the manufacturer's instructions, except transfecting with mimic/inhibitor instead of siRNA oligos. Briefly, cells were seeded to reach 70% confluence in antibiotic-free media before mimic/inhibitor was diluted in Opti-MEM and Lipofectamine 2000 (Thermo, 11668027) and added for a final concentration of 10 μM. Samples were collected at 24 hours post transfection.

mirVana oligos used

- miR-9 mimic (has miR-9-5p mirVana mimic ID: MC10022, 4464066)
- miR-9 inhibitor (hsa miR-9-5p mirVana miRNA, ID: MH10022, 4464084

2.4 Western Blot

Whole cell extracts were first prepared in RIPA buffer (Tris-HCl pH 7.5 20 mM, NaCl 150 mM, EDTA 1mM, EGTA 1 mM, NP40 1%, NaDOC 1%) supplemented with proteas inhibitor cocktail (Sigma, P8340) and phosphatase inhibitor cocktails 2 (Sigma, P5726) and 3 (Sigma, P0044) at 1:1000 dilutions. Protein concentrations were quantified using the Bradford assay according to the manufacturer's protocols (Bio-Rad 500-0006). Protein samples were diluted and boiled for 5 minutes in sample buffer (Tris-HCl pH 6.8, SDS, glycerol, bromophenol blue) at 95 ºC before loading onto a gel. Equal amounts of protein (7.5-10 μg/lane) was then loaded onto a Nu-Page Novex 4-12% Bis-Tris gel (Invitrogen, NP0322) and run in MOPS buffer (Invitrogen, NP0001), after which protein was transferred to nitrocellulose membranes (Sigma, GE10600001) in transfer buffer (25 mM Tris-base, 250 mM glycine, 20% ethanol). Membranes were then blocked for 90 minutes in 5% milk or 5% bovine serum albumin (BSA) (Sigma, A7906) in PBS/0.2% Tween (PBS-T) as per antibody manufacturer instructions. Primary antibodies diluted in 5% milk or 5% BSA in PBS-T were then incubated with membranes overnight at 4ºC. Membranes were then washed three times in PBS-T before incubating with secondary antibody diluted in 5%

milk or 5% BSA in PBS-T for one hour at room temperature. Secondary antibody was visualized using Luminata Crescendo HRP substrate (Merck, WBLUR0100) and developed onto Amersham Hyperfilm (GE Healthcare Life Sciences, 28906836) and a XOGRAF Compact X4 film processor.

2.5 Antibody List

Protein	Host	Supplier	Cat. No.
actin	mouse	Cell Signalling Technology	4967
Akt pS473	rabbit	Cell Signalling Technology	9271
emerin	mouse	abcam	ab204987
Gamma-H2AX pS345	mouse	Cell Signalling Technology	20E3
GAPDH	mouse	Genetex	GT239
Lamin A	rabbit	abcam	ab26300
Lamin A pS22	rabbit	Cell Signalling Technology	D2B2E
Lamin B1	rabbit	abcam	ab16048
RPA2 pS4/8	rabbit	Bethyl Laboratories	A300-245A-3
RPA2 pS33	rabbit	Bethyl Laboratories	A300-246A
tubulin	mouse	Millipore	MAB3408
Vinculin	rabbit	abcam	ab129002
Yap1	mouse	Santa Cruz	sc-271134
Active-Yap1	rabbit	abcam	ab205270

Table 2.1: primary antibodies used in this research project.

Antibody	Host	Supplier	Cat. No.
Anti-mouse HRP	Goat	Fisher Scientific	PA1-74421
Anti-rabbit HRP	Goat	Fisher Scientific	PA1-31460
Alexa Fluor 488 anti-rabbit IgG (H+L)	Goat	Life Technologies	A11008
Alexa Fluor 488 anti-mouse IgG (H+L)	Goat	Life Technologies	A11029
Alexa Fluor 647 anti-rabbit IgG (H+L)	Goat	Life Technologies	A21244
Alexa Fluor 647 anti-mouse IgG (H+L)	Goat	Life Technologies	A21235

Table 2.2: secondary antibodies used in this research project.

2.6 Reverse transcriptase (RT)-qPCR

RNA was first extracted using a Qiagen RNeasy Plus Mini Kit (Qiagen, 74134) per the manufacturers instructions. The RT reaction was performed using the One Step Mesa Blue Mastermix (Eurogentec, 032XNR), supplemented with Euroscript Reverse Transcriptase/RNase inhibitor (Eurogentec, RT-0125-ER). Total reaction voluems were 14 µL per well, consisting of 7 µL master mix, 1.5 µL each of forward and reverse primers (5 µM) and 4 µL of RNA (20 ng/µL). All samples were loaded in triplicate and each experiment contained at least three biological repeats.

The reactions were run using a BioRad CFX Connect qPCR machine under the following programme.

- 30 minutes at 48ºC
- 5 minutes at 95 ºC
- 3 seconds at 95ºC → 45 seconds at 60ºC (repeat 40 cycles)
- 10 seconds each at 65 – 85 ºC for melt curve analysis

Data was analysed with levels of target gene mRNA (e.g., LMNA) in each condition (24h, 24h with c-Myc, 48h, 48h with c-Myc) normalized to levels of *GAPDH* in the same condition (control gene) and averaged across three statistical replicaes. These levels were then compared between different conditions at the same timepoints (24h with and without c-Myc, 48h with and without c-Myc) to obtain fold change expression per target gene at 24h and 48h with c-Myc for a single biological replicate. Three replicates were taken and an average fold change expression was calculated and tested for statistical significance.

Gene	**Sequence 5'-3'**
ACTB Fw	TCCACGAAACTACCTTCAACTC
ACTB Rv	CAGTGATCTCCTTCTGCATCC
BANF1 Fw	CTCTCTGGGAAGCTCTCAATC
BANF1 Rv	CGGAGGTGAGTACGACAATAG
EMD Fw	GGACGCTTTACTCTACCAGAGC
EMD Rv	CTGGTGATGGAAAGCGTCAGCA
GAPDH Fw	GAAATCCCATCACCATCTTCCAGG
GAPDH Rv	GAGCCCGAGCCTTCTCCATG
LBR Fw	CTATGTGGTGGATGCTCTCTGG
LBR Rv	CCACACCAAGTCTCCAAAAGCC
LMNA Fw	CGGTTCCCACCAAAGTTCA

LMNA Rv	CTCATCCTCGTCGTCCTCAA
LMNB1 Fw	GAAAAAGACAACTCTCGTCGCA
LMNB1 Rv	GTAAGCACTGATTTCCATGTCCA
LMNB2 Fw	AGAAGTCCTCGGTGATGCGTGA
LMNB2 Rv	CATCACGTAGCAGCCTCTTGAG
MAN1 Fw	GCCCACTACTTGTCGATGTT
MAN Rv	AGATACTCCTGTCCCTCTCATT
PLEC Fw	AGCGTGAGAAGGAGAAGCTCCA
PLEC Rv	CAGAGAGGAAGCTTTGCTGCAG
SUN1 Fw	CTGTGAGACAGTGGATGCCGTA
SUN1 Rv	AGCATCGTCTGCAAGTCGCCTT
SUN2 Fw	GGTGTGATTGGAGTGACAGAGG
SUN2 Rv	CTCGTAGGTCTCAGAACATCGG
SYNE1 Fw	AGAGCCAAGTCCTCAACCACCT
SYNE1 Rv	CACCGAAGCATTTGACAGGTCAC
SYNE2 Fw	CAAAGCACAGGAAACTGAGGCAG
SYNE2 Rv	AGACAGTGGCAACGAGGACATG
TUB1A Fw	CTCCTTGCCAATGGTGTAGTGC
TUB1A Rv	CAGTGATCTCCTTCTGCATCC

Table 2.3: primer pair sequences used in this research project.

2.7 Flow Cytometry

DNA content measurements using propidium iodide (PI) staining was performed to validate cell cycle dynamics on addition of Cdk inhibitor drugs. Cells were first trypsinised, washed in PBS and fixed in 70% ethanol at -20ºC overnight. Cells were then spun down and pellet washed in PBS and resuspended in 50 mg/mL PI and 100 mg/mL RNase A in PBS and incubated for 2 hours at room temperature. Samples were then measured using a BD LSRII flow cytometer with DIVA software (BD) and analysed using FlowJo software.

2.8 Immunofluorescence

Non-extracted cells. Cells were seeded on glass coverslips pre-coated in fibronectin (Sigma, F1141) and washed in PBS before fixing with 4% paraformaldehyde (PFA) for 20 minutes at room temperature. They were then permeabilized using 0.2% Triton x-100 (Sigma, T8787) solution in PBS for 5 minutes before washing twice with PBS

at room temperature. Cells were then blocked in 2% BSA in PBS-T for 2 hours at room temperature before overnight incubation with primary antibody diluted in 2% BSA in PBS-T at 4ºC. After washing three times with PBS, cells were incubated with secondary antibody diluted in 2% BSA in PBS-T for two hours at room temperature. Cells were then washed three times again with PBS before incubation with Hoechst 3342 (Invitrogen, H3570) at 1:10000 dilution in PBS for 5 minutes at room temperature in the dark before washing in PBS and water and mounting on glass slides with Fluoroshield (Sigma, F6182). Slides were then air-dried for 15 minutes at 30ºC before sealing with nail varnish. Images of fixed cells were acquired using a Leica TCS SPE2 and SPE3 confocal microscopes under a 40x or 63 objective lens before analysis in Fiji software.

Extracted cells. Cells were seeded on glass coverslips pre-coated with fibronectin and washed in PBS before cells were extracted to remove protein not bound to chromatin. For extraction, cells were incubated in ice-cold PBS (4ºC) 0.2% Triton x-100 for 1 minute, before washing twice with PBS at room temperature and fixing with 4% PFA for 20 minutes at room temperature. Cells were then washed twice with PBS at room temperature before blocked with 2% BSA in PBS-T for 2 hours at room temperature. Processing was then performed as described above using the same protocol for non-extracted cells.

2.9 Live-cell imaging

For transient transfection of pCDH-NLS-copGFP-EF1-BlastiS plasmid (Addgene, 132772) (Denais et al., 2016), a forward transfection protocol was used. Briefly, cells were seeded in antibiotic-free media to reach 70% confluence before 2 µg plasmid diluted in 5 µL Lipofectamine 2000 and Opti-MEM was added to each well of a 6-well plate. Samples were then imaged 6 hours later using a Nikon Ti inverted widefield timelapse confocal microscope. NE rupture was visualized by taking images every 5 minutes for a 24 hour time course. For 48 hour c-Myc activity, cells were seeded with c-Myc activity for 24 hours prior to plasmid transfection and imaging. Analysis was performed using Fiji software.

2.10 Preparation of polydimethylsiloxane (PDMS) gels

Coverslips were first cleaned using 1M HCl and sonication for 30 minutes at room temperature, before two washes with water and further sonication for 15 minutes in water and air-drying for 30 minutes in a fume hood.

PDMS (Sylgard 184 Elastomer kit) mixture was prepared using by measuring specific weights of PDMS base and curing agent and mixing manually using a Pasteur pipette. The mixture was then centrifuged to remove air bubbles before curing for two hours at room temperature and pouring into plates for seeding. For coating coverslips, a vacuum spin-coater was used to ensure uniform thickness in layer. A drop of PDMS mixture was added to the coverslip inside the spin coater before a two-step programme was followed of 500 rpm for 10 seconds, followed by 4000 rpm for 60 seconds for each coverslip. Once PDMS has set, the surface was cleaned using a plasma clean device that sterilized the surface for cell culture by treating with oxygen plasma for 30 seconds at 50% power.

Finally, the PDMS surface was functionalized by coating with fibronectin at 50 µg/mL in PBS and incubating for 5 hours at 37ºC. Once complete, the PDMS surface was washed three times with sterile PBS and cells were seeded for experiments.

2.11 Image Analysis

Images were obtained and analysed on Fiji software using several automated macros, outlined below. Original macros to generate maximum intensity projections, segment nuclei and measure signal intensities were written by Betheney Pennycook (formerly of the de Bruin lab); specific parts were modified by myself for my own use (generation of nuclear parameters, generation of smaller nuclear masks for nucleoplasmic intensity measurements).

Generation of maximum intensity projections from image stacks (example image below)

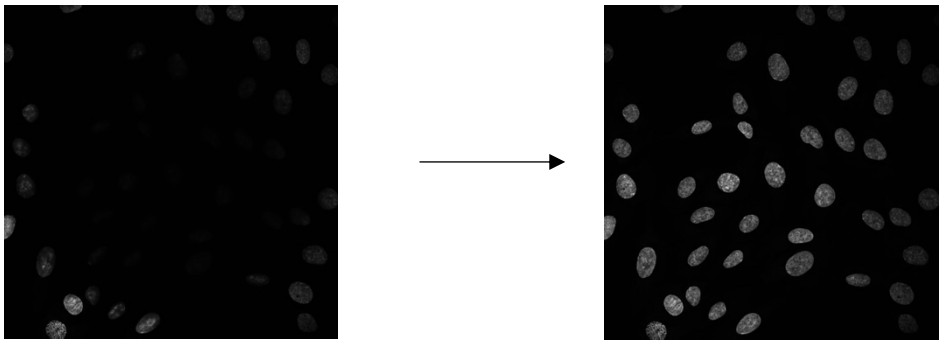

(Left): image stack of nuclei stained with Hoechst

(Right): Maximum intensity projection generated from code outlined below

```
imgArray = newArray(nImages);
for (i=0; i<nImages; i++)
{
        selectImage(i+1);
        imgArray[i] = getImageID();
}
for (i=0; i< imgArray.length; i++)
{
        selectImage(imgArray[i]);
        run("Z Project...", "start=1 stop=100 projection=[Max Intensity]");
}
```

Segmentation of nuclei using Hoechst staining, generation of nuclear parameters

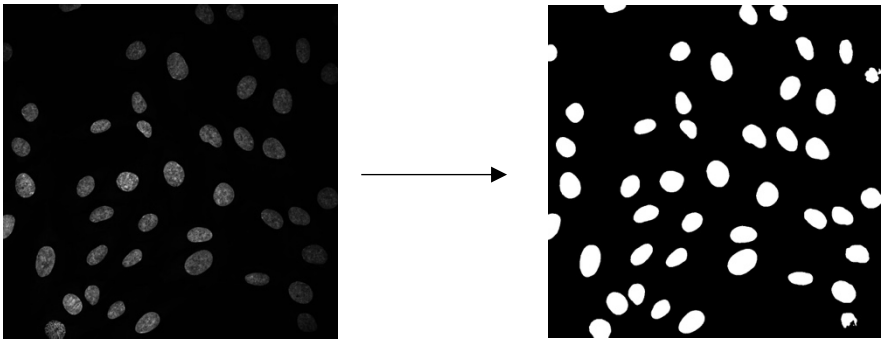

(Left): Maximum intensity projection generated; (Right): nuclear masks generated through segmentation using code below

```
ti=getTitle();

run("Gaussian Blur...", "sigma=3");
setAutoThreshold("Huang dark");
run("Create Mask");
run("Watershed");

run("Analyze Particles...", "size=15.00-Infinity circularity=0.00-1.00 show=Nothing
exclude clear add");
waitForUser("Pause","Correct ROIs");
selectWindow(ti);
run("Set Measurements...", "circularity redirect=None decimal=3");
```

```
roiManager("Measure");
waitForUser("Pause","Copy results");
selectWindow("mask");
close();
selectWindow(ti);
close();
```

Segmentation of nuclei using Hoechst staining, measurement of signal intensities

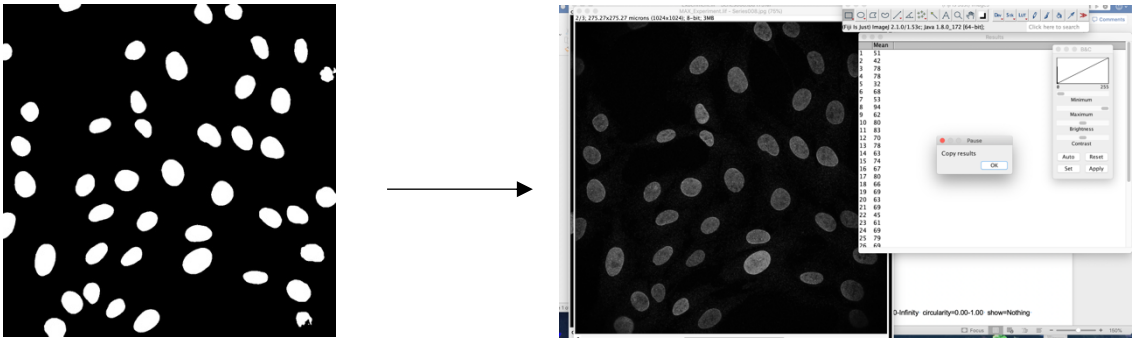

(Left): nuclear masks generated through segmentation using code below; (Right): Measurements of signal intensities in other channels (e.g., lamin A) using nuclear masks as regions of interest

```
ti=getTitle();
setSlice(3);
run("Gaussian Blur...", "sigma=3");
setAutoThreshold("Huang dark");
run("Create Mask");
run("Watershed");
//this doesn't work for myc nuclei

run("Analyze Particles...", "size=15.00-Infinity circularity=0.00-1.00 show=Nothing exclude clear add");
waitForUser("Pause","Correct ROIs");

selectWindow(ti);
run("Set Measurements...", " mean redirect=None decimal=0");
setSlice(2);
roiManager("Measure");
```

```
waitForUser("Pause","Copy results");
setSlice(1);
roiManager("Measure");

waitForUser("Pause","Copy results");
selectWindow("mask");
saveAs("png");
close();
```

Generation of smaller nuclear masks to segment nucleoplasm and measure nucleoplasmic intensities of protein

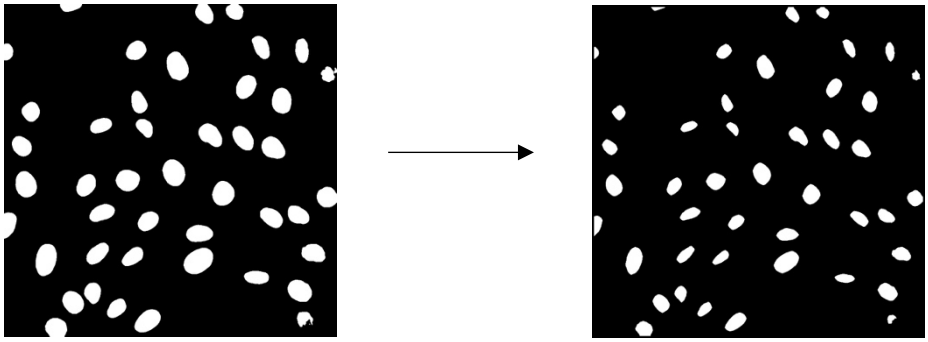

(Left): nuclear masks generated through segmentation using code below; (Right): eroded nuclear masks generated from original nuclear masks to measure signal of proteins of interest in nucleoplasm

```
ti=getTitle();
setSlice(2);
run("Gaussian Blur...", "sigma=3");
setAutoThreshold("Huang dark");
run("Create Mask");
run("Watershed");
run("Erode");
run("Erode");
run("Erode");
run("Erode");
run("Erode");
run("Analyze Particles...", "size=15.00-Infinity circularity=0.00-1.00 show=Nothing exclude clear add");
```

```
waitForUser("Pause","Correct ROIs");
selectWindow(ti);
run("Set Measurements...", " standard redirect=None decimal=3");
setSlice(1);
roiManager("Measure");

waitForUser("Pause","Copy results");

selectWindow("mask");
close();
```

Quantification of laminar homogeneity values.

Line sections were generated using Fiji and manually aligned with the longitudinal axis of each nucleus. Traces were produced using the measurement tool and the intensity values at opposing peaks were noted and recorded in Excel.

Once intensity values were generated, parametric one-way ANOVA was used for statistical analysis between multiple conditions in Prism v8.

2.12 Classification of nuclei in time-courses (intact vs NER vs apoptosis).

Individual nuclei were identified through GFP signal and classed into three phenotypes depending on their behavior throughout the time-course. If there was no leakage of GFP signal from the nucleus into the cytoplasm at any point throughout the time-course (excepting when the nucleus divides through mitosis), they were classed as intact. If at any point the nucleus experienced a transient decrease in nuclear GFP signal, accompanied by an increase in surrounding cytoplasmic GFP signal (as nuclear GFP leaked into the cytoplasm), which was then resolved with a recovery of nuclear GFP signal (due to NE membrane repair) between 15 minutes to an hour (3 to 20 frames), they were classed as having undergone one NE rupture events. If nuclei underwent blebbing and fragmentation, in which nuclear GFP signal became scattered into distinct and separate fragments, they were classed as having undergone apoptosis.

3. The effects of c-Myc activation on nuclear morphology and nuclear architecture

In this chapter I will outline the results of my investigation into the observed changes to nuclear morphology and nuclear architecture on c-Myc activation. c-Myc is a well-established example of an oncogene whose activation can lead directly to tumorigenesis, with both *in vitro* and *in vivo* assays for transformation phenotypes classing it as one of the most potent oncogenes currently known (Sheiness et al., 1978, Alitalo et al, 1983).

However, none of the currently known mechanisms of c-Myc induced oncogenesis involve directly induced changes to nuclear morphology or nuclear architecture. Some of the more well studied consequences of c-Myc activity include an acceleration of DNA replication and S-phase entry (Cerni et al., 1986) or the generation of increased GIN via the blockage of ds-DNA repair and increase oxidative damage (Vafa et al., 2002).

I wanted to therefore study the direct effects of short-term c-Myc activation on nuclear morphology and the levels of NE proteins that constitute nuclear architecture, which so far remain unexplored.

3.1 c-Myc induction causes acute changes to nuclear morphology

To test if c-Myc had any effects on gross nuclear morphology, I first decided to directly image fixed cells at early timepoints following c-Myc activation. For the entirety of this research project, I have used a cell line originally derived from immortalized non-transformed retinal pigment epithelium (RPE1) hTERT cells where cell cycle chcekpoints remain intact and basal expression levels of *ESR1* are minimal (Jin et al., 2023). These cells have been modified to stably express a fusion protein of c-Myc with the oestrogen receptor protein (ER) tagged at its C-terminus. This cell line will be referred to as RPE1 c-Myc ER cells (Bertoli et al., 2016). Addition of 4-hydroxytamoxifen (4-OHT) to cell culture media containing these cells leads to activation of c-Myc via the activation and subsequent translocation of the fusion protein from the cytoplasm to the nucleus, where c-Myc binds to its target genes and upregulates their transcription within as short as 8 hours post induction.

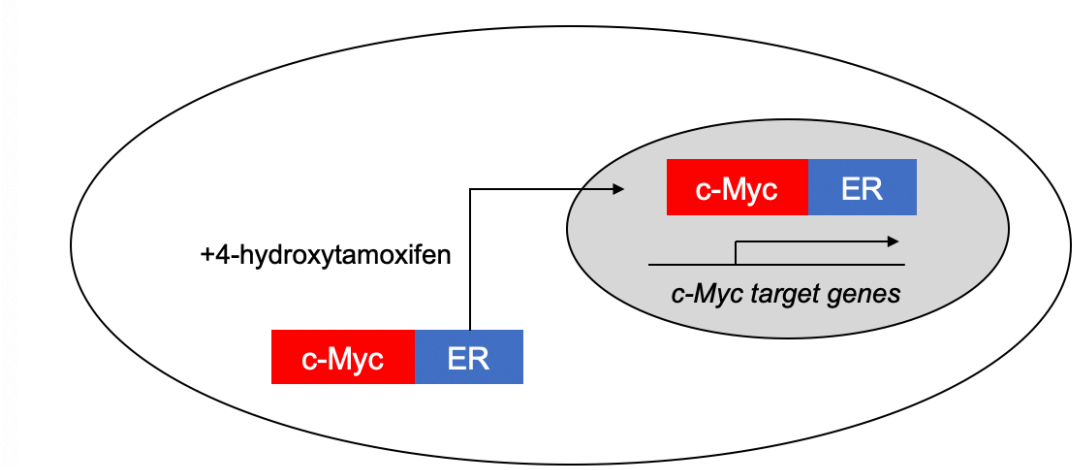

Figure 3.1: Schematic of the c-Myc inducible system. In untreated cells, the fusion protein of c-Myc and oestrogen receptor (ER) remains in the cytoplasmic and target genes are not upregulated. On addition of 4-OHT (hereafter tamoxifen), the fusion protein translocates to the nucleus where c-Myc activates the transcription of its target genes.

At timepoints of 8, 24 and 48 hours after activation of c-Myc, RPE1 c-Myc-ER cells were fixed and DNA stained with Hoechst dye to visualize the nucleus and its outline. They were then imaged via fixed-cell immunofluorescence using a confocal microscope. These samples were then compared to those where c-Myc remained inactive.

Figure 3.2A shows representative images of Hoechst-stained nuclei at the three separate time points. We can see from 3.2B that c-Myc activity leads to changes to nuclear morphology at the later two timepoints, from as early as 24h post induction that was maintained at 48h. This is in the form of reductions to nuclear circularity, with the reductions themselves becoming larger over time. Nuclear circularity (C) as a parameter is obtained by fitting measurements of nuclear area (A) and perimeter (P) to the equation $C = 4\pi*A/(P\hat{}2)$. It takes a value between 0 and 1, with 1 representing maximum circularity and corresponding to a regular circle. It is a commonly used method for quantifying nuclear shape and has been used in a variety of studies looking at nuclear dysfunction in cancer (Takaki et al., 2017, Antmen et al., 2019) and other disease contexts, such as the laminopathy HGPS (Goldman et al., 2004). Some studies have also suggested circularity values alone can be used as a reliable diagnostic marker to separate between melanomas in histological samples (Schöchlin et al., 2014).

This observation of increasingly irregular nuclear morphology on c-Myc activation is strengthened by 3.2C, which represents a bar graph showing the data from the same images with nuclei categorized by visual scoring into one of three categories (examples also shown): circular, elliptical and irregular, with the former two representing wild-type nuclear morphology. This shows that untreated cells contain c. 15% irregularly shaped nuclei. These proportions increase to 15.9% after 8 hours, 65.5% after 24 hours and 57.8% after 48 hours of c-Myc activity, a phenomenon seen after three separate experiments. Both 3.2B and 3.2C therefore indicate that c-Myc activation leads to an increase in frequency of nuclei with irregular morphologies compared to cells with no c-Myc activity.

We also see from 3.2D that c-Myc causes a slight reduction in cross-sectional nuclear area at 8h, which becomes significant at 24h post induction. These reductions likely represent an accelerated passage of the c-Myc induced cells through the cell cycle, resulting in a shortened interphase and consequently shortened G1 and G2 phases, where nuclei would usually grow in size. There is no change in cross sectional nuclear area at 48h, and interquartile ranges of nuclear size at all three timepoints remained unaffected with c-Myc activation (3.2E).

In this initial set of experiments, it is important to note that two controls are missing that would need to be added to further validate that the effects seen on nuclear morphology are truly down to c-Myc activity. Firstly, evidence of c-Myc expression would need to be inserted to prove that the c-Myc-ER system is functioning properly and that addition of 4-OHT would leads to c-Myc target genes being turned on. When the RPE1 c-Myc-ER cell line was first characterized, c-Myc activity was validated by measuring fold change in transcript levels of c-Myc target genes eIF4E and cyclin E following 4-OHT addition and comparing to fold change on the same treatment using control cells that do not contain c-Myc. These control cells are identical to RPE1 c-Myc ER cells, but do not contain the c-Myc-ER fusion protein. Instead, this cell line (hereafter termed “ER-empty cells”) contains a truncated version of the same plasmid as the c-Myc ER cell line that only contains ER protein on its own, without its fusion to c-Myc. This results in all ER-empty cells lacking c-Myc, meaning that any effect of 4-OHT that is seen in c-Myc ER cells, but not these ER-empty cells would be a direct result of c-Myc activation. In this thesis, evidence of c-Myc activity through upregulation of target genes are only shown in RT-qPCR experiments, where an increase in *eIF4E* levels after 4-OHT addition is used as a positive control. This

positive control would need to be performed and included in this initial set of studies characterising nuclear morphology.

A second control to be added would be to ensure that the effects seen are not due to 4-OHT addition alone. For this negative control, the same experiment would need to be performed on RPE1 ER-empty cells that lack the c-Myc fusion protein, where cells are imaged 24 and 48h after addition of 4-OHT and compared to untreated samples to verify that nuclear morphology remains unaffected when 4-OHT is added to the cell line that does not contain the c-Myc ER fusion protein.

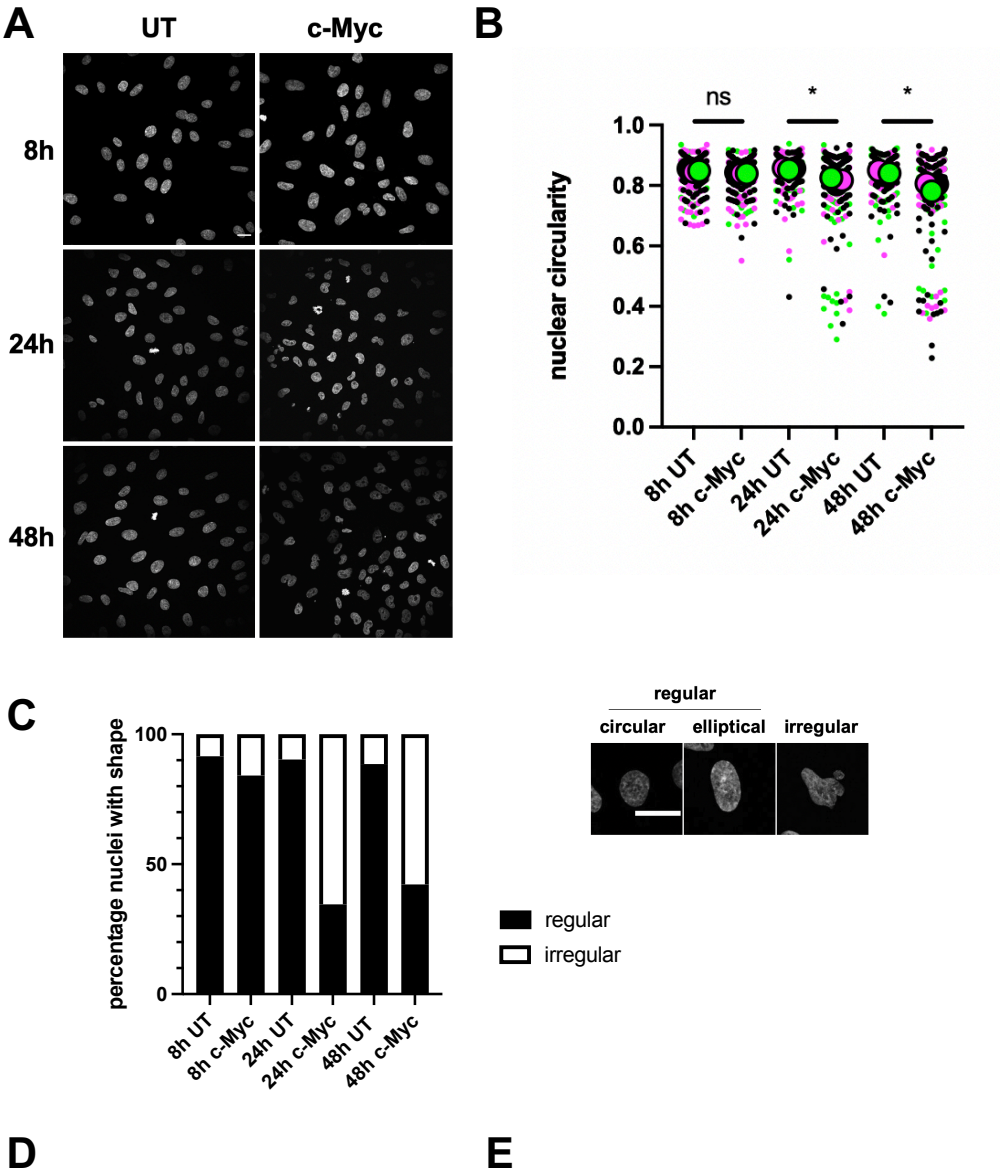

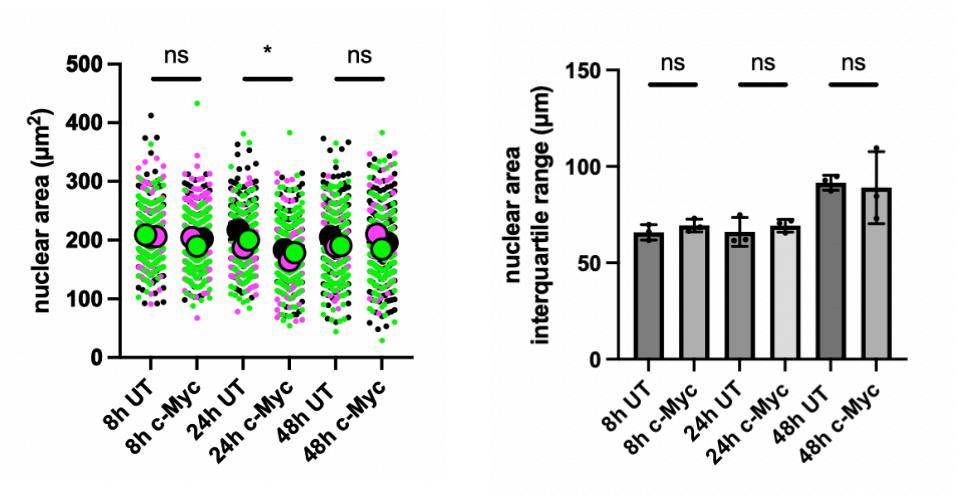

Figure 3.2 (previous): c-Myc induction causes acute changes to nuclear morphology. **(**A) RPE-1 c-Myc ER cells were untreated (UT) or treated with tamoxifen (c-Myc) for 8h, 24h and 48h before fixation, nuclear staining with Hoechst and imaging via immunofluorescence. Representative images were taken from n = 3 independent experiments, c. 100-200 cells per experiment. Scale bar = 20 µm. (B) Column scatter graph of nuclear circularity of the same cells at 8h, 24h and 48h with or without c-Myc activation. Each colour represents a separate independent experiment (black, magenta, green, n = 3, 100-200 cells per condition per experiment). Large coloured circles represent mean values per experiment. Small circles represent individual cells per independent experiment. (C) Bar graph indicating percentage of nuclei that displayed either regular (a combination of circular and elliptical shapes) or irregular morphologies, as determined by visual scoring with examples of nuclei in each category shown to the right. Scale bar = 20 µm. Representative of n = 3. (D) Column scatter graph of nuclear area (µm^2) of the same cells at 8h, 24h and 48h with or without c-Myc activation. Each colour represents a separate independent experiment (black, magenta, green, n = 3, 100-200 cells per condition per experiment). Large coloured circles represent mean values for nuclear area per experiment, small circles represent individual cells per independent experiment. (E) Bar graphs showing total interquartile range of areas of same cells at 8h, 24h and 48h with or without c-Myc activation. All graphs show mean ± SD. Representative of n = 3. All statistical analyses were performed using a paired student's t-test on mean values of circularity, area and interquartile range between conditions. (* $p < 0.05$, ** $p < 0.01$, *** $p < 0.001$, **** $p < 0.0001$).

3.2 c-Myc induction causes changes to the composition of the nuclear lamina and cytoskeleton.

Having established that c-Myc activity causes acute and significant changes to nuclear morphology, I next wanted to investigate potential causes for these changes. As previously discussed, there are three main canonical determinants of nuclear mechanics and therefore nuclear morphology: the nuclear lamina, the cytoskeleton and chromatin. I decided to first investigate the composition of the NE and see whether there were any alterations to the levels of NE proteins that contribute towards the maintenance of nuclear structure.

To measure this, I first performed an RT-qPCR to measure the levels of mRNA transcripts of genes coding for components of the nuclear lamina, as well as cytoskeletal proteins actin and tubulin on c-Myc activation at 24h and 48h (Figure 3.3). I used the levels of *eIF4E* as a positive control, since it is a well-established c-Myc target gene whose levels increase several-fold on c-Myc activation (Ruggero 2009). We see a significant increase in *eIF4E* transcript levels at both 24h and 48h following addition of tamoxifen, indicating c-Myc has been activated and is functioning as expected. We can then see that there is a significant reduction in levels of *LMNA* and *LMNB1* mRNA transcript at both time points on c-Myc activation, with *LMNA* being reduced to around half the levels of untreated cells after 48h. c-Myc activity's effects on *LMNB2* transcript levels were more variable, where levels show a slight increase at 24h before appearing to return to untreated levels after 48h following c-Myc activation. Overall, this data suggests that c-Myc activity has a direct effect on inducing alterations to transcript levels of lamina proteins that are normally found underneath the NE and help maintain nuclear integrity and nuclear function. The reduction in levels of mechano-protective *LMNA* transcript, as well as *LMNB1*, involved in maintaining nuclear elasticity following deformation (Lammerding et al., 2006) is especially striking and warrants further investigation as possible mediators of c-Myc's effects on dysregulated nuclear morphology. *LMNB2* is a less well studied isoform, though there is some recent evidence suggesting it supports lamin A/C in modulating nuclear deformability (Vortmeyer-Krause et al., 2020) and its slight increase at 24h could reflect a compensatory response of the nucleus to c-Myc induced decreases in the other two isoforms.

Furthermore, we can see that c-Myc activity resulted in significant decreases in cytoskeletal transcript levels of certain key actin and tubulin subunits, with significant reductions in both *ACTB* (beta-actin) and *TUBA1A* (tubulin-1-alpha) at both timepoints. This suggests that c-Myc can also induce a dysregulated transcription of cytoskeletal proteins as well as those found within the nucleus proper, likely through inducing a global transcriptional imbalance due to its pleiotropic actions as a master regulator. The implications for such decreases towards cytoskeletal dynamics remains unclear but hints at its importance.

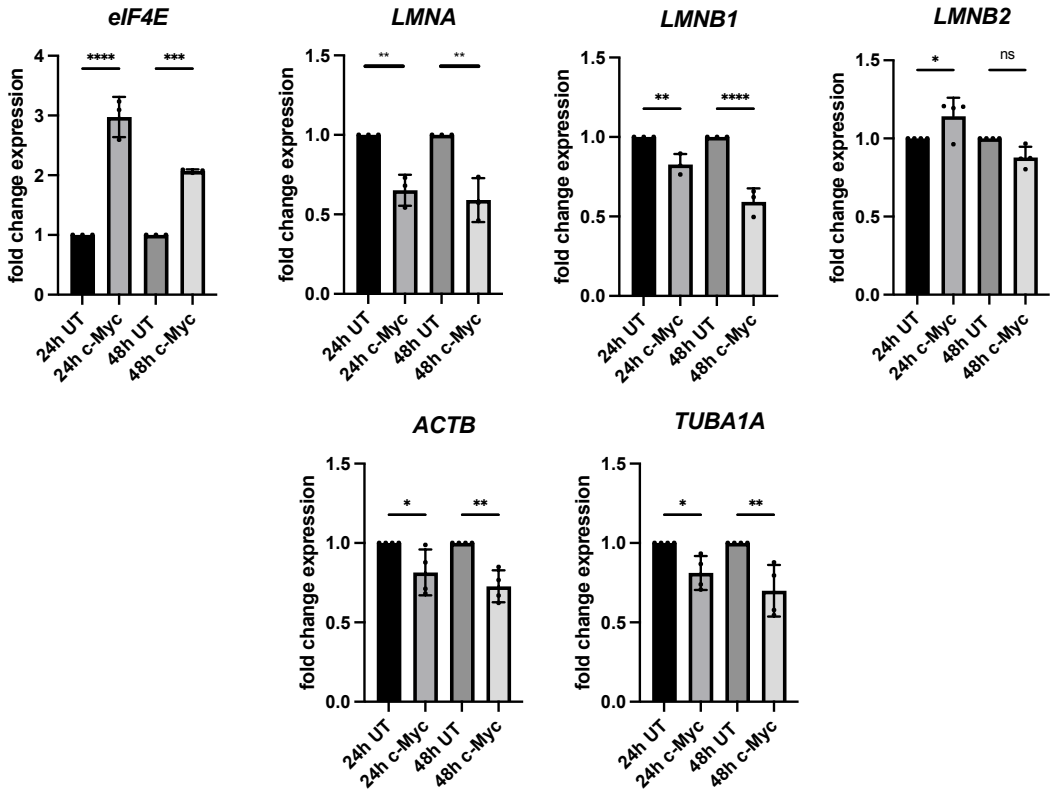

Figure 3.3: c-Myc induction causes reductions in transcript levels of key proteins in the nuclear lamina and cytoskeleton. RPE-1 c-Myc ER cells were untreated (UT) or treated with tamoxifen (c-Myc) for 24h and 48h. Quantifications of fold change in mRNA levels of *LMNA, LMNB1, LMNB2, ACTB* and *TUBA1A*. *eIF4E* is included as a positive control, representing a target gene whose transcription is upregulated on c-Myc activation. All graphs show mean ± SD. Representative of n = 3 separate biological replicates, except for *LMNB2* where n = 4. All statistical analyses were performed using a one-way ANOVA (* $p < 0.05$, ** $p < 0.01$, *** $p < 0.001$, **** $p < 0.0001$).

Following on from this, I measured the corresponding protein levels of the above transcripts except lamin B2 (due to lack of antibody availability) via Western blot at the same two timepoints to investigate whether they reflect the changes seen in transcript levels (Figure 3.4). 3.4A and 3.4B confirm this to be the case and both show that these largely recapitulate the changes in mRNA transcript levels I saw using RT-qPCR. c-Myc activation causes significant reductions in lamin A, beta-actin and beta-tubulin protein levels at both timepoints, whilst lamin B1 shows a slight decrease at 24h, which becomes a significant reduction by 48h.

One thing to note here is that I have looked at beta-tubulin protein levels, whereas in the previous figure I have measured mRNA transcript levels of alpha-tubulin. The two isoforms are usually found at a 1:1 stoichiometry within microtubules and so it is expected that a decrease in one would reflect a decrease in another, though without direct measurement of either alpha-tubulin protein or beta-tubulin mRNA levels this is

not a firm conclusion. Overall however put together, this data indicates that c-Myc causes reductions in both transcript and protein levels of the genes investigated. It also hints at a potential mechanism for these changes as being transcriptional rather than translational in nature.

Next, I wanted to see whether c-Myc activity caused any significant alterations in a panel of other key NE proteins, to shed light on which candidates on which to focus as the most significant contributors to nuclear morphology alterations.

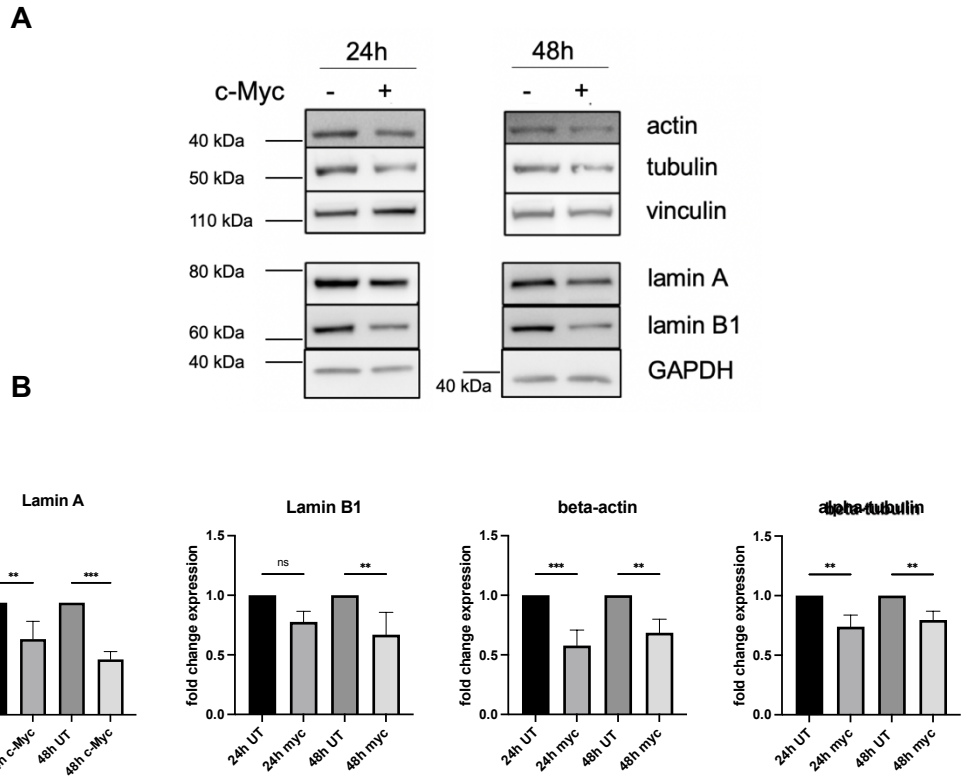

Figure 3.4 (previous): c-Myc induction causes reductions in protein levels of key components of the nuclear lamina and cytoskeleton. (A) RPE-1 c-Myc ER cells were untreated (UT) or treated with tamoxifen (c-Myc) for 24h and 48h. Whole cell lysates were taken from cells at and samples probed for protein levels of lamin A, lamin B1, beta-actin and beta-tubulin. Vinculin and GAPDH were used as loading controls. Representative blot from n = 3. (B) Quantifications of band intensities as proxy for protein expression levels of lamin A, lamin B1 (normalised to GAPDH), beta-actin and alpha-tubulin (normalised to vinculin) with or without c-Myc activity. Fold change was obtained by calculating the ratio of intensities of target protein between UT and c-Myc conditions. All graphs show mean ± SD. Representative of n = 3. All statistical analyses were performed using a one-way ANOVA (* $p < 0.05$, ** $p < 0.01$, *** $p < 0.001$, **** $p < 0.0001$).

3.3 c-Myc induction causes changes to the protein composition of the nuclear envelope (NE).

Finally, I used RT-qPCR to measure transcript levels of other key NE proteins on c-Myc activation at the same two timepoints (Table 3.1). These were four isoforms of the LINC complex (*SUN1, SUN2, SYNE1, SYNE2*) as well as INM proteins emerin (*EMD*), plectin (*PLEC*), lamin B receptor (*LBR*), LEM-domain containing protein-3 (*MAN1*) and barrier to autointegration factor 1 (*BANF1*). All of these proteins have been implicated in the maintenance of regular nuclear function, and there is evidence linking their dysregulation in a cancer context.

As discussed previously, the LINC complex is key to nuclear mechanotransduction and cytoskeletal organisation. SUN1/2 are a candidate for anti-tumour therapy (Chen et al., 2019), due to its roles in attenuating DNA damage and maintaining genome stability (Lei et al., 2012). Nesprin-1 mutation or depletion has been linked to altered nuclear shape, increased GIN and alterations to the DNA damage response (Sur et al., 2014, Sur-Erdem et al., 2020). Nesprin-2 has roles in cellular migration, though its roles if any in cancer are unclear.

Emerin is perhaps the second most well studied lamin A/C binding partner protein, with roles in the regulation of gene expression, mechanotransduction, cell signalling and nuclear architecture. Importantly, there is growing evidence implicating it in the maintenance of nuclear morphology in cancer, with a recent study linking its deregulation to nuclear shape instability and an increase in metastatic potential (Reis-Sobrero et al., 2018). Man1 is a similar Lem domain protein, though its functions are far less well studied. Within a cancer context however, it has been shown to be a negative regulator of TGF-β signalling and thus a candidate for anti-cancer treatments.

Banf1 (similar to lamin A/C) has been linked to the maintenance of nuclear integrity specifically during migration (Halfmann et al., 2019), with depletions in Banf1 increasing the frequency of NE ruptures during migration. Of additional interest, it also has roles in mediating membrane repair following NE rupture (Denais et al., 2016), meaning its loss would increase the levels of DNA damage and GIN, potentially leading to catastrophic cell death in migrating cells. Lamin B receptor (LBR) protein is a lamin B1 binding partner and is shown to play a role in post-mitotic NE reassembly and heterochromatin organisation, where its loss can lead to changes in chromatin

organisation and cellular senescence following irradiation (Lukasova et al., 2017). Plectin is especially important in regulating cytoskeletal dynamics and thus nuclear mechanics. Disruption of keratin network through plectin loss has been shown to cause increased actomyosin contractility, leading to greater nuclear deformations (Almeida et al., 2015). In addition, plectin overexpression has been used as a cancer biomarker for pancreatic ductal carcinoma (PDAC).

Protein Family	Gene	Protein	Notes/Location
SUN domain proteins	*SUN1*	Sun1	Component of LINC complex (spans INM)
	SUN2	Sun2	Component of LINC complex (spans INM)
KASH domain proteins	*SYNE1*	nesprin-1	Component of LINC complex (spans ONM)
	SYNE2	nesprin-2	Component of LINC complex (spans ONM)
LEM domain proteins	*EMD*	emerin	INM protein
	MAN1	Man1	INM protein
BAF	*BANF1*	Banf1	INM protein
Tudor domain protein	*LBR*	Lamin B receptor	INM protein
Plakin	*PLEC1*	Plectin-1	Cytolinker, variable localisation

Table 3.1: Summary of NE proteins investigated.

We can see from Figure 3.4 that c-Myc's effects on transcript levels of these proteins is variable, reflecting both the complex regulatory networks that govern their expression levels and the pleiotropic nature of c-Myc activity in controlling and influencing many target genes.

There were significant reductions in *SUN2* mRNA levels at both timepoints, as well as *LBR* at 48h, as well as strikingly significant increases in *EMD* levels at both timepoints. *SUN1* showed slight but not significant upregulation at both timepoints, and the levels of the remaining transcripts *SYNE1, SYNE2, PLEC, MAN1* and *BANF1* remain unchanged at both 24 and 48h.

Of these findings, the most intriguing represent the upregulation of emerin mRNA and the downregulation of SUN2. Whilst there is currently no evidence suggesting emerin is a c-Myc target gene, it would be an attractive mechanism to explain such an

increase in transcription 24h after c-Myc activation. However, given c-Myc's direct transcriptional upregulation of its target genes takes place on the order of hours (Butt et al., 2008), further experiments to validate this would be necessary. Firstly, an investigation into levels of *EMD* transcript at an earlier timepoint (e.g., 8h post c-Myc induction) and secondly, a ChIP-seq study to identify cites of potential c-Myc binding in the emerin promoter region. Overall, emerin has a plethora of roles that can all contribute towards increasing a cell's invasiveness and deregulating is nuclear morphology, indicating it to be a promising mediator of c-Myc induced dysregulation of nuclear morphology.

SUN2 silencing represents a trickier phenomenon to explain, since the functional differences between it and SUN1 are currently unclear. There is some evidence they play partially redundant roles in nuclear anchorage (Lei et al., 2009) and possibly DDR (Lei et al., 2012) but untangling their individual contributions towards nuclear morphology and GIN, as well as understanding why c-Myc seems to upregulate one but silence the other, is likely more complex than focusing on the previously observed changes to the lamina, cytoskeleton and emerin.

Having established a broad set of phenotypes in the levels of NE proteins following c-Myc activation, I next wanted to see whether any of these significant changes were reflecting in alterations to their localization within the nucleus proper. To do this, I first focused on the lamina proteins lamin A and B1, as they have well-designed antibodies, well-characterised distributions under physiological conditions and show some of the largest reductions in mRNA and protein levels.

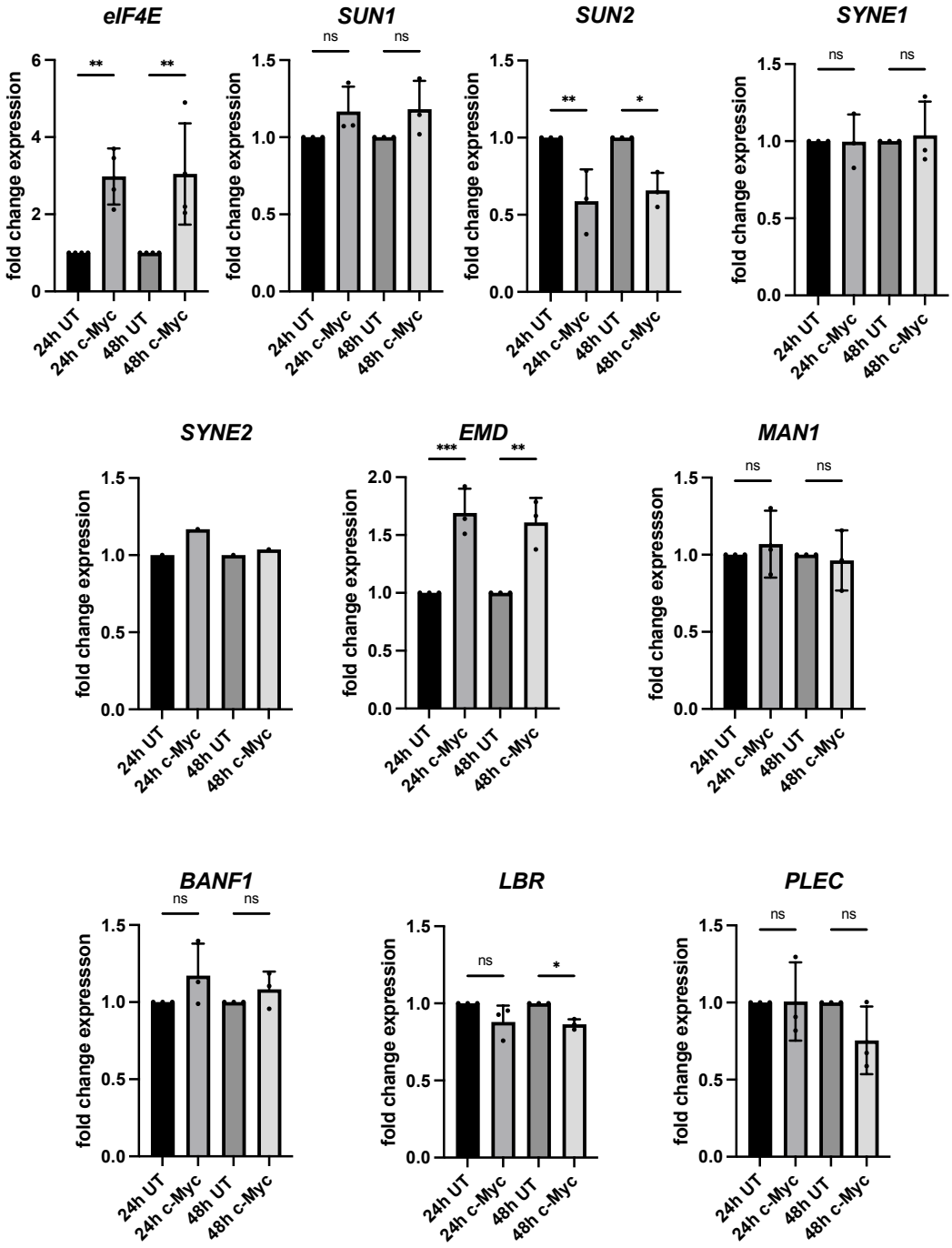

Figure 3.5: c-Myc activity alters the levels of a subset of NE proteins. RPE-1 c-Myc ER cells were untreated (UT) or treated with tamoxifen (c-Myc) for 24h and 48h. Quantifications of fold change in mRNA levels of key NE proteins. *eIF4E* is included as a positive control. All graphs show mean ± SD. Representative of n = 3 independent experiments except for *eiF4E* where n = 4 and *SYNE2* where n = 1. All statistical analyses were performed using a one-way ANOVA (* $p < 0.05$, ** $p < 0.01$, *** $p < 0.001$, **** $p < 0.0001$).

3.4 c-Myc induction causes changes to the localization of lamins A and B1.

To assess lamin localisation, I next performed fixed-cell immunofluorescence on c-Myc induced cells, which were fixed at 24 and 48h, stained for lamin A and B1 (Figure 3.6).

3.6A confirmed the phenotype I first observed in 3.1A that c-Myc causes changes to nuclear morphology at both timepoints. Under untreated conditions, lamins are distributed regularly throughout the nucleus (3.6B), with a very thin area of high intensity around the nuclear edge (the lamina) and a 'mobile pool' found throughout the nuclear centre (nucleoplasm). c-Myc activation led to dramatic changes in the localization of both lamin A and B1 throughout the nucleus. Particularly prominent are the sections indicated by the white arrowheads, which indicate sections of the nuclear lamina where lamins are absent. These can occur both in conjunction with an absence or presence of DNA. The former could indicate direct chromatin herniation or leakage into the cytoplasm, whilst the latter the beginning of a potential NE rupture event, which often starts as discussed with a small break in the continuity of the lamina. Both can lead to increases in DNA damage and GIN and contribute towards oncogenesis.

To quantify the degree of nuclear mislocalisation I see in my images, I used two approaches (3.6B). For nucleoplasmic localisation, eroded masks of nuclei excluding the lamina were taken and standard deviations of intensity values measured as proxies for degree of mislocalisation, with larger values representing more heterogeneity. Laminar mislocalisation proved more challenging, as the thickness of the lamina itself was not sufficient to automate a process that reliably acquired annular sections excluding the cytoplasm. Instead, a line selection along the longitudinal axis across the nucleus was taken. A profile of mean intensities across the line was created and the ratio of the intensity values on opposing peaks were calculated. A ratio of 1 represents a uniform distribution, as both peaks have the same intensity value; decreases represent increasing laminar heterogeneity.

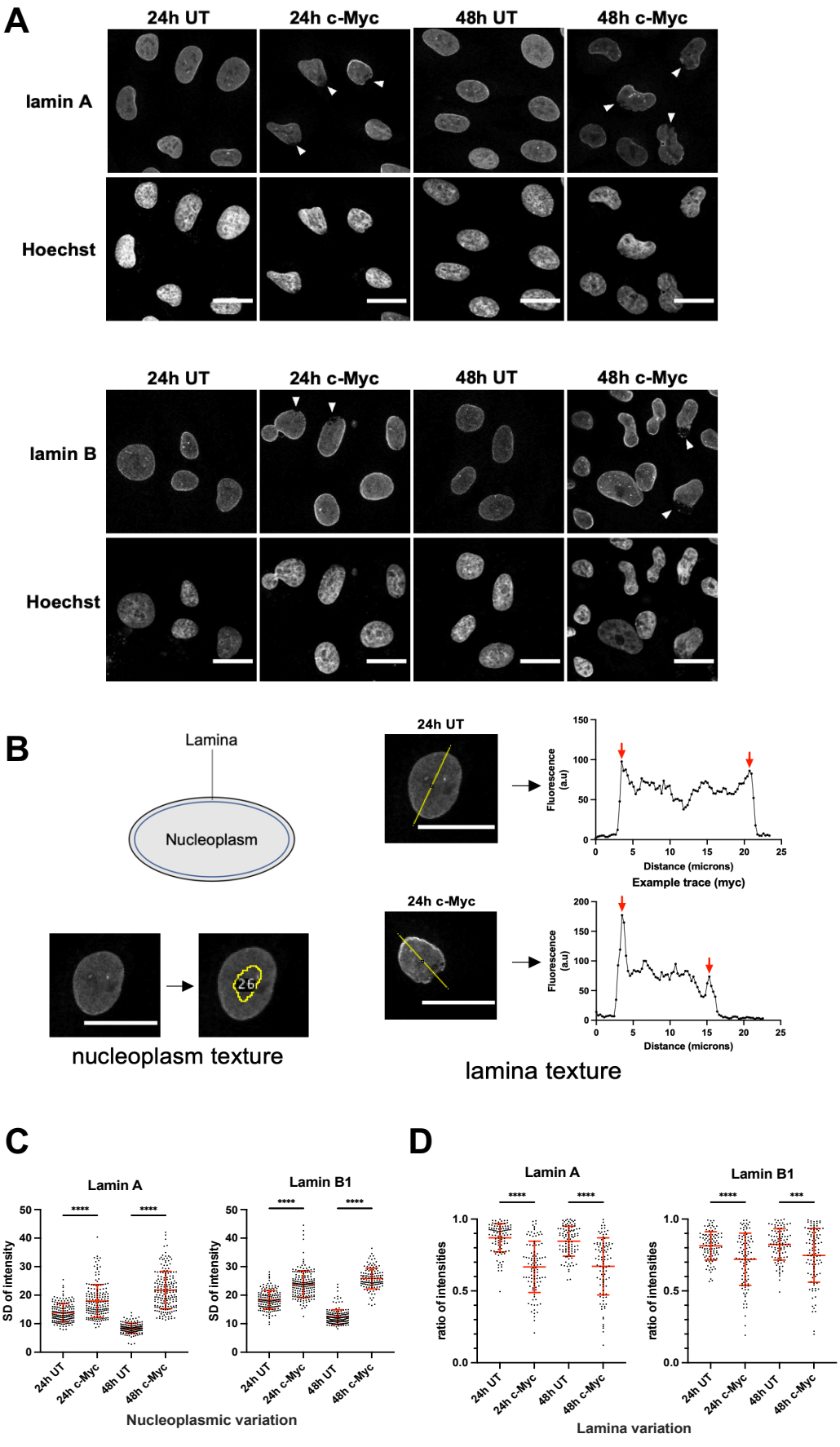
A
24h UT
24h c-Myc
48h UT
48h c-Myc
lamin A
Hoechst
lamin B
B
Lamina
Nucleoplasm
nucleoplasm texture
24h UT
24h c-Myc
Fluorescence (a.u)
Distance (microns)
Example trace (myc)
lamina texture
C
Lamin A
Lamin B1
SD of intensity
Nucleoplasmic variation
D
ratio of intensities
Lamina variation

Figure 3.6 (previous): c-Myc induction causes mislocalisation of lamins A and B1. (A) RPE-1 c-Myc ER cells were untreated (UT) or treated with tamoxifen (c-Myc) for 24h and 48h before fixation, nuclear staining with Hoechst/antibodies against lamin A and B1 and imaging via immunofluorescence. White arrowheads indicate areas in the lamina where lamins are absent from nucleus despite presence of nuclear DNA as indicated by Hoechst. Scale bar = 20 μm. (B) Schematic indicating two sections of nucleus: lamina and nucleoplasm and how variation in each was quantified. Scale bar = 20 μm. (C) Column scatter graphs of the SD of nucleoplasm intensity values for cells at 24h and 48h with or without c-Myc induction. Representative of n = 3, 150-200 cells per experiment. (D) Column scatter graphs of lamina peak ratio values for cells at 24h and 48h with or without c-Myc induction. Representative of n = 3, 100 cells per experiment. All graphs show mean ± SD. All statistical analyses were performed using a one-way ANOVA (* $p < 0.05$, ** $p < 0.01$, *** $p < 0.001$, **** $p < 0.0001$).

We can see from 3.6C that c-Myc induction led to significant increases in nucleoplasmic mislocalisation for lamin A and B1 at both timepoints. This was shown by significant increases in nucleoplasmic heterogeneity. 3.6D shows corresponding significant decreases in the ratio of values represent laminar intensities, in both proteins and at both timepoints. These also therefore indicate c-Myc induction causes a significant mislocalisation of laminar protein as well. Taken together, this shows that c-Myc activation causes rapid changes to both the levels and localisation of the two key lamin proteins A and B1, with direct implications both for nuclear morphology and possible downstream genome stability.

3.5 c-Myc activation causes an upregulation and mislocalisation of emerin.

I next wanted to return to my results in Figure 3.5 and investigate the most striking of the changes seen on c-Myc activation in the qPCR screen of NE protein levels: namely, the upregulation of the *EMD* transcript at both 24 and 48h post c-Myc induction.

I first performed the analogous experiment to Figure 3.4, probing for emerin protein. 3.7A shows that c-Myc induction caused increases in its levels at both 24 and 48h relative to untreated cells. I next wanted to see whether this is reflected in any changes to its nuclear distribution, as seen from immunofluorescence, stained against emerin. 3.7B and 3.7C show a striking and significant increase in emerin signal intensity at both timepoints following c-Myc activation.

The nature of emerin localization was also drastically altered. In untreated cells it is located within the NE, with a small cytoplasmic pool just outside the ONM (3.7B). On c-Myc activation however it is upregulated both within the NE and the cytoplasm, with areas of cytoplasmic emerin clustering ('perinuclear emerin') forming near some nuclei, as shown by the white arrowheads. This is seen from 3.7D, which quantifies the percentage of nuclei with perinuclear emerin clusters, which increases from 2% to 15% at 24h and from 4% to 41% at 48h, a trend seen across three separate experiments. These perinuclear emerin clusters appear to be localized in areas of high local membrane curvature, where the nuclei appear to be experiencing local deformations; raising the intriguing possibility that they represent a cellular response to an increase in nuclear fragility brought about by the global silencing of lamins A and B1. This will be discussed in the next chapter.

One aspect to note with the emerin staining observed in this experiment was that there was a moderate level of diffuse emerin staining (background), even within areas of the cytoplasm further away from the NE. A necessary follow-up would be to first find an optimal (lower) concentration of primary emerin antibody that minimizes this background staining whilst still maintaining a strong signal at or near the NE; the experiment can then be repeated using this new concentration of antibody.

In addition to titrating the primary antibody to determine optimal concentrations for signal to noise ratio, there are several additional steps that would improve the results of this experiment. Antibodies were validated by confirming their expected molecular weight (through Western blot) and expected subcellular localization (through immunofluorescence microscopy). However, the high background signal seen in the emerin staining shows that further optimization of staining conditions could have been performed. This would involve titrating concentrations of BSA and secondary antibody, again to minimize background signal.

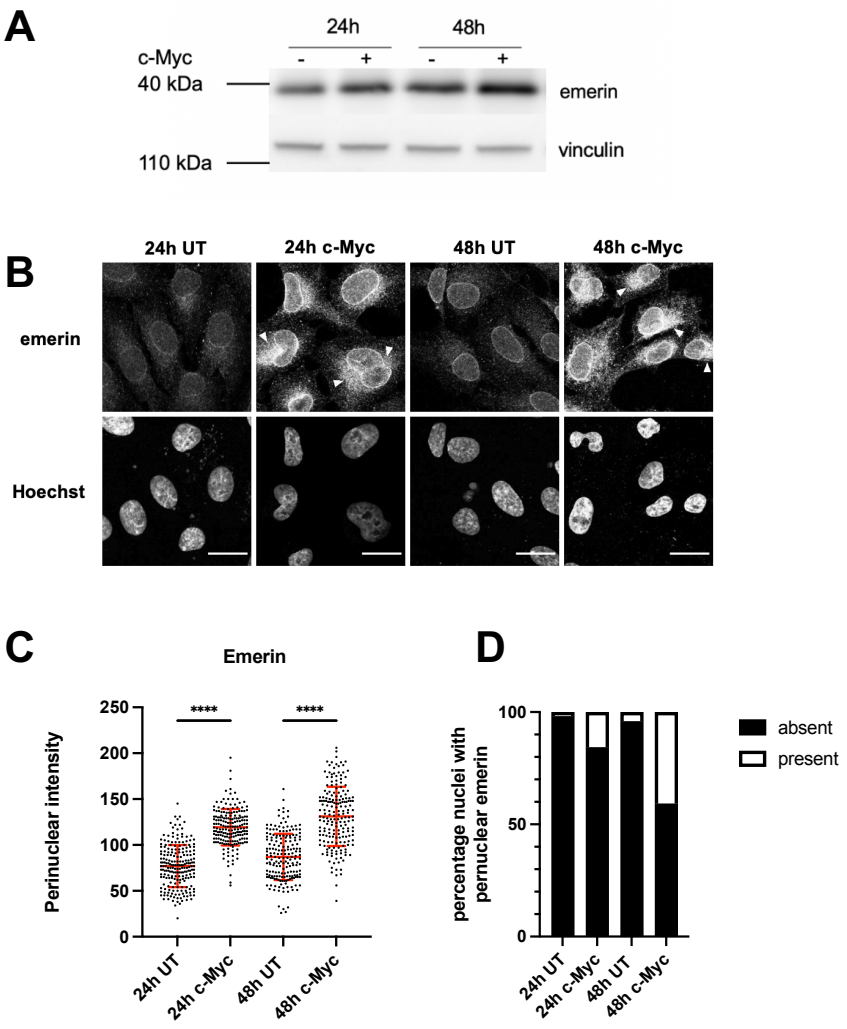

Figure 3.7: c-Myc activation causes an upregulation and mislocalisation of emerin. (A) RPE-1 c-Myc ER cells were untreated (UT) or treated with tamoxifen (c-Myc) for 24h and 48h before analysis by Western blot. Representative blot from n = 2. (B) Representative immunofluorescence images taken from cells either with or without c-Myc activity at 24h and 48h, stained for emerin/Hoechst. White arrowheads indicate areas of particularly high perinuclear emerin that form distinct clusters proximal to the NE. Scale bar = 20 μm. (C) Column scatter graphs of emerin intensity values for cells at 24h and 48h with or without c-Myc induction. Representative of n = 3, c. 150 cells per experiment. All graphs show mean ± SD. Statistical analysis was performed using a one-way ANOVA (* $p < 0.05$, ** $p < 0.01$, *** $p < 0.001$, **** $p < 0.0001$). (D) Bar graph indicating percentage of nuclei that had perinuclear emerin clusters present or absent as determined by visual scoring, representative of n = 3.

Having established a key set of phenotypes produced with c-Myc activity, I then wanted to see whether silencing lamin A alone was enough to recapitulate downstream phenotypes commonly seen shortly after c-Myc activation.

3.6 Lamin A silencing recapitulates phenotypes caused by c-Myc induction.

Given the central role that lamin proteins, particularly A-type lamins play in nuclear structure, as well as processes such as DNA transcription, replication and signaling, it is likely that reduced lamin A levels serves to be the most significant contributor towards c-Myc induced increases in DNA damage and genome instability, as well as its induction of abnormal nuclear morphologies. As such, I transfected cells with either non-targeting siRNA (siControl) or siRNA against *LMNA* (siLMNA) and imaged samples 24h and 48h following silencing.

Given the abundance of evidence linking lamin A depletion to irregular nuclear morphology, 3.8A shows perhaps unsurprisingly that *LMNA* silencing alone leads to this, as seen by significant reductions in nuclear circularity (3.8B) and nuclear area (3.8C) at both timepoints. The reduction in nuclear area seen at 48h of *LMNA* silencing is interesting, as this is not seen with c-Myc activation. There are several possible explanations for lamin depletion induced decreases in average nuclear area. The first is that given lamin A's role in protecting pRB from degradation (Johnson et al., 2004), its depletion may lead to decreases in Rb levels, allowing cells to pass the G1/S transition in the presence of DNA damage without undergoing arrest. As a result, cells could accelerate through the cell cycle, leading to a shorter interphase and less time for the nuclei to grow before mitosis. A second simpler but unexplored theory is that since lamin A synthesis needs to keep up with the rate of nuclear growth during G1 and G2 phase to allow more lamin A to be deposited at the NE, silencing *LMNA* would reduce synthesis rates, imposing a limiting factor on how large the nuclei themselves can grow before the cells undergo mitosis; resulting in smaller nuclei on average.

Finally, I wanted to investigate whether silencing *LMNA* would lead to the same increases in replication stress and DNA damage seen with c-Myc activation 24 and 48 hours after induction. I therefore analysed whole cell lysates of silenced and control cells and probed for markers of replication stress (pRPA-S33), DNA damage (pγH2AX S139) and activation of the DNA damage response (pRPA-S4/8). I found an increase in all three markers at both timepoints following *LMNA* silencing, supporting the idea that c-Myc induced lamin A silencing was a significant contributor towards downstream increases in GIN via increases in DNA damage and replication stress (RS).

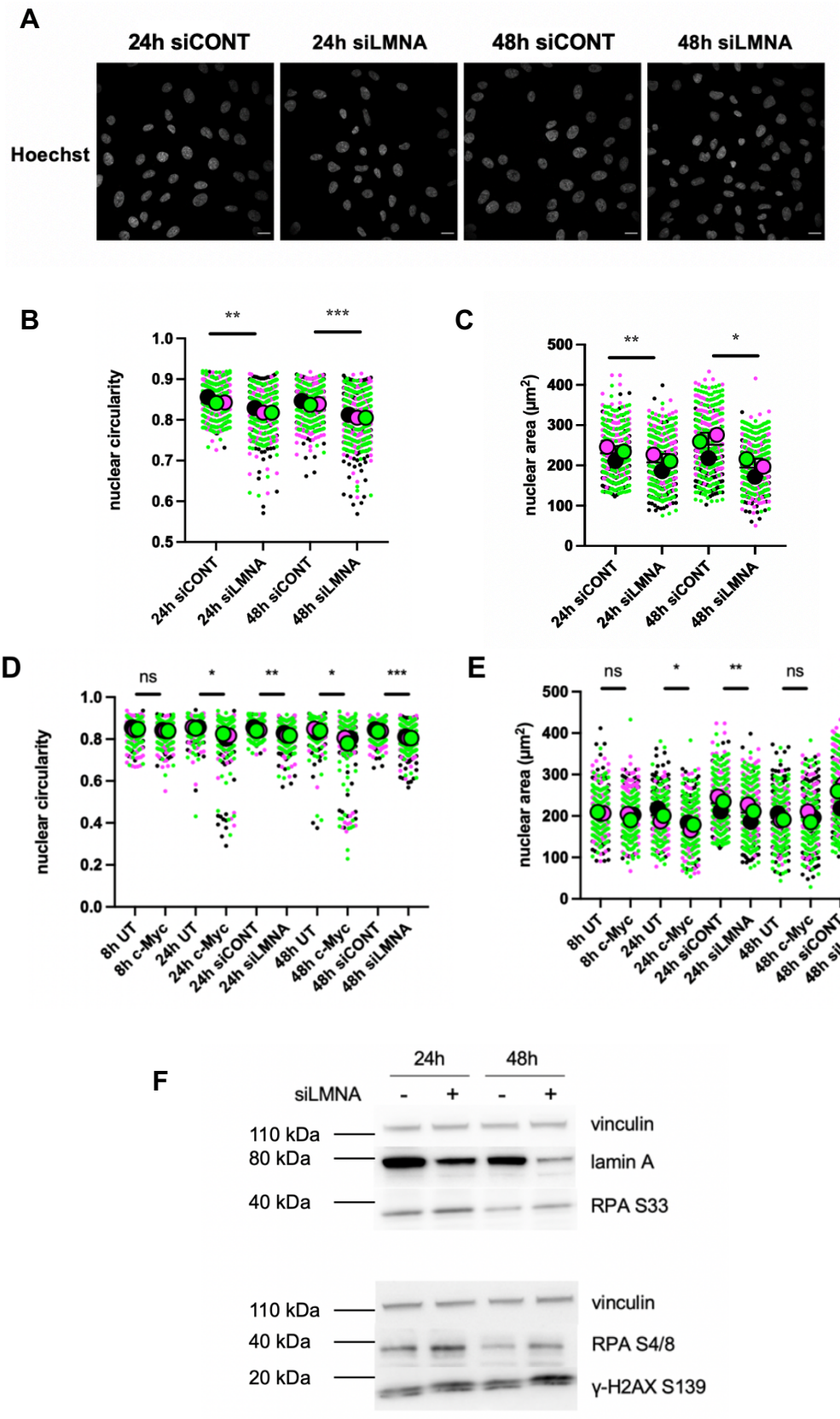
A
24h siCONT
24h siLMNA
48h siCONT
48h siLMNA
Hoechst
B
nuclear circularity
1.0
0.9
0.8
0.7
0.6
0.5
**
***
24h siCONT
24h siLMNA
48h siCONT
48h siLMNA
C
nuclear area (µm²)
500
400
300
200
100
0
**
*
24h siCONT
24h siLMNA
48h siCONT
48h siLMNA
D
nuclear circularity
1.0
0.8
0.6
0.4
0.2
0.0
ns
*
**
*
***
8h UT
8h c-Myc
24h UT
24h c-Myc
24h siCONT
24h siLMNA
48h UT
48h c-Myc
48h siCONT
48h siLMNA
E
nuclear area (µm²)
500
400
300
200
100
0
ns
*
**
ns
*
8h UT
8h c-Myc
24h UT
24h c-Myc
24h siCONT
24h siLMNA
48h UT
48h c-Myc
48h siCONT
48h siLMNA
F
24h
48h
siLMNA
-
+
-
+
110 kDa
80 kDa
40 kDa
vinculin
lamin A
RPA S33
110 kDa
40 kDa
20 kDa
vinculin
RPA S4/8
γ-H2AX S139

Figure 3.8 (previous): Lamin A silencing recapitulates downstream phenotypes seen on c-Myc activation. (A) Representative images of RPE-1 c-Myc ER cells were treated with non-targeting (siCONT) or siLMNA for 24h and 48h. Scale bar = 20 μm. (B, C) Column scatter graph of nuclear circularity (B) and nuclear area (C) of the same cells at 24h and 48h with or without lamin A silencing. Each colour represents a separate independent experiment (black, magenta, green, n = 3, 100-200 cells per condition per experiment). Large coloured circles represent mean values per experiment. Small circles represent individual cells per independent experiment. All graphs show mean ± SD. All statistical analyses was performed using a paired student's t-test on mean values of circularity and area between conditions. (* $p < 0.05$, ** $p < 0.01$, *** $p < 0.001$, **** $p < 0.0001$). (D, E): Column scatter graphs of nuclear circularity (D) and area (E) compared to data from Fig 3.2 (with and without c-Myc activation). (F) . Representative blot of cells probed for replication stress (RS) markers pRPA S4/8 and S33 and DNA damage marker pγH2AX S139. Representative of n = 3.

These results are again perhaps unsurprising as studies have shown that lamin A depletion leads to impaired restart of stalled forks during RS as an initial step in DNA repair via HR (Singh et al., 2013). Recent work has also shown lamin A plays a role in base excision repair (Maynard et al., 2019), providing further evidence that its depletion would lead to accumulations of DNA damage as seen in γH2AX phosphorylation.

3.7 Summary

In this chapter I have shown the wide range of effects that c-Myc activity has both on nuclear architecture and nuclear morphology, mainly through its alterations in the expression levels and localisations of key NE proteins that are involved in the maintenance of regular nuclear function and shape (summarized Figure 3.9). They represent the first direct evidence linking acute oncogenic c-Myc activity to changes to nuclear morphology. I found that c-Myc activation leads to significant reductions to nuclear circularity and shape, as well as changes to nuclear area at 24 hours post c-Myc activation. I then found that c-Myc activity causes decrease in lamins A, B1, actin and tubulin within the cell at both the transcript and protein level. Expanding the scope of investigation to other NE proteins, I found that the INM protein emerin and LINC complex protein SUN2 display significant alterations in their transcript levels.

I then investigated the localisations of lamins A and B1 and found them to be mislocalised throughout the nucleus at both the periphery and the centre. Emerin protein was similarly upregulated and mislocalised, with intriguing deposits of perinuclear emerin found at certain sites of membrane deformation. Finally, I found that lamin A depletion alone in cells untreated with tamoxifen was sufficient to produce several downstream markers of c-Myc induced oncogenesis, including an increase in

DNA damage, activation of the DNA damage response and an increase in replication stress.

Lamin A is by far the most well studied NE protein due to its many roles in nuclear structure and mechanics, as well as nuclear processes such as DNA damage repair which have important implications in disease contexts such as cancer. As such, I decided to narrow down to c-Myc induced lamin A silencing as a promising contributor of c-Myc induced changes to nuclear architecture. My next salient questions (as seen in Figure 3.9) are the mechanisms by which c-Myc silences lamin A at the mRNA and protein level (A) and the pathway by which this silencing translates into mislocalisation within the nucleus (B). These will both be addressed in Chapter 4.

It is important to note several controls that would first need to be implemented for the results of these experiments to be further validated. Firstly, while c-Myc activity on 4-OHT addition was verified by observing upregulation of target genes when the cell line was first created in the lab, it is key to test whether this is still the case while conducting my own set of studies. To do this, mRNA levels of c-Myc target genes (*eIF4E* and *CCNE*) should be measured in c-Myc-ER cells on 4-OHT addition, and levels and localization of c-Myc should be directly visualized using immunofluorescence microscopy to verify that nuclear c-Myc levels increase as expected. A fractionated western blot of c-Myc should also be taken to verify an increase in c-Myc levels within the nuclear fraction on 4-OHT addition.

A negative control should also be added to rule out any effects caused by addition of 4-OHT alone; this would involve the addition on RPE1 cells that do not contain the c-Myc ER fusion protein (RPE1 ER-empty cells, described previously) and checking whether nuclear morphology remains unchanged at every timepoint post 4-OHT addition. An additional insight that would be generated with this control is the direct comparison between the nuclei of ER-empty cells and c-Myc ER cells that have not had 4-OHT added. If there is no significant diffnerence in morphology between the two conditions, this would verify that the nuclei of untreated c-Myc ER cells are not significantly affected by any basal c-Myc activity that may be seen through a c-Myc western blot of untreated c-Myc ER cells.

Another area for optimization would be further validation of the antibodies used for the immunofluorescence visualization of protein localization. This is especially the case for Fig 3.7, which studied emerin localization as all conditions (including

untreated cells) had a moderate level of background staining on the cytosolic side of the nuclear envelope, where emerin is not usually found (as it is localized on the nucleoplasmic side of the NE). Titration of antibody concentration to find a set of conditions that minimizes this background signal but retains strong signal around the NE is an important next step in cleaning up this diffuse signal.

Finally, several controls should be added to Fig 3.8, which investigated the impact of lamin A transcript silencing on downstream nuclear morphology, replication stress and DNA damage. Firstly, a vehicle control where cells are treated with transfection reagent (Lipofectamine RNAiMAX) but not with siRNA is needed to verify that the transfection agent itself is not causing any phenotypic changes to the cells by itself. This can be done by comparing nuclei from cells treated with the vehicle control to cells that were untreated with any transfection reagent or siRNA during the same timeframe and checking that there is no significant difference in nuclear morphology and levels of DNA damage and replication stress markers between the two conditions. Off-target controls can also be further minimized; the experiment used Smartpool siRNA, which uses four separate lamin A specific siRNAs in a single pool that reduces individual siRNA concentrations and reduces the risk of off-target effects. It is important to note however that since Smartpool reagents contain four separate oligonucleotides that target different parts of the target mRNA, there is a higher probability of cumulative off-target effects arising from the four sequences, despite the lowered concentration of each of the individual sequences. As a result, the usage of individually designed siRNAs with high specificity to the target sequence within the target mRNA is a way to further reduce the risk of off-target effects. However, usage of individual sequences may lead to a lowered knockdown efficacy of the target gene compared to combination treatments such as Smartpool. In addition, each sequence requires careful validation of knockdown efficacy at different concentrations before usage in experiments. The best solution to the reduction of off-target effects whilst achieving knockdown would therefore be the use of one or two validated sequences that target a smaller number of sequences but have been shown to achieve adequate knockdown.

A further way to validate that the phenotype seen was due specifically to lamin A silencing would be to perform a simultaneous RT-qPCR on *LMNA* transcript levels 24h and 48h after *LMNA* silencing to verify whether silencing was indeed occurring alongside the observed phenotypic changes. RT-qPCR on *LMNA* transcript levels can also be used to determine the minimum concentration of siRNA reagent necessary to

achieve *LMNA* silencing by comparing *LMNA* transcript levels using different concentrations of siRNA to levels on c-Myc activation following 4-OHT addition at the same timepoints. This would further reduce the risk of off-target effects by minimizing the concentration of siRNA used in the experiment.

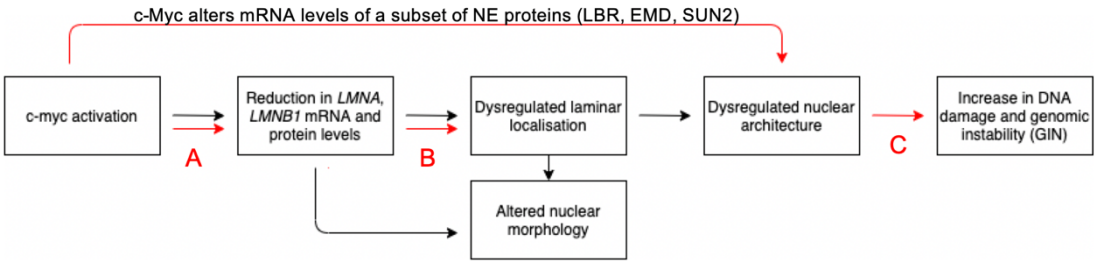

Figure 3.9: Summary of model so far (Chapter 3). Three salient questions will be addressed in the following chapters. A: How does c-Myc activation lead to acute reductions in lamin A and B1 levels so soon after activation? (Chapter 4) B: How does this reduction then lead to its mislocalisation within the nucleus? C: How does this dysregulation of nuclear architecture then lead to increases in DNA damage and GIN that contribute towards oncogenesis? (Chapter 5)

4. The mechanism of c-Myc induced changes to nuclear architecture and morphology.

In this chapter I will discuss the results of my investigations into the possible mechanisms of c-Myc induced transcriptional and protein silencing of lamin A, which I have interpreted as the most significant contributor towards c-Myc's dysregulation of nuclear architecture and morphology.

The robust silencing seen is likely a multi-factorial event and not just dependent on a single pathway, especially as c-Myc induced transcriptional silencing is a more complex phenomenon to explain than for instance c-Myc induced transcriptional upregulation. Specific mechanisms of lamin A gene regulation have been discovered (see section 1.6.3) and some of these will be investigated in the following sections.

4.1 c-Myc induction does not cause an increase in lamin A phosphorylation or degradation.

One mechanism of silencing at the protein level could be via a combination of decreased transcription and an increased turnover of the mature lamin A protein, through altered post-translational modifications. Several papers (Buxboim et al., 2014. Kochin et al., 2014) have observed an increase in phosphorylation of lamin A at S22 (one of two so-called 'mitotic sites' that Cdk1 acts on for mitotic laminar disassembly) following a reduction in stiffness of the extracellular matrix, that then leads to its localization to the nucleoplasm and its subsequent degradation. Though the fate of nucleoplasmic lamin A is unclear, increased S22 phosphorylation would result in lamin A relocalisation away from the nuclear periphery, reducing nuclear stiffness and increasing deformability, contributing towards alterations to nuclear morphology.

Figure 4.1A shows whole cell lysate samples probed for levels of both lamin A and phosphorylated lamin A (pS22) on c-Myc ER cells after 24 and 48 hours of c-Myc activity. We can see reductions in both total and phosphorylated lamin A by the same proportion, indicating that c-Myc activation does not cause an increase in S22 phosphorylation.

Another possible mechanism is through a c-Myc induced increase in cleavage and degradation of lamin A protein, such as is seen during apoptosis by caspase-6 (Ruchaud et al., 2002). Studies have indicated this results in an increase in the formation of smaller kDa cleavage products at around 50 and 30 kDa (Mahajan et al., 2017). Figure 4.1B shows however that c-Myc activity does not result in an increased generation of these smaller lamin A fragments at lower molecular weights. This indicates that there is no increase in lamin A degradation at the protein level, at least by caspase-6 as seen in the onset of apoptosis.

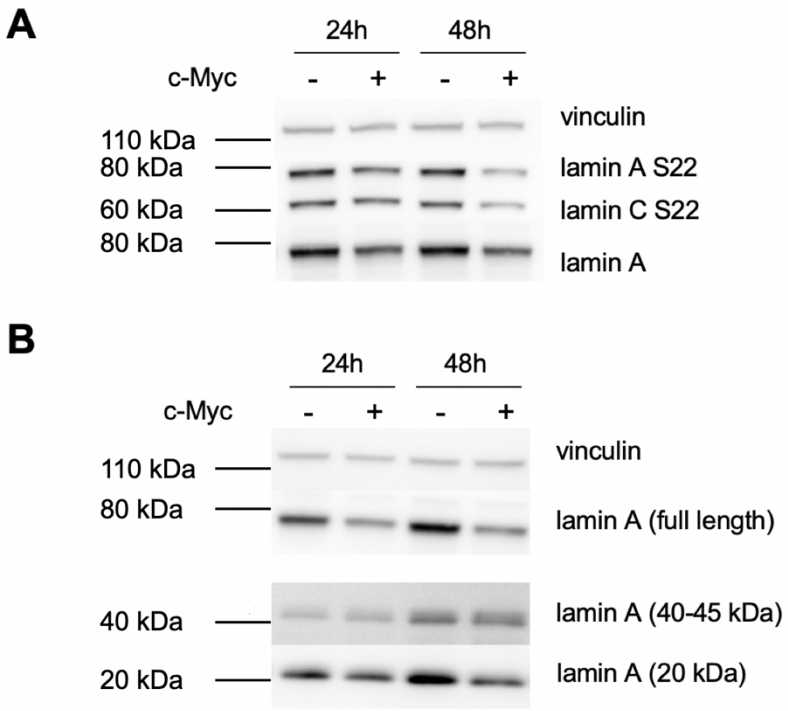

Figure 4.1: c-Myc induction does not caused increased lamin A phosphorylation or fragmentation. (A) Representative blot of RPE-1 c-Myc ER cells that were untreated (UT) or treated with tamoxifen (c-Myc) for 24h and 48h and probed for lamin A, lamin A phosphor-serine 22. (B) Representative blot cells probed for lamin A, and lamin A fragments at 40-45 and 20 kDa. Both blots representative of n = 2.

It should be noted that this does not rule out changes to lamin A post-translational modifications. Work in Akt signalling has shown that lamin A is a phosphorylated by Akt at S404 and that targets the prelamin A precursor for proteasomal degradation (Bertacchini et al., 2013). This was further supported by a recent study by Jan Lammerding's group that showed that an increase in Akt hyperactivation mediated lamin A downregulation in a panel of breast cancer cell lines that correlated with an enhanced ability of the cells to migrate, invade and metastasise (Bell et al., 2022). To test this hypothesis in my c-Myc inducible system, I probed for phospho-Akt S473,

which is a proxy for Akt activity and is the canonical signalling event upstream of lamin A S404 phosphorylation (Bertacchini et al., 2013).

Figure 4.2 shows however that c-Myc does not cause an increase in Akt activity, and surprisingly shows reduced levels of pAkt at both 24 and 48 hours after activation. Since total Akt levels were not probed, it is difficult to say whether this is a result of an overall reduction in Akt protein expression, or a specific effect on Akt activity. Given that both c-Myc and Akt signalling represent highly active pathways in cancer cells, this sort of complex relationship is perhaps to be expected. For instance, Akt signalling via mTOR activity is seen to enhance the translation of *MYC* mRNA (Chen et al., 2018). This can then feedback and act as a negative feedback loop to reduce Akt activity once the c-Myc oncogene is activated.

A more direct measure and a necessary follow up to this experiment would be the direct probing of lamin A S404 to measure whether its levels are increased on c-Myc activation.

Taken together, c-Myc's downregulation of lamin A protein levels is unlikely to proceed through an increase in post-translational modifications or Akt or caspase-mediated degradation. I next wanted to study the effect of the lamin binding partner protein emerin on its expression and localisation to see whether it played a significant role.

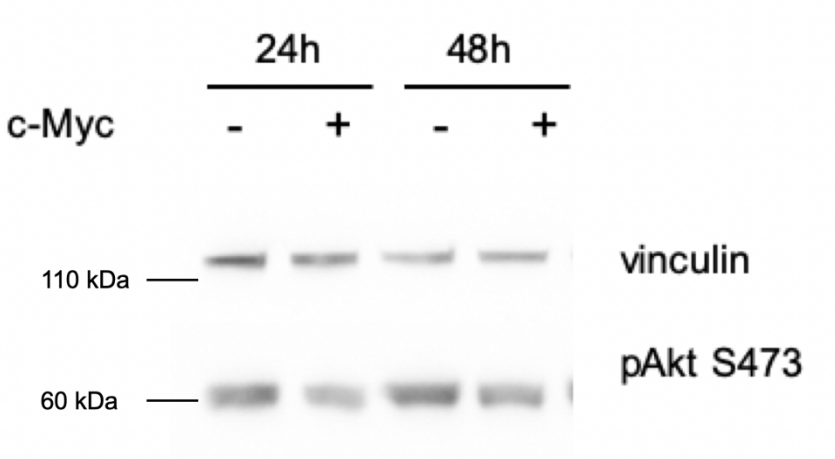

Figure 4.2: c-Myc induction does not caused increased Akt activity. Representative blot of RPE-1 c-Myc ER cells that were untreated (UT) or treated with tamoxifen (c-Myc) for 24h and 48h and probed for phosphor-Akt S473. Representative of n = 2.

4.2 c-Myc induced emerin upregulation is a separate event to c-Myc induced lamin A silencing

Returning to the phenomenon of c-Myc induced emerin upregulation, since these both occurred within the same 24 and 48h timeframe, it was intriguing to hypothesise whether the two pathways of lamin A silencing and emerin upregulation were interlinked, especially as they were both binding partners to each other, with a direct interaction between the two first noted *in vitro* (Clements et al., 2000). The hypothesis was that either pathway could enhance the other; that is, c-Myc induced lamin A silencing could contribute to emerin upregulation, or vice versa. If the latter were the case, it would provide a simple mechanism for the sudden silencing we see after 24 hours of c-Myc activity.

To test this, a simple experimental at the transcriptional level was to investigate the effects of silencing one gene on the transcript levels of the other (Figure 4.3). c-Myc ER cells were transfected with siRNA against *LMNA* or *EMD* with or without c-Myc activity and the corresponding levels of both transcripts were measured using RT-qPCR.

4.3A (left) first confirms that c-Myc induction leads to partial and significant reductions in *LMNA* mRNA (compare two black bars of siControl). Next we see that the *LMNA* silencing has worked as there are significant reductions in *LMNA* when treated with siLMNA (compare each black with each grey). Interestingly, siLMNA and c-Myc appear to be acting through similar pathways in *LMNA* silencing as inducing both does not lead to an additive effect (compared each grey bar). 4.3A (right) indicates however that lamin A silencing in both untreated and c-Myc induced cells on its own does not cause an increase *EMD* mRNA. Perhaps the most key comparison is between the two c-Myc induced conditions, where we see that further silencing of *LMNA* does not lead to further increases in the levels of *EMD* mRNA, suggesting that the two processes are surprisingly not linked at the transcriptional level.

If we perform the converse experiment of silencing *EMD* and investigating levels of *LMNA*, we see the same trend. 4.3B (left) shows firstly that c-Myc induction leads to the aforementioned upregulation of *EMD* (compare two black bars of siControl). Next we see the efficiency of *EMD* knockdown as a positive control. 4.3B (right) shows c-silencing of *LMNA* is unaffected by knockdown of *EMD* (compare two black and grey

bars) in both untreated and c-Myc induced cells. Taken together, this indicates that the two processes of emerin upregulation and lamin A silencing are separate but parallel pathways that occur post c-Myc activity, and that they do not appear to influence each other at the transcriptional level. A useful follow up would be to perform

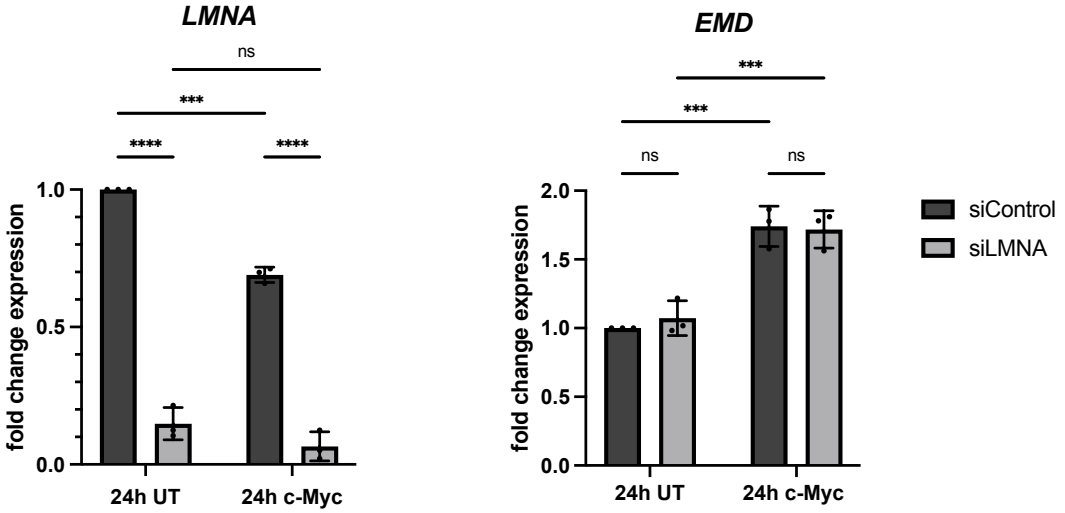

the analogous experiment at the protein level to see whether they are linked.

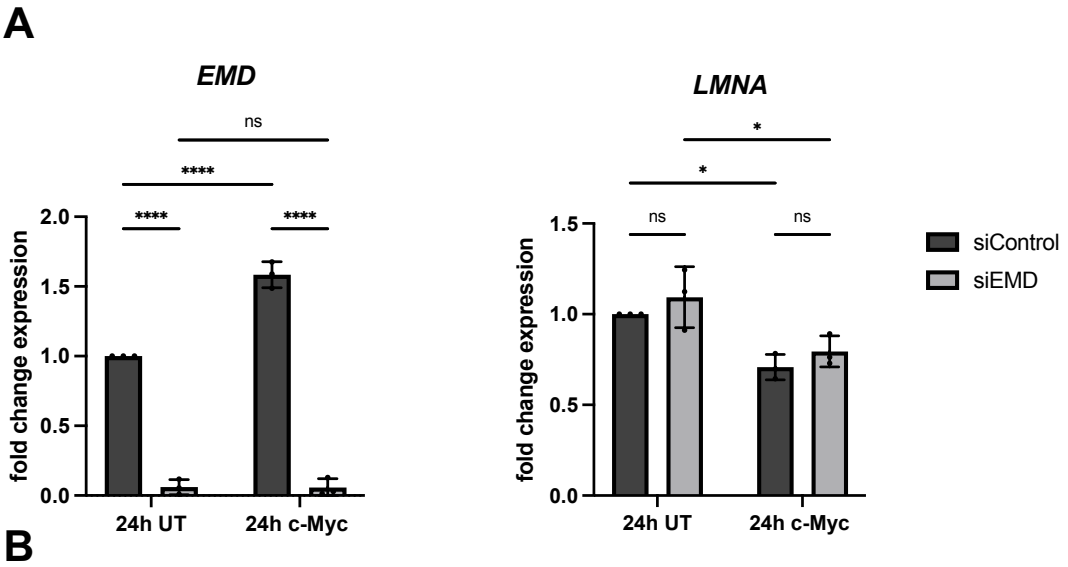

Figure 4.3: Lamin A silencing does not lead to upregulation of emerin and downregulation of emerin does not rescue lamin A silencing. RPE-1 c-Myc ER cells were untreated (UT) or treated with tamoxifen (c-Myc) for 24h with or without lamin A silencing. Quantifications of fold change in mRNA levels of *LMNA* and *EMD*. (B) Quantification of fold change following corresponding experiment using emerin silencing. All graphs show mean ± SD. Representative of n = 3 separate biological replicaes. All statistical analyses were performed using a two-way ANOVA (* $p < 0.05$, ** $p < 0.01$, *** $p < 0.001$, **** $p < 0.0001$).

Despite the seeming lack of dependence that each gene had on levels of the other at the mRNA level, it was interesting to then speculate whether their localisations may

be affected using the same silencing protocol. It has been shown that lamin A is necessary for the correct localization of emerin to the INM (Vaughan et al., 2001, Holt et al., 2003). It would be possible that this relationship was also the case in reverse, with lamin A localization (but not transcriptional regulation) dependent on emerin levels for localization. c-Myc's upregulation of emerin could therefore drive aberrant lamin A localization and the reduction of emerin levels might rescue this mislocalisation phenotype.

To test this, I next transfected cells with siEMD to silence emerin and stained for lamin A and emerin protein under fixed-cell immunofluorescence, in untreated and c-Myc induced cells (Figure 4.4).

4.4A confirmed firstly that emerin silencing had worked at the protein level, with almost complete abolition of emerin signal in both untreated and c-Myc induced cells. Surprisingly, lamin A localization appeared to have little dependence on emerin levels, as nucleoplasmic variation (a proxy for nuclear heterogeneity in lamin A distribution) remained unchanged on emerin silencing (4.4C). Similarly, emerin silencing appeared to have little effect on nuclear morphology (4.4B), indicating that it was a less significant contributor towards its maintenance than lamin A.

Interestingly, silencing emerin in c-Myc induced cells appeared to have no effect on rescuing lamin A mislocalisation or nuclear circularity. Again, this suggests that there is little interplay between the two processes and that silencing emerin in c-Myc induced cells may induce larger and more gross changes to nuclear function than already seen. Another experiment worth performing would be immunofluorescence of emerin protein on lamin A silencing, though given it remained upregulated at the transcriptional level (4.3A), it is highly unlikely that their protein levels or localization would be rescued or altered.

Taken together, this work suggests an additive nature to the two c-Myc pathways and also that they occur in parallel instead of one after another. This is unsurprising as c-Myc induced changes to nuclear morphology is unlikely to be due to a single protein or pathway and also explains the differences in severity of phenotypes we see between the nuclei of c-Myc induced cells compared to when lamin A alone is silenced; the former has additional mechanisms contributing towards nuclear dysregulation that we have not been investigated.

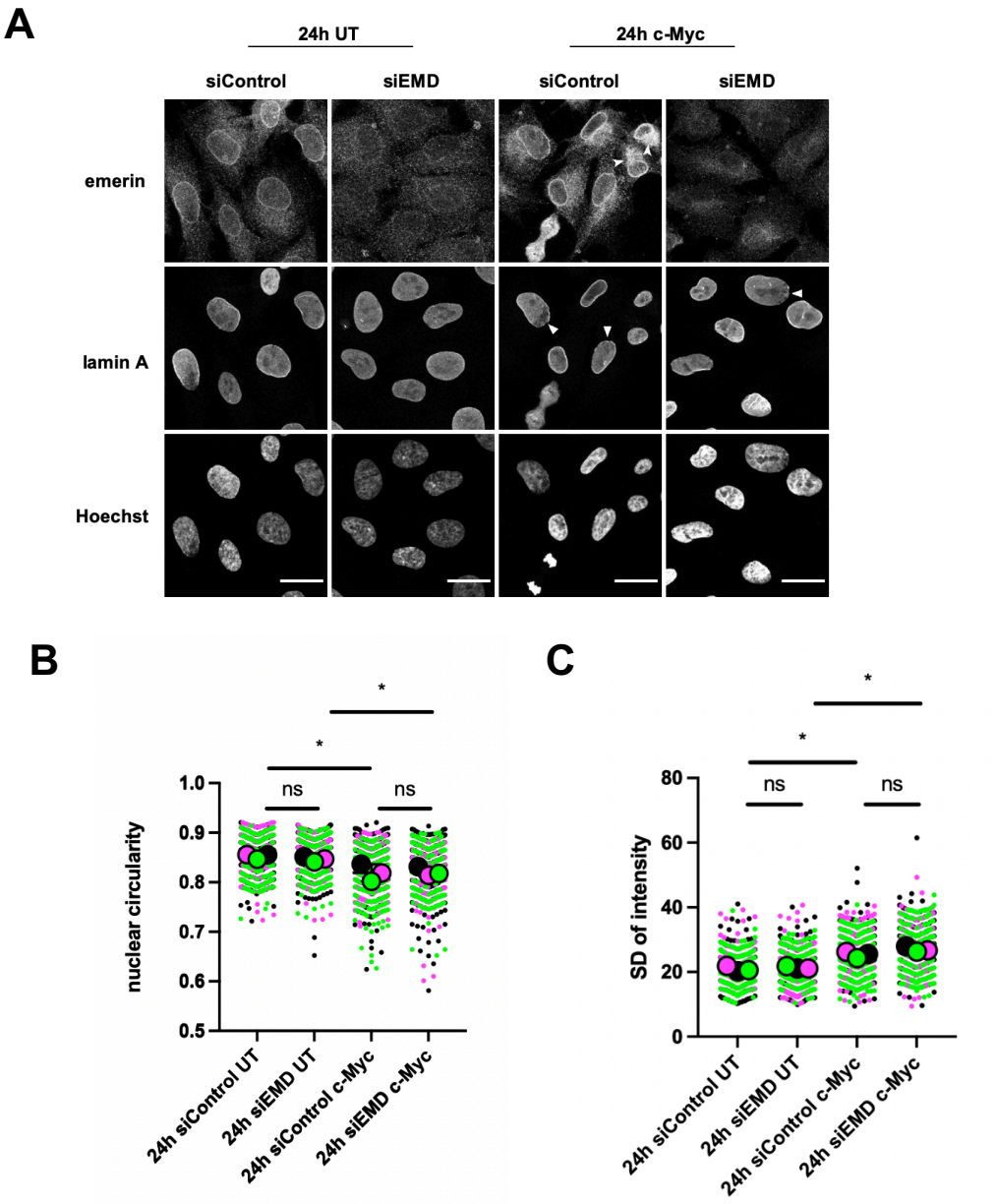

Figure 4.4: Emerin silencing does not rescue c-Myc induced nuclear morphology defects. RPE-1 c-Myc ER cells were untreated (UT) or treated with tamoxifen (c-Myc) for 24h with or without emerin silencing. Quantifications of fold change in mRNA levels of *LMNA* and *EMD*. (B/C) Column scatter graph of nuclear circularity (B) and nuclear area (C) of the same cells at 24h with or without emerin silencing in conjunction with or without c-Myc activation. Each colour represents a separate independent experiment (black, magenta, green, n = 3, 100-200 cells per condition per experiment). Large coloured circles represent mean values per experiment. Small circles represent individual cells per independent experiment. All graphs show mean ± SD. All statistical analyses were performed using a paired student's t-test on mean values of circularity and area between conditions. (* $p < 0.05$, ** $p < 0.01$, *** $p < 0.001$, **** $p < 0.0001$).

4.3 c-Myc induced lamin A silencing may be mediated by mi-R9.

I next wanted to explore another possible way by which c-Myc could silence lamin A. As discussed in section 1.6.3, there are several studies that implicate the micro-RNA miR-9, which has roles in promoting metastasis. Two studies have provided encouraging preliminary data that support this conclusion (Figure 4.5). Firstly, Ma et al., (2010) have found, using an extremely similar c-Myc inducible cell system and ChIP that expression of miR-9 is directly activated and controlled by c-Myc that binds to the *mir9-3* gene locus. This, coupled with the fact that miR-9 was seen upregulated in non-metastatic cells (Ma et al., 2007), led to the hypothesis that c-Myc induced miR-9 upregulation occurred early in oncogenesis before tumours become fully metastatic. Next, Jung et al., (2012) found that miR-9 actively silenced lamin A but not lamin C, by binding to the 3' UTR of mature prelamin A that targeted it for degradation in brain tissue. Combined, these studies provided an elegant pathway by which c-Myc activation could lead to fast silencing of lamin A.

Direct measurement of miR-9 levels were experimentally challenging, as miR-9 was found to only be expressed in high levels in brain and neural tissues undergoing neurodevelopment. Direct detection on c-Myc activation in the c-Myc-ER system would require a sensitive form of RT-qPCR that would have presented challenges in designing primers specific enough for miR-9 to ensure efficient and specific amplification and low abundance of miR-9 would mean extraction efficiency would need to be extremely high and results susceptible to variability in RNA extraction, genomic DNA removal, amplification and normalization (to small RNA controls e.g., U6 snRNA).

To test this hypothesis on miR-9's effects on lamin A I therefore decided to use an indirect approach to first see whether c-Myc's silencing of lamin A could be rescued by the use of a specially designed miR-9 inhibitor oligo that bound to miR-9 and prevented its activity. This was used in conjunction with a miR-9 mimic molecule to first test its validity.

Figure 4.5 shows the results of said experiment. RT-qPCR of *LMNA* levels were performed on non c-Myc induced RPE c-Myc ER cells that were treated with various combinations of mimic, inhibitor and tamoxifen to induce c-Myc activation. We can first see that there is a slight reduction in *LMNA* levels on addition of miR-9 mimic, though surprisingly this is not significant. Next, we see that the inhibitor is functioning

as expected, since this slight reduction is rescued and *LMNA* levels restored to untreated levels on addition in conjunction with the mimic. c-Myc activity again reduces *LMNA*, though the miR-9 inhibitor does not have a significant effect on its levels when added in conjunction with c-Myc activity. Further studies are needed to therefore verify whether c-Myc induced lamin A silencing is at least partially mediated by its upregulation or activation of the intermediary miR-9. A necessary follow up would be direct measurement of miR-9 levels with the c-Myc inducible system, by Northern blotting or real time qPCR. Both have advantages and drawbacks, such as the inapplicability of Northern blotting for short miRNAs such as the 18 nt miR-9, and the high rate of false positives and difficulties in primer design for qPCR (Ye et al., 2019). A further follow-up would be the addition of an appropriate vehicle control within the experiment (i.e., addition of inhibitor delivery agent Lipofectamine RNAiMAX only) to verify that it does not have any significant effects on *LMNA* levels on its own.

Overall, this experiment demonstrates that c-Myc likely does not follow a single pathway for *LMNA* silencing and highlights the difficulties in investigate many mechanisms that each contribute a small part to the overall result. It is also important to note that this pathway does not explain c-Myc's effects on decreasing lamin B1 levels which follow a slightly different kinetics to lamin A, as the reduction is more mild at 24 hours but becomes more significant after 48.

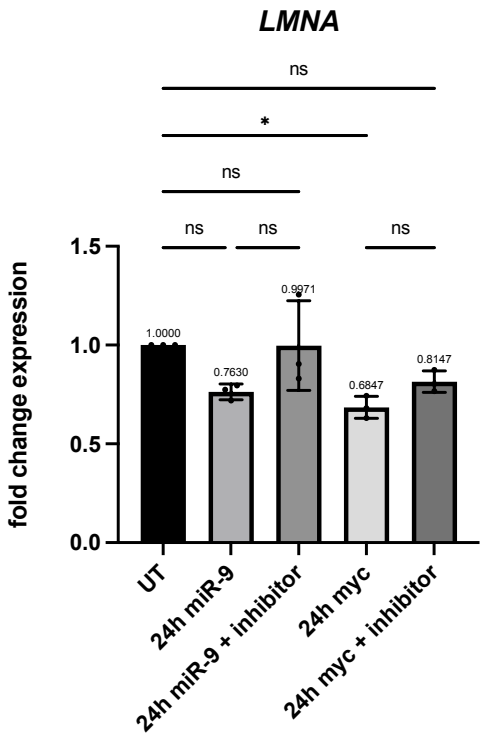

Figure 4.5 (previous): c-Myc's effects on lamin A levels may be mediated through miR-9. RPE-1 c-Myc ER cells were untreated (UT) or treated with miR-9 mimic, mimic/inhibitor, tamoxifen (c-Myc) with or without inhibitor for 24h. Quantifications of fold change in mRNA levels of *LMNA*. All graphs show mean ± SD. Representative of n = 3 separate biological replicates. All statistical analyses were performed using a two-way ANOVA (* $p < 0.05$, ** $p < 0.01$, *** $p < 0.001$, **** $p < 0.0001$).

Additional recent evidence has also emerged which further complicates the picture. A study that followed much of the same reasoning of lamin A expression, investigated the phenotype of low lamin A expression in metastatic lung adenocarcinoma cells (Guinde et al., 2020). It found surprisingly that miR-9 expression was shown to be reduced in lamin A negative cells, indicating that it was not involved expression levels in that particular system. This suggests that lamin A silencing is context dependent and has multiple causes.

4.4 c-Myc induced alterations to nuclear morphology are affected by cell cycle dynamics

Finally, I wanted to investigate how lamin A silencing results in its mislocalisation and subsequent abnormal nuclear morphology. The precise dynamics of lamins during interphase are surprisingly understudied, though it is accepted that it is continuously synthesised throughout and incorporated into the lamina (Gerace et al., 1984), especially during G1 phase where nuclei grow significantly in volume. Lamin-LAP2 interaction during interphase also appears to have a role in regulating nuclear growth (Yang et al., 1997) by ensuring the nuclei reach a certain size before entry into S phase. A recent paper found that lamin A synthesis rates scale with nuclear size, ensuring that nuclei growing during interphase maintain their mechanics and constant incorporation of new lamins into the lamina (Zhironkina et al., 2016). Though incorporation of new lamin proteins occurs during interphase, mitosis is the only point at which the nuclear lamina is disassembled and subsequently reassembled post-mitotically. It is tempting to hypothesise therefore that c-Myc induced lamin A silencing leads to dilution of lamin concentration at the nuclear lamina and nucleoplasm, that then leads to mislocalisation and subsequent reductions in nuclear circularity only after the first entry into mitosis (Figure 4.6).

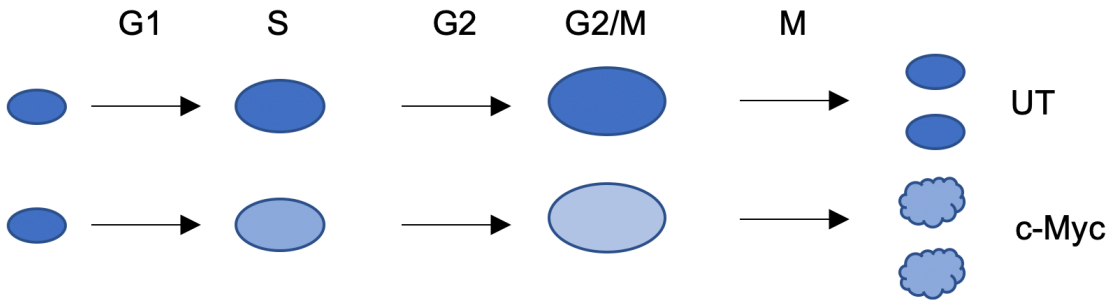

Figure 4.6: model of how c-Myc induced lamin A silencing could result in nuclear morphology defects only *after* exit from mitosis. In untreated (UT) cells, lamins (blue) are synthesised throughout interphase and the nucleus maintains a constant concentration of lamin protein, which is divided into two daughter cells following mitosis. In c-Myc induced cells, reduced lamin A synthesis due to transcriptional *LMNA* silencing could lead to dilution of nuclear concentration throughout the first interphase, ultimately leading to a short supply of lamins to distribute amongst daughter cells once mitosis is complete, abnormal localisation during reassembly and subsequent abnormal nuclear morphology.

To test this hypothesis, I investigated nuclear circularities in c-Myc induced cells, which were also treated with the reversible Cdk1 inhibitor RO-3306, which arrests cells at the G2/M transition and is often used to synchronise cell populations into the same phase of the cell cycle (Vassilev et al., 2006).

Figure 4.7A first shows that addition of RO-3306 to both untreated and c-Myc induced cells leads to a rapid and significant increase in the proportion of G2 phase cells and 24h after treatment, indicating success cell cycle arrest at the G2/M transition. 4.7B and 4.7C then show that c-Myc ER cells that have been treated with both c-Myc and RO-3306 display a rescue of regular nuclear morphology, as seen by the significant increase in nuclear circularity when compared to single treatment with tamoxifen alone. This provides strong evidence that c-Myc induced effects on nuclear morphology are mitosis-dependent, and that cells who have c-Myc active but are arrested at G2 phase do not display altered nuclear morphologies.

One necessary control to add to this experiment would be a solvent (DMSO)-only control. This would be to confirm that DMSO alone does not affect the cell cycle profile or nuclear circularity and to ensure that the effects seen on addition of RO-3306 to the cell cycle and nuclear circularity are due to the drug.

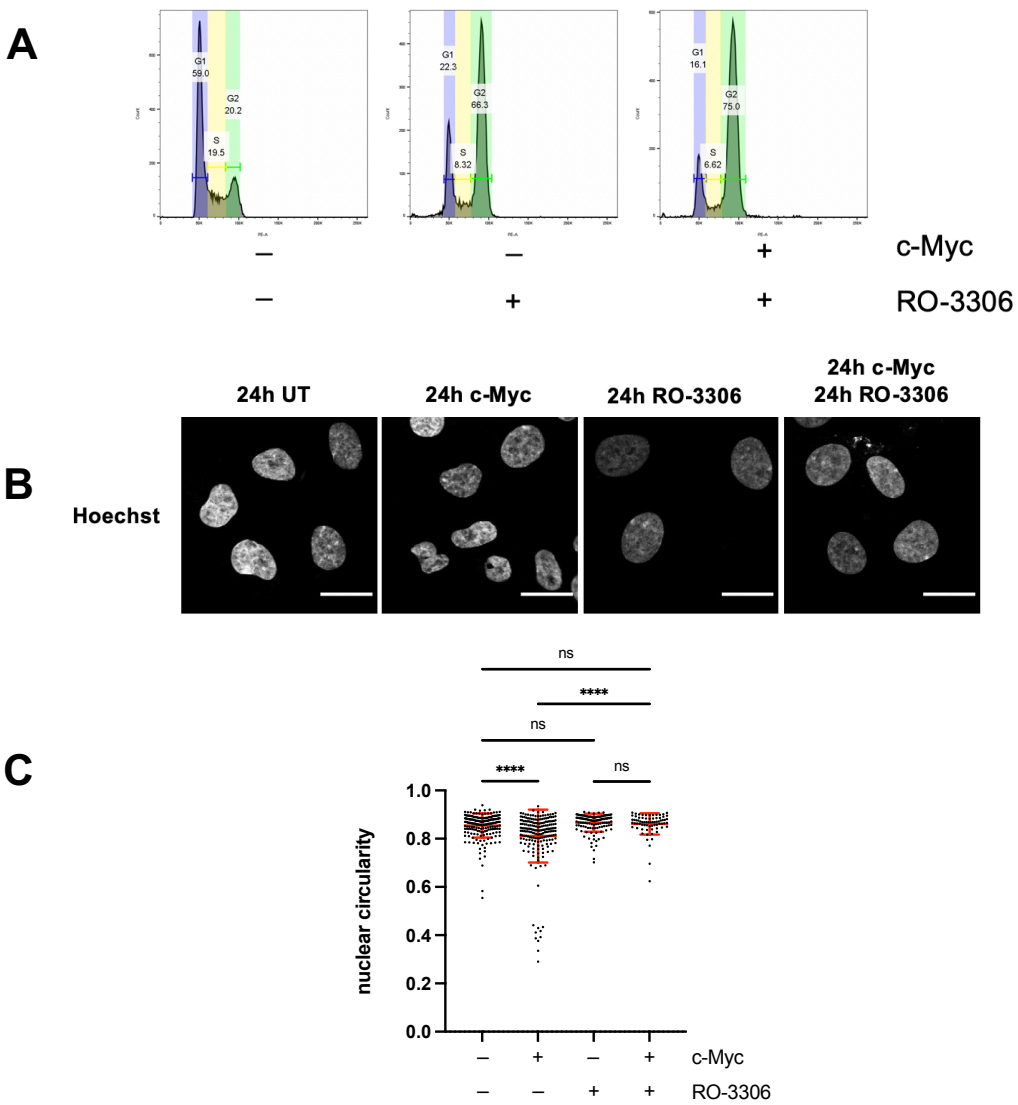

Figure 4.7: c-Myc's dysregulation of nuclear morphology requires entry into mitosis. (A) RPE1 c-Myc ER cells were untreated or treated with RO-3306 (9 μM) alone or in combination with tamoxifen (c-Myc) for 24 hours, before cell cycle profiles were analysed by propidium iodide (PI) staining. (B) Representative images of RPE-1 c-Myc ER cells that were untreated (UT) or treated with tamoxifen, RO-3306 or in combination for 24h before fixation, nuclear staining with Hoechst and imaging via immunofluorescence. Taken from n = 3 independent experiments, c. 150-200 cells per experiment. Scale bar = 20 μm. (C) Column scatter graphs of nuclear circularity of the same cells. All statistical analyses were performed using a two-way ANOVA (* $p < 0.05$, ** $p < 0.01$, *** $p < 0.001$, **** $p < 0.0001$).

I next wanted to see whether this dependence on mitosis of c-Myc effects on nuclear morphology extended to lamin A mislocalisation, and whether this effect could be seen in cells arrested over a longer time scale. To do this, an extended protocol was performed, outlined in Figure 4.8A. Three time courses were followed. Firstly, (1) and (2) were repeats of the previous experiment, with cells treated either with RO-3306 alone or with c-Myc. (3) and (4) represent washout experiments, to investigate whether previously G2-arrested but now cycling cells would undergo the same c-Myc

induced nuclear morphology and lamin A mislocalisation defects as expected. (5) and (6) represent experiments in which cells that have been treated with RO-3306 for 48h are either left untreated or with 24h c-Myc halfway to see whether defects arise in cells that are already arrested.

4.8C confirms firstly that nuclear circularity does not decrease and remains unaffected in cells arrested in G2 phase in both untreated and c-Myc active cells. This is accompanied by 4.8D, which shows that lamin A remains regularly localised, suggesting lamin A deposition during interphase is perhaps unaffected in c-Myc active cells despite the silencing and reduced rates of synthesis. Next, we see that both morphology defects and nuclear mislocalisation return once cells are cycling again and c-Myc is induced for 24 hours post RO-3306 washout. Finally, we can see that these two defects are rescued again when c-Myc is added to cells which are already robustly arrested in G2.

Taken together, this extends the conclusion one can draw from the previous figure, indicating that c-Myc activity does not lead to mislocalisation of lamin A or nuclear morphology defects in G2 arrested cells, though they become apparent once cells are released following washout of RO-3306. Similar to Fig 4.7, a DMSO-only control should be added to each condition that uses RO-3306 to verify that solvent alone does not cause this rescue of nuclear circularity.

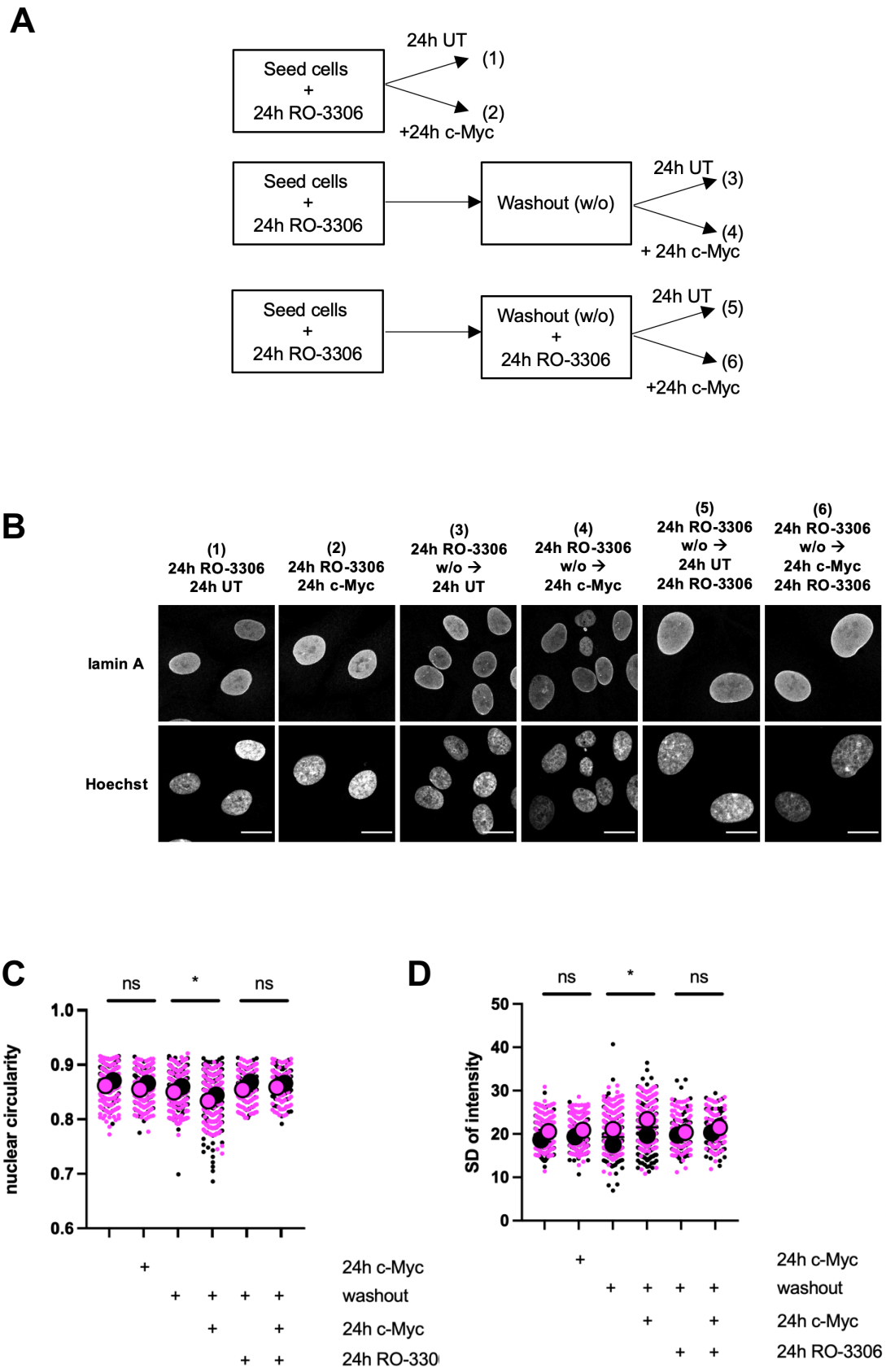
A
Seed cells + 24h RO-3306
24h UT
(1)
(2)
+24h c-Myc
Seed cells + 24h RO-3306
Washout (w/o)
24h UT
(3)
(4)
+ 24h c-Myc
Seed cells + 24h RO-3306
Washout (w/o) + 24h RO-3306
24h UT
(5)
(6)
+24h c-Myc
B
(1) 24h RO-3306 24h UT
(2) 24h RO-3306 24h c-Myc
(3) 24h RO-3306 w/o → 24h UT
(4) 24h RO-3306 w/o → 24h c-Myc
(5) 24h RO-3306 w/o → 24h UT 24h RO-3306
(6) 24h RO-3306 w/o → 24h c-Myc 24h RO-3306
lamin A
Hoechst
C
nuclear circularity
ns
*
ns
1.0
0.9
0.8
0.7
0.6
24h c-Myc
washout
24h c-Myc
24h RO-330
D
SD of intensity
ns
*
ns
50
40
30
20
10
0
24h c-Myc
washout
24h c-Myc
24h RO-3306

Figure 4.8 (previous): c-Myc does not induce dysregulation of nuclear morphology and lamin A mislocalisation in G2 arrested cells. (A) Schematic showing six experimental conditions of varying treatments with RO-3306 and tamoxifen. (B) Representative images of RPE-1 c-Myc ER cells that were untreated (UT) or treated with tamoxifen, RO-3306 or in combination for 24h before fixation, staining with lamin A and Hoechst and imaging via immunofluorescence. Taken from n = 3 independent experiments, c. 150-200 cells per experiment. Scale bar = 20 μm. (C, D) Column scatter graphs of nuclear circularity (C) and nucleoplasmic lamin A signal variation (D) of the same cells at under each condition. Each colour represents a separate independent experiment (black, magenta, n = 2, 100-200 cells per condition per experiment). Large coloured circles represent mean values per experiment. Small circles represent individual cells per independent experiment. All statistical analyses were performed using a paired student's t-test on mean values of circularity and area between conditions. (* $p < 0.05$, ** $p < 0.01$, *** $p < 0.001$, **** $p < 0.0001$).

I next wanted to investigate whether arresting cells during interphase, specifically during the G1 phase of the cell cycle produced the same rescue of c-Myc induced nuclear defects. To do this, I used the Cdk4/6 inhibitor palbociclib, which reversible arrests cells in G1 and has similarly been used to induce a synchronisation of cell lines in the literature (Scott et al., 2020, Trotter and Hagan, 2020).

Analogous to the previous figure, 4.9A outlines the six conditions tested. Three time courses were followed. Firstly, (1) and (2) were simply to investigate the effects of G1 arrest on nuclear morphology and lamin localisation in untreated cells. (3) and (4) represent an investigation into whether c-Myc activation in G1-arrested cells generates any nuclear defects. (5) and (6) represent washout experiments, to investigate whether previously G1-arrested but now cycling cells would undergo the same c-Myc induced nuclear morphology and lamin A mislocalisation defects as expected.

4.9C confirms firstly that nuclear circularity does not decrease and remains unaffected in cells arrested in G1 phase in both untreated cells. 4.9D also shows that lamin A remains regularly localised. Next, surprisingly, we see that both morphology defects and nuclear mislocalisation return in G1-arrested cells with 24h c-Myc activity. This is in contrast to the lack of such a phenotype in G2 arrest. Finally, we see that once cells are cycling again and c-Myc is induced for 24 hours post palbociclib washout, mislocalisation and circularity decreases return.

Taken together, this presents an interesting picture of the dynamics of lamin A mislocalisation and nuclear morphology. What it shows is that c-Myc's effects on lamin A mislocalisation firstly require laminar disassembly and reassembly following mitosis. However, the presence of mislocalisation and irregular morphologies in G1-

arrested cells suggests that it is not that simple. Since G1 represents a phase where nuclei are growing and lamins are actively synthesised and incorporated in the lamina, and that lamin A is highly dynamic and regulated, G1 arrest could lead to abnormal deposition or exchange of existing lamin A between the lamina and nucleoplasm under c-Myc that causes nuclear defects in a separate process to cycling cells. There is also the influence of c-Myc induced changes to chromatin organisation, which will be discussed later. Similar to the previous two figures (4.7 and 4.8), a DMSO-only control is necessary to check that these changes to nuclear circularity are being caused by palbociclib and not the solvent itself.

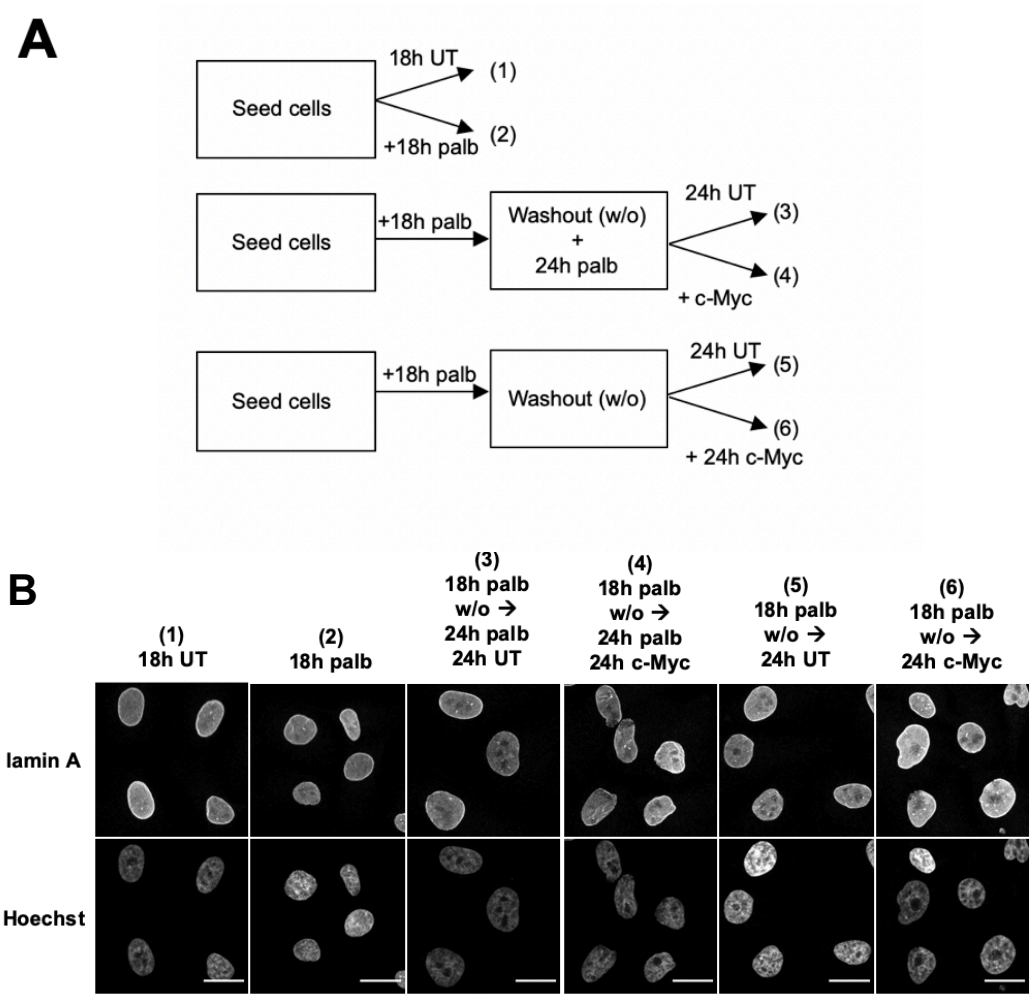

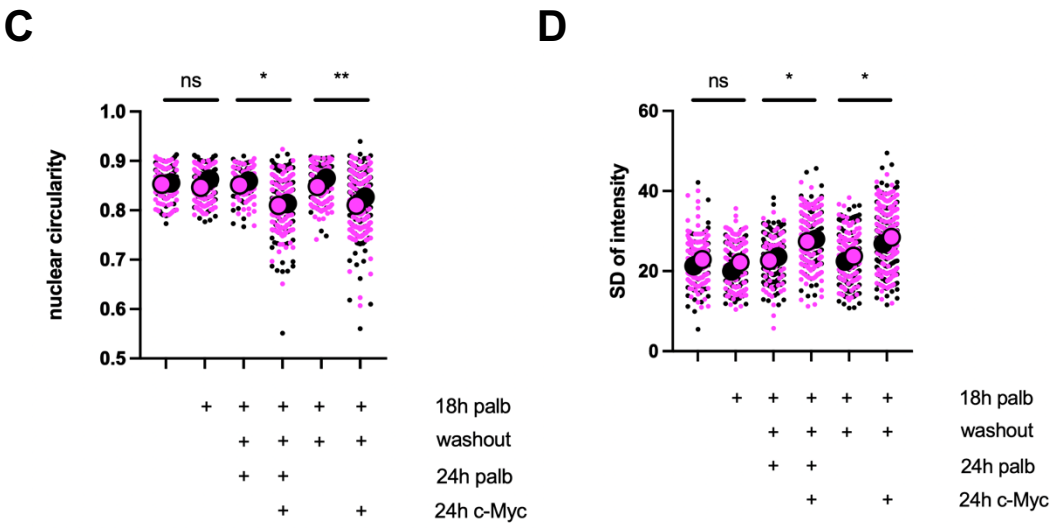

Figure 4.9 (previous): c-Myc's dysregulation of nuclear morphology and mislocalisation of lamin A still takes place in G1 arrested cells. (A) Schematic showing six experimental conditions of varying treatments with palbociclib (palb, 150 nM) and tamoxifen. (B) Representative images of RPE-1 c-Myc ER cells that were untreated (UT) or treated with tamoxifen, palbociclib or in combination before fixation, staining with lamin A and Hoechst and imaging via immunofluorescence. Taken from n = 3 independent experiments, c. 150-200 cells per experiment. Scale bar = 20 μm. (C, D) Column scatter graphs of nuclear circularity (C) and nucleoplasmic lamin A signal variation (D) of the same cells at under each condition. Each colour represents a separate independent experiment (black, magenta, n = 2, 100-200 cells per condition per experiment). Large coloured circles represent mean values per experiment. Small circles represent individual cells per independent experiment. All statistical analyses were performed using a paired student's t-test on mean values of circularity and area between conditions. (* $p < 0.05$, ** $p < 0.01$, *** $p < 0.001$, **** $p < 0.0001$).

4.5 Summary

To summarise, in this chapter I have shown the results of an investigation into a range of potential mechanisms by which c-Myc could firstly induce lamin A silencing, and secondly how this could lead to nuclear morphology defects and lamin mislocalisation. I have seen that several well studied pathways, such as lamin A phosphorylation or degradation are unlikely to play a role in c-Myc induced silencing, whereas the contribution of miR-9 activation needs to be further studied, as current results are inconclusive. The key follow-up experiment here would be direct measurement of miR-9 levels on c-Myc activation to validate whether an increase in miR-9 levels are seen following an increase in c-Myc activity.

The surprising lack of interaction between emerin upregulation and lamin A downregulation is a fruitful topic for further study. Ultimately, they likely represent parallel pathways by which c-Myc dysregulates nuclear architecture and both can contribute in distinct ways towards oncogenesis.

Finally, the dependence of c-Myc's nuclear effects on the cell cycle was an unexpected but interesting finding. Though initial observations suggested it was purely dependent on cycling and completion of mitosis, the experiments using G1 inhibitor palbociclib hinted that that is not the whole picture, since non-cycling cells also displayed c-Myc induced nuclear defects. It is important with this set of experiments (Fig 4.7, 4.8 and 4.9) to repeat the studies with the addition of a DMSO control to ensure that both the effects seen on cell cycle profile and nuclear morphology are due specifically to the drugs used (RO-3306 and palbociclib) and not the DMSO itself. This is especially relevant in light of evidence suggesting that DMSO by itself at concentration as low as 1-2% can induce a reversible G1 arrest in Chinese hamster ovary (CHO) cells (Fiore et al., 2002), underscoring the need to verify that DMSO alone is not causing any changes to cell cycle profile within the c-Myc-ER cell line used. This is in conjunction with more recent work suggesting that DMSO treatment can induce alterations to protein secondary structure, indicating a wide range of cellular processes that may be disrupted at concentrations as low as 0.1% (Tuncer et al., 2018), which is far lower than those used in the experimental setup for Figure 4.7, 4.8 and 4.9 (1-10%).

Having seen these changes in the nucleus at 24 and 48 hours post c-Myc activation, it is now important to put them in the context of early stage oncogenesis. In the next chapter I investigate the question of how dysregulation in nuclear architecture can ultimately contribute towards tumorigenesis by increasing DNA damage and GIN, both hallmarks of cancer and key steps in the transformation process.

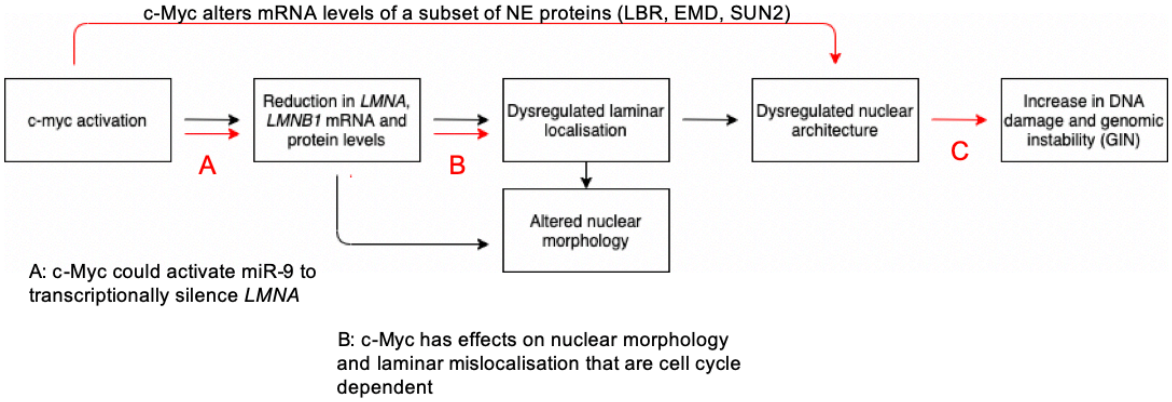

Figure 4.11: Summary of model so far (Chapter 4). Two questions (A and B) have been investigated. The remaining one is C: How does this dysregulation of nuclear architecture then lead to increases in DNA damage and GIN that contribute towards oncogenesis? (Chapter 5)

5. The consequences of c-Myc induced changes to nuclear architecture and morphology

In this chapter I will discuss the results of my investigations into several downstream phenomena that occur due to c-Myc induced alterations to nuclear architecture. I have focused on the process of NE rupture, which has long since been associated with defects or depletions in lamin proteins within the nuclear lamina (De Vos et al., 2011, Zwerger et al., 2013, Earle et al., 2020). As I see robust reductions in both lamins A and B1 (at the protein and transcript level), I hypothesized that this alteration to nuclear structure could contribute towards an increased in NE rupture events.

Depletion of lamins could contribute towards an increase in NE rupture frequency through several ways. Firstly, reduction in lamin A/C could increase nuclear fragility, decrease stiffness and render nuclei more deformable under the same external stresses. Secondly, a reduction in both A and B-type lamins and their subsequent mislocalisation at the lamina could create areas of local lamina deficiency, which provide points at which NE rupture could be initiated due to the increased membrane curvature that results from a lack of protection against local forces (Figure 5.1A).

5.1 c-Myc activation causes an increased frequency of NE rupture events

To test the effects of c-Myc activation on NE rupture, I used a transfection approach in which I transiently transfected a plasmid containing copGFP fused to a nuclear localization signal (NLS). This is a well-established system for visualizing NE rupture events. Once expressed, the copGFP localizes to the nucleus due to the attached N-terminal NLS. Upon NE rupture, it leaks into the cytoplasm, leading to a reduction in nuclear signal and a corresponding increase in cytoplasmic signal; once the site of rupture is repaired, this cytoplasmic signal decreases once more as the protein is localized back into the nucleus, resulting in the same signal localization as before the NE rupture event (Figure 5.1B). 5.1C shows a schematic of the pipeline I followed. I first seeded RPE1 c-Myc ER cells to attach for a full day, after which I transiently transfected them with the copGFP plasmid (Addgene 132772) and treated them with tamoxifen to induced c-Myc activity for the 48h timepoint. I then imaged the cells 24 hours after transfection for a further 24 hours using a widefield time-lapse microscope,

acquiring every 5 minutes. This led to the acquisition of several 24-hour time course movies showing the fluorescence signal from the nuclear localized copGFP expressed from the transfected plasmid (example montages shown in 5.1D).

A

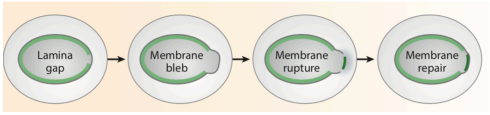

B

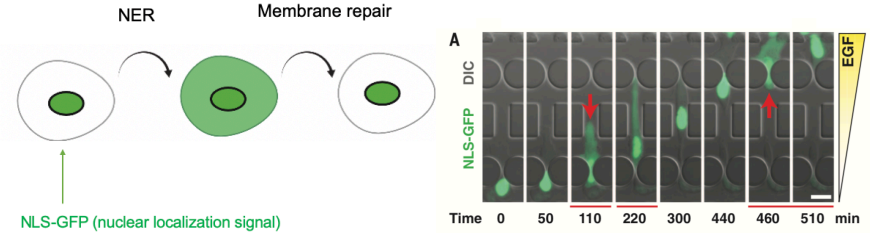

C

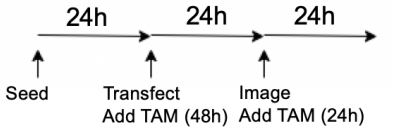

D

untreated or 24h c-Myc

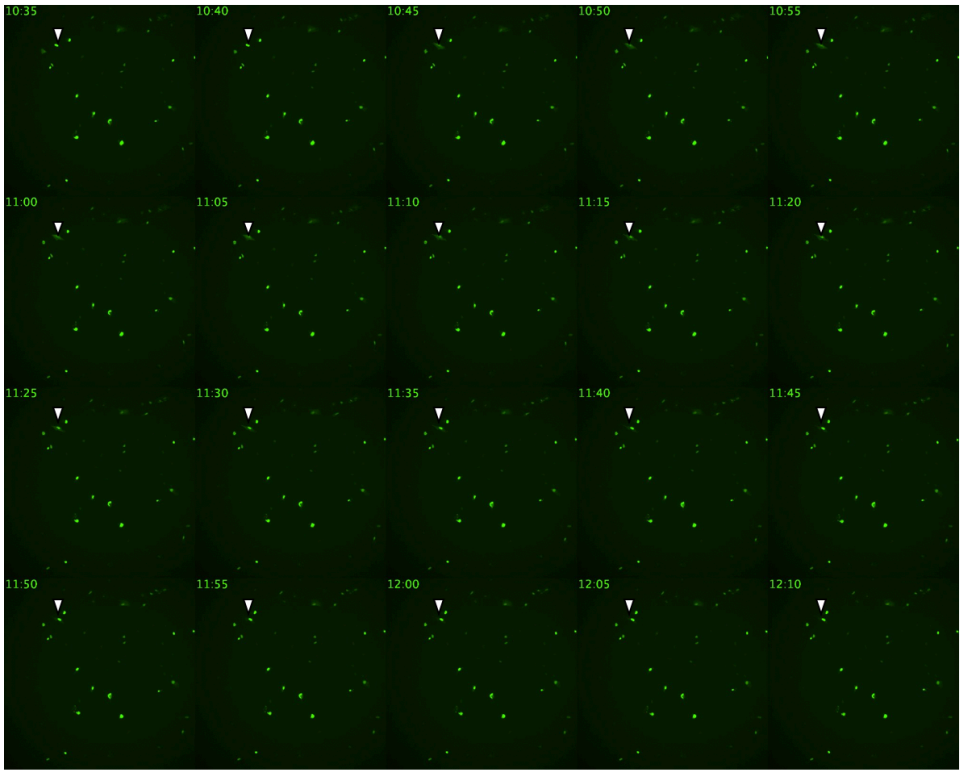

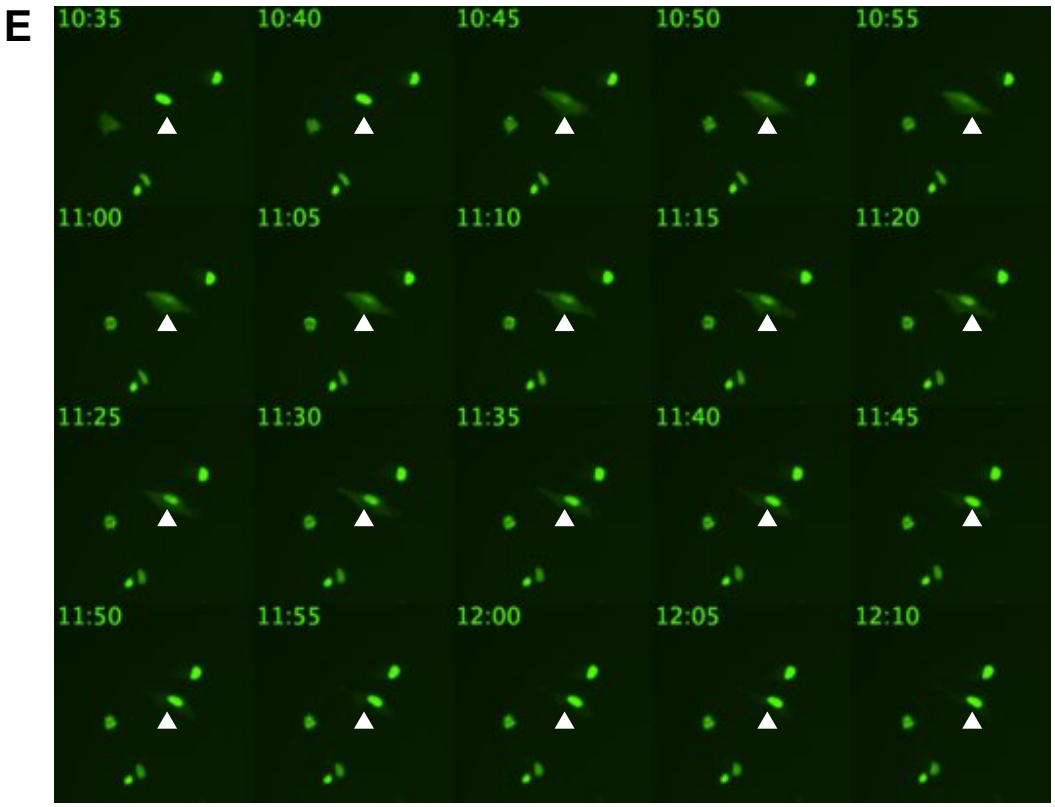

Figure 5.1 (previous): Experimental setup for visualizing NE rupture events in c-Myc induced cells. (A) Diagram showing the main steps of NE rupture and repair. Of note is that rupture events are initiated at sites of where there are gaps in the underlying lamina. (Figure taken from Maciejowski and Hatch, 2020). (B) Left: Diagram showing the signal localization of NLS-GFP under normal conditions, that then leaks into the cytoplasm upon NE rupture, after which membrane repair leads to its reuptake into the nucleus. Right: An example of an NE rupture event as visualized by this set up; rupture occurs in this case during nuclear migration through narrow constrictions, after which membrane repair restores NE integrity (Taken from Denais et al., 2016). (C) Schematic showing timings of transfection, drug treatments and imaging for untreated, 24h c-Myc and 48h c-Myc induced cells. (D) Example montage generated from acquired 24-hour movies, with white arrowheads showing a transient single NER event. (E) Close up of NER event shown at white arrowhead in panel D.

Although there are available methods of automation with NE rupture event analysis, their reliance on the signal intensity of a second, cytoplasmic marker as well as the NLS-GFP signal meant that these were unavailable to use for this experimental setup. In addition, automated tracking and segmenting individual nuclei, which tended to migrate long distances and often moved in close proximity to each other over the 24 hour time-course was challenging, meaning the simplest way to analyse the data was direct visual scoring of individual NE rupture events and their frequency (Figure 5.2).

5.2A shows the results of the experiment. Nuclei underwent one of three possible fates during the time-course. Firstly, they could have remained intact with no NE rupture events throughout the imaging process (left). Secondly, they could have undergone one or several NE rupture events, accompanied by nuclear membrane

repair and cellular survival. These events were characterized by a transient reduction in nuclear GFP signal, a corresponding increase in cytoplasmic signal, and a restoration of the original localization on the order of 15 minutes to one hour. A third possible outcome was apoptosis, characterized by nuclear blebbing and fragmentation and indicative of cell death. This could have been due to phototoxicity of the prolonged imaging process, or catastrophic GIN caused by NE rupture leading to loss of viability and death.

5.2B shows the numbers of nuclei in each of the outcomes for three conditions for one representative experiment. We can see that c-Myc activity at 24h increases both the number of nuclei undergoing at least one NE rupture event and cell death. This increase is even more pronounced at 48 hours of activity, with more cells that have ruptured than remained intact within the sample. 5.2C shows the same data across three separate experiments, with the proportion of nuclei that had ruptured at least once during the time-course. We can see that c-Myc activity causes significant increases in this value at both 24 and 48 hours of activity, and that longer c-Myc activity leads to a higher proportion of nuclei that have ruptured. Similarly, 5.2D shows that c-Myc activity causes a significant increase in the percentage of nuclei that have apoptosed compared to untreated cells. Finally, 5.2E shows that c-Myc activation significant increases in the average number of rupture events per nucleus compared to untreated cells, again that correlates with longer c-Myc activity.

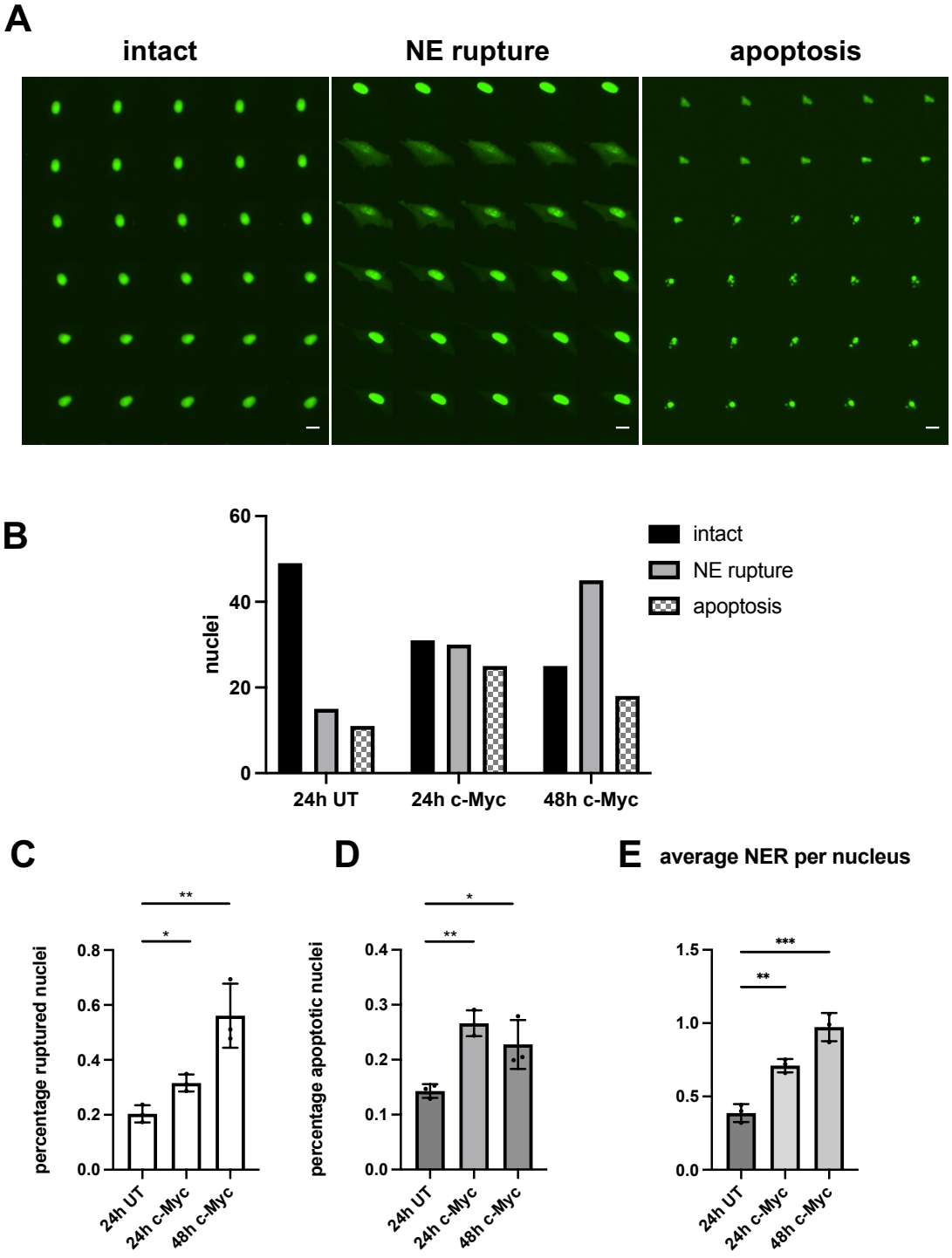

Figure 5.2: c-Myc activity causes an increase in frequency of NE rupture events. (A) Representative montages (30 frames, 150 minutes) of the three possible outcomes a cell can undergo within the time-course (details on phenotypes in methods). Left: nuclei remain intact throughout. Centre: nuclei undergo at least one NE rupture event. Right: nuclei undergo blebbing and fragmentation due to apoptosis. Scale bar = 20μm. (B) Representative bar graph showing numbers of nuclei in each of the three categories. (C) Bar graph showing percentage of nuclei that have undergone at least one NE rupture event. (D) Bar graph showing percentage of nuclei that have undergone at apoptosis. (E) Bar graphs showing average number of NE rupture event per nucleus in each condition. All graphs show mean ± SD. Representative of n = 3, 50-100 nuclei per condition. All statistical analyses were performed using an unpaired student's t-test (* $p < 0.05$, ** $p < 0.01$, *** $p < 0.001$, **** $p < 0.0001$).

Taken together, these results demonstrate that c-Myc activity leads to a downstream increase in frequency of NE rupture events. What is striking is that this seems to correlate with duration of c-Myc activity, with proportionately almost twice as many nuclei rupturing during the time-course when c-Myc is induced for 48 hours compared to 24 hours. The next outstanding question would be to establish conclusively whether this result is due specifically to c-Myc induced changes in the nuclear lamina, and not some indirect consequence of other processes that it deregulates. To do this, a rescue experiment would need to be set up, in which levels of lamin A are restored to untreated under c-Myc activity and NE rupture event frequencies analysed.

c-Myc's effects on apoptosis are also complex. Whilst the simple explanation would be to state that an increase in catastrophic GIN due to c-Myc induced NER causes this increased cell death, the fact that there was little difference in apoptotic proportions between 24 and 48 hours of c-Myc suggests other processes are at play. Furthermore, even just over 10% untreated cells underwent cell death, most likely due to the low level of phototoxicity the experiment necessitated, as both the length of the movie and the need to acquire images every 5 minutes for a high resolution of rupture events meant that cells were not subjected to physiological conditions.

One intriguing follow up would be to observe these cells for longer time-courses and investigate whether there was a link between c-Myc induced cells that underwent more NE rupture events and their levels of DNA damage and GIN. This could be done by co-transfecting with a marker for DNA damage, such as γ-H2AX or 53-BP1 and visualizing the frequency and localization of their foci in cells with multiple NE rupture events compared to ones whose nuclei have remained intact. This would then shed light on the functional consequences of NE rupture in early stage oncogenesis and its contribution towards tumour cell evolution. Overall however, this data provides promising preliminary evidence suggesting c-Myc induced changes to nuclear architecture could directly lead to downstream increases in NE rupture events and subsequent GIN.

5.2 c-Myc activation causes increased Yap1 signalling

Yap1 is a transcriptional co-activator implicated in a number of oncogenic processes such as metastasis and tissue regeneration. It has also been shown to be mechano-sensitive, with one landmark paper found that Yap activity and localization was regulated by ECM stiffness, with cells plated on stiff (40 kPa) hydrogels displaying nuclear localization of Yap1, whereas those on 0.7 kPa gels had Yap1 in its cytoplasm (Dupont et al., 2011). Further work has established Yap1 as a key downstream effector of cytoskeletal contractility (via its sensing Rho GTPase activity). I wanted to therefore see if c-Myc activity and its changes to nuclear mechanics led to altered activation of this mechanosensitive signalling pathway due to increased nuclear sensitivities to mechanical forces.

To test this, I first imaged cells using fixed cell immunofluorescence, staining for total levels of Yap1 protein. I found that c-Myc activity caused a significant increase in levels of Yap1 found within the nucleus at both 24 but not 48 hours after c-Myc activation (5.3B). I then followed this up by looking at levels specifically of active Yap1 (non-phosphorylated) bound directly to chromatin, as a proxy for levels of Yap1 activity. In this experiment, cells were first extracted to remove all proteins not directly bound to chromatin before fixation, blocking, staining and imaging. Here, I found that again, c-Myc activity caused a significant increase in levels of active chromatin-bound Yap1 at both timepoints (5.3D). Taken together, these results show that c-Myc activity leads to an increase in both nuclearly localized Yap1 and chromatin-bound non-phosphorylated (active) Yap1, suggesting that c-Myc causes an increase in Yap1 signalling.

While this result is striking, further work is needed to untangle cause and effect in this situation. It is tempting to speculate that c-Myc induced changes to nuclear mechanics rendered nuclei more sensitive to cytoskeletal tension, that then led to upregulation of Yap1. However, that is one of many possible pathways in this situation; For instance, c-Myc could directly upregulate Yap1 expression. It has already been shown to enhance Yap1 protein expression independent of transcription (Xiao et al., 2013). c-Myc and Yap1 signalling are also linked, with evidence suggesting the two even work together at the transcriptional level (Croci et al., 2017). There are other indirect routes; for instance, there is evidence to suggest c-Myc causes F-actin remodeling (Lewinska et al., 2019), that could then feedback onto Yap1 signalling through its increased generation of tension onto the nucleus. One thing to note would be the

relative timescales of c-Myc's effects on both lamin A and Yap1 levels. While both lamin A reduction and Yap1 increase occur within 24 hours of c-Myc activation, lamin A reduction appears to be a more sustained phenomenon, with decreases seen even 48 hours after c-Myc activation, whereas Yap1 localization to the nucleus appears to lessen by this point. However, levels of chromatin-bound Yap1 are still sustained, indicating Yap1 signalling is likely still increased.

A

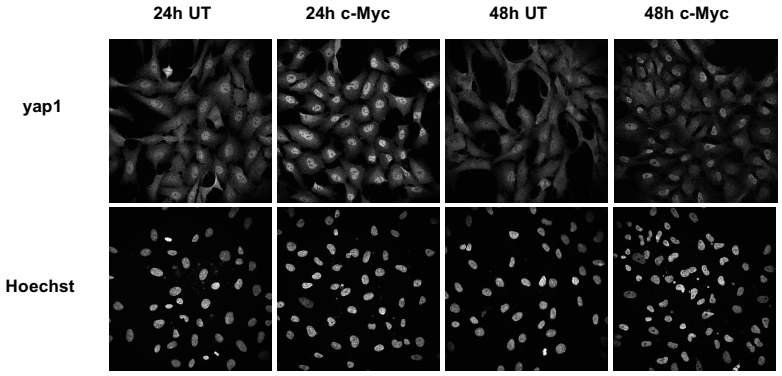
24h UT
24h c-Myc
48h UT
48h c-Myc
yap1
Hoechst

B

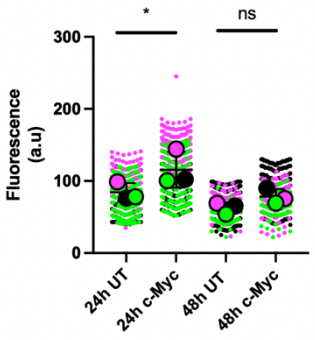
*
ns
300
200
100
0
Fluorescence (a.u)
24h UT
24h c-Myc
48h UT
48h c-Myc

C

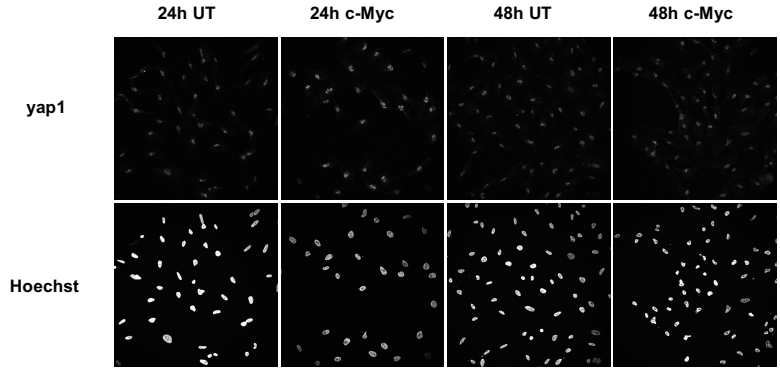
24h UT
24h c-Myc
48h UT
48h c-Myc
yap1
Hoechst

D

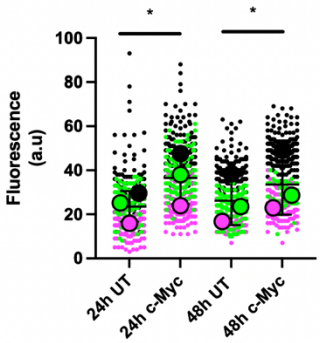
*
*
100
80
60
40
20
0
Fluorescence (a.u)
24h UT
24h c-Myc
48h UT
48h c-Myc

Figure 5.3 (previous): c-Myc activity causes an increase in Yap1 signaling. (A) RPE-1 c-Myc ER cells were untreated (UT) or treated with tamoxifen 24h and 48h before fixation, nuclear staining with Hoechst and Yap1. Scale bar = 20μm. (B) Column scatter graph of signal intensity of nuclearly localized Yap1 protein of the same cells at 24h and 48h with or without c-Myc activation. Each colour represents a separate independent experiment (black, magenta, green, n = 3, 100-200 cells per condition per experiment). Large coloured circles represent mean values per experiment. Small circles represent individual cells per independent experiment. (C) A) RPE-1 c-Myc ER cells were untreated (UT) or treated with tamoxifen 24h and 48h before fixation, nuclear staining with Hoechst and active Yap1. Scale bar = 20μm. (D) Column scatter graph of signal intensities of chromatin-bound active Yap1 protein of the same cells at 24h and 48h with or without c-Myc activation. Each colour represents a separate independent experiment (black, magenta, green, n = 3, 100-200 cells per condition per experiment). Large coloured circles represent mean values per experiment. Small circles represent individual cells per independent experiment. All graphs show mean ± SD. Representative of n = 3. All statistical analyses were performed using a paired student's t-test on mean values of circularity, area and interquartile range between conditions. (* $p < 0.05$, ** $p < 0.01$, *** $p < 0.001$, **** $p < 0.0001$).

5.3 c-Myc's effects to nuclear morphology and architecture are not dependent on substrate stiffness

One last aspect of nuclear mechanics that I studied was the possible dependence of c-Myc induced nuclear alterations on the stiffnesses of the substrates on which the cells were plated. To test this, cells were plated onto 2D polymer polydimethylsiloxane (PDMS) substrates with tunable stiffnesses varying from no substrates (plastic) to 40 kPa (Figure 5.4A). The substrates themselves were first plasma cleaned and coated with fibronectin to ensure cell adhesion.

5.4B shows that c-Myc induces an increase in cells passing through S-phase 24 hours after activation, indicating an accelerated passage through the cell cycle. However, these changes are not dependent on substrate stiffness. Similarly, 5.4C shows that c-Myc induced silencing of lamin A does not change based on substrate stiffness, nor does its induction if DNA damage (as seen by the marker γ-H2AX). Taken together, these studies suggest that c-Myc-induced changes to the nuclear lamina are not affected by mechanical alterations to bulk substrate stiffness.

One caveat however with the usage of PDMS was that the range of stiffnesses tested do not reflect a physiological range. For instance, bone tissue has a stiffness of around 100 kPa, while brain tissue just 1 kPa. Whilst these differences are large, they are nowhere near the orders of magnitude differences that I investigated, meaning that any physiological dependence of c-Myc activity on stiffness likely was not observed due to this lack of resolution. Further systems using polyacrylamide (PA) hydrogels, which vary both bulk stiffness and adhesion ligand density (Trappman et al., 2012) will provide a more accurate picture, as these are more representative of

varying matrix stiffness in an *in vivo* context, with more finely tuned differences (on the order of 0.7 to 50 kPa).

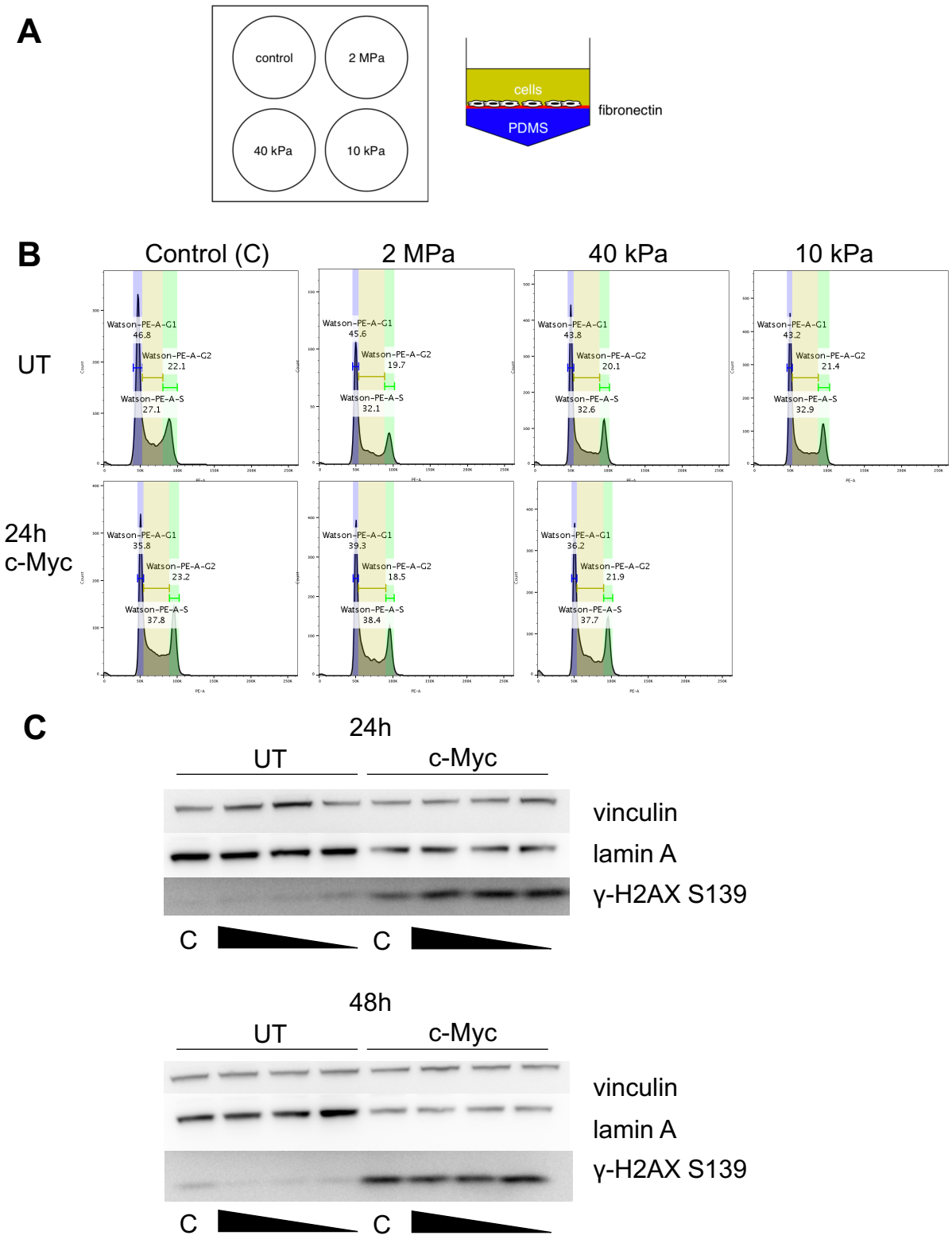

Figure 5.4: c-Myc's effects on the cell cycle, nuclear architecture and DNA damage are not dependent on substrate stiffness. (A) Schematic showing the experimental setup for plating cells on PDMS substrates of varying stiffness (Young's modulus). (B) RPE1 c-Myc ER cells were plated on PDMS and untreated or treated with tamoxifen (c-Myc) for 24 hours, before cell cycle profiles were analysed by propidium iodide (PI) staining. Representative of n = 2.

Figure 5.4 continued. (C) Representative blot of cells that were plated on PDMS substrates and untreated (UT) or treated with tamoxifen (c-Myc) for 24h and 48h and probed for vinculin, lamin A and γ-H2AX (S139) Both blots representative of n = 3.

5.4 Summary and Model

To summarise, I have found that c-Myc induced nuclear alterations lead to an increased frequency of NE rupture events (Figure 3.5). This represents a key link between the molecular changes that c-Myc activation causes in the short term and further long-term contributions towards tumorigenesis, as NE rupture is one of the most well studied processes by which cells experience increases in DNA damage and loss of genome integrity. Further work should focus on characterizing the precise consequences of c-Myc induced NE rupture and how it may differ from rupture events generated in other scenarios (such as during migration through narrow constrictions).

I have also shown that c-Myc activity causes an increase in Yap1 signalling through an increase in nuclear and active Yap1. The causality here is unclear, and there is already extensive evidence linking c-Myc and Yap1 signalling, meaning it is perhaps unsurprising that one would influence the other so robustly. Further experiments focusing on c-Myc induced changes to upstream Yap1 regulators, such as Rho GTPase activity or ECM stiffness will be necessary to tease apart the sequence of events. Finally, I have found that c-Myc's effects on the nucleus appear to be independent of substrate stiffness, though smaller trends may have been masked by the range of stiffnesses used in my initial set up.

My overall model is shown in Figure 5.5. c-Myc activation causes a rapid and significant silencing of lamin A and lamin B1 mRNA and protein. This then leads to their mislocalisation at both the nuclear lamina and nucleoplasm, resulting in the abnormal nuclear morphologies that I first saw. As a result of this dysregulation in nuclear architecture c-Myc induced nuclei undergo an increased frequency in NER events that increase the levels of DNA damage and GIN that these cells experience, contributing to the process of early cell oncogenesis.

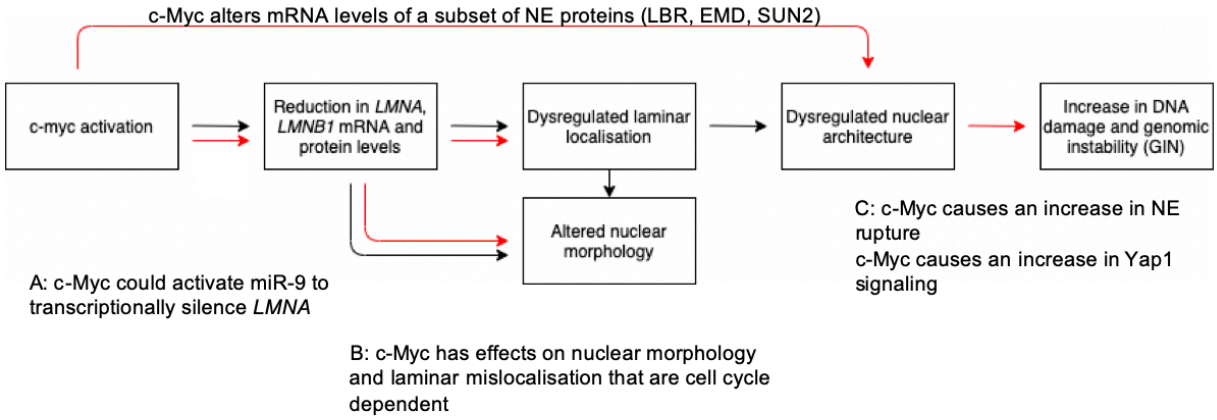

Figure 5.5: summary of model (Chapters 3-5). C-Myc induced increases in NE rupture frequency are the first link between the short-term molecular alterations to nuclear architecture and longer term increases in GIN, a hallmark of cancer.

6. Discussion

Abnormal nuclear morphologies are a common and widespread phenotype of cancer nuclei and have been recorded for some time (Fischer et al, 2020). Until recently however they were used mainly as a reliable diagnostic tool to identify tumour tissue in histological samples. There was comparatively little study devoted towards either the mechanistic pathways these nuclei take develop their irregular appearance, or their potential contribution towards the tumorigenic process itself, such as the effect of abnormal morphologies towards nuclear function and gene expression. Research into these areas would help shed light on a fundamentally conserved and therefore key feature of tumour evolution and may eventually provide previously unknown key targetable features in tumour cells that are involved in the maintenance of nuclear morphology, to be used either as diagnostic biomarkers or even as selective agents that disrupt the function of tumour cells whilst leaving normal cells unharmed (to be discussed later in this chapter).

Given that the mechanisms that underly these changes are cancer-type dependent and multifactorial, my project aimed specifically to study the generation of abnormal nuclear morphologies and architectures within the context of oncogene activity, using a c-Myc inducible cell line as a model for early cell oncogenesis. My work contained two main aims: firstly, to describe and investigate the effects of c-Myc activity on nuclear architecture and nuclear morphology. Secondly, to then further investigate the contribution of these c-Myc induced changes to nuclear morphology and architecture towards early oncogenesis and subsequent tumour evolution.

6.1 c-Myc induces acute and significant alterations to nuclear morphology and nuclear architecture

Whilst nuclear atypia is a common feature of cancerous tissue, the mechanisms of its formation is unclear and likely both complex and multi-factorial (Fischer et al., 2020). Indeed, there was limited evidence in the literature suggesting that increased oncogene activity alone could produce nuclear atypia, with a study finding that artificial introduction of the *RET/PTC* oncogene to thyroid epithelial cells led to direct alterations (referred to as ‘NE irregularities) at 18 and 24 hours after injection (Fischer et al., 2003). The presence of these defects in pre-mitotic nuclei suggested that post-

mitotic NE re-assembly was not required for their generation, though the precise mechanistic details are still unclear. Whilst this was encouraging proof of concept, there was no evidence specifically linking c-Myc activity to the regulation of nuclear morphology. In Chapter 3, I first found using an oncogene inducible cell line that c-Myc activity alone was sufficient to lead to changes in nuclear morphology (in the form of reductions to nuclear circularity and changes to nuclear area) from 24 hours post activation, which was maintained with longer c-Myc activity, at the 48 hour timepoint. This increase in the proportion of irregularly shaped nuclei is seen by visual scoring of the same data and overall suggests that c-Myc activity causes direct changes in nuclear shape. This first result provided encouraging evidence that the c-Myc inducible system was a valid model to study the induced changes to nuclear morphology that occur in very early stage oncogenesis. Two essential additions to these initial studies would be a positive control to verify c-Myc activity (e.g., through measuring transcript levels of target genes) and a negative control to verify the effect is not due to 4-OHT alone (comparison with 4-OHT treated RPE1 ER-empty cells that do not contain c-Myc-ER).

As I found such a striking increase in the frequency of irregularly shaped nuclei, I then investigated whether c-Myc activity has any effects on altering the dynamics of the main regulators of morphology in non-cancerous nuclei. As discussed in Chapter 1, there are three main determinants of nuclear morphology: the nuclear lamina, the cytoskeleton and chromatin. I found that c-Myc activity resulted in alterations to transcript levels of two main lamin isoforms (lamins A and B1), as well as those of beta-actin and alpha-tubulin. This was accompanied by corresponding reductions in the protein levels of the first three proteins, as well as beta-tubulin. This was further evidence that c-Myc activity could lead directly to changes to nuclear morphology and mechanics through its potential effects on the reduction of key structural components to the nuclear lamina, perhaps through rendering c-Myc induced nuclei more mechanically fragile and prone to deformation. I also found significant changes in transcript levels of certain other proteins found at the NE, most notably reductions to levels of *SUN2* (SUN2) and *LBR* (lamin B receptor) and significant increases to *EMD* (emerin) mRNA levels. The most striking of these was the induced increase to *EMD* transcript levels, which I then followed up in a later set of experiments.

In terms of cytoskeletal dynamics, studies have shown that contractile forces generated by actomyosin stress fibres can indent the surface of the nucleus and result in nuclear fragmentation and morphological abnormalities, leading to increased

genome instability (Takaki et al., 2017). Indeed, the impact of cytoskeletal dynamics on genome stability can be seen in several studies have shown that F-actin fibers themselves exert compressive forces directly onto the NE that lead directly to nuclear deformations and NE rupture events (Hatch and Hetzer, 2016).

Within this context, it is plausible that c-Myc's effects on nuclear morphology defects can be partially mediated through its potential impact on cytoskeletal dynamics through the levels and/or polymerization state of actin filaments. One study in medulloblastoma (MB) cells has already demonstrated that c-Myc activity can promote cytoskeletal remodeling through its induction of an oxidative stress response pathway that promotes the nuclear translocation of the actin polymerization regulator cofilin (Lewinska et al., 2019). Other work has also demonstrated the presence of transcriptional cross-regulation between the c-Myc and RhoA signaling pathways, with c-Myc activity leading to the blockage of specific branches of the RhoA pathway resulting in altered dynamics of stress fibre induction and contractility (Sauzeau et al., 2010).

My preliminary work has highlighted the potential effect c-Myc activity has on the levels of key components of the cytoskeletal network, through its apparent reductions in the mRNA and protein levels of actin and tubulin subunits. Whilst not followed up in my project, further work using microscopy to image actin polymerization and localization would be an intriguing avenue of research, especially if c-Myc activation leads to increased actomyosin contractility that can then exert direct forces upon the nucleus. Very preliminary work (data not shown) has indicated that c-Myc activation may induce the formation of a higher density of F-actin stress fibres compared to untreated cells, but higher resolution imaging approaches are needed to elucidate their precise dynamics. A separate line of inquiry that would be important here is the usage of chemicals that modify actin dynamics (such latrunculin A) to investigate whether depolymerization or reduction of F-actin stress fibre formation can rescue c-Myc induced nuclear abnormalities.

I then focused on c-Myc's potential effects on levels of proteins that compose the nuclear lamina. This was because the lamin proteins that compose the nuclear lamina are very well studied and their levels have been shown to vary widely within different cancers (thus providing my data a clinically relevant context). A third reason would be that they provided attractive and relatively mechanistically straightforward processes

to study, compared to the complexity of assessing c-Myc's effects on cytoskeletal dynamics or chromatin organisation (discussed later).

Using fixed-cell immunofluorescence, I then found that the localisations of both lamins A and B1 were heavily disrupted at both the edge and centre of c-Myc induced nuclei. Whilst this abnormal distribution would likely have significant effects on resultant nuclear mechanics, what was especially striking was the presence of areas of the lamina where one or another of the lamins was absent, leading to visible gaps. This was illuminating as these gaps could encourage the initiation of NE rupture events through chromatin leakage into the cytoplasm. Such events have been well studied and are well-established generators of increased DNA damage and GIN, important to the tumour evolution process. The presence of these gaps and irregular localisation of lamins also suggests that c-Myc induced nuclei are more fragile and mechanically vulnerable to deformation than those of untreated cells, providing an explanation for the irregular morphologies seen and the downstream increases in GIN. Lamin silencing has already been linked to an increase in nuclear fragility and a decrease in nuclear stiffness in many systems, but direct measurements of nuclear stiffnesses between untreated and c-Myc induced nuclei using atomic force microscopy (AFM) would be one further experiment that could support this hypothesis within my system.

Nucleoplasmic lamins were also mislocalised, with alterations in their levels between untreated and c-Myc induced nuclei. The functions of these lamins are less well-studied, though it is speculated that their roles are less structural and more towards the regulation of nuclear processes such as cell cycle progression, differentiation and gene expression (Dorner et al., 2007). What is clear from this initial set of experiments is that c-Myc has profound effects on the levels and localization of lamin proteins that themselves play a wide range of key roles that impact both nuclear function and mechanics. Due to this, lamin silencing is an attractive mediating mechanism to explain c-Myc's wide ranging effects, though it is of course unlikely to be the only contributor towards abnormal nuclear morphology.

I then investigated the effects of c-Myc's induced increase in emerin transcript levels. Emerin is perhaps the second most well studied NE protein behind the lamins, is a key lamin A binding partner and has roles in regulating nuclear morphology in ovarian cancer cells (Watabe et al., 2022), with its silencing linked to both nuclear shape instability (Reis-Sobreiro et al., 2018) and cancer progression and metastasis (Liddane et al., 2021). I found that the abovementioned increase in *EMD* transcript

levels came with a corresponding upregulation of emerin protein and an altered localization, with a larger frequency of nuclei containing prominent clusters of cytoplasmic emerin close to the ONM ('perinuclear emerin') at sites of high local NE curvature. Further antibody validation would help to reduce the signal to noise ratio in these images to generate images with potentially higher resolution into the precise localisations of both this perinuclear and NE emerin deposits.

Whilst these perinuclear emerin foci are intriguing, further work is necessary to elucidate their precise role in nuclear morphology. Given emerin's role in capping actin filaments (Holaska et al., 2004) and regulating actin flow (Chang et al., 2013), it is tempting to speculate that their increased levels are a response to c-Myc induced increases in F-actin stress fibre formation that lead to an increase in contractile forces upon the nuclei (leading to their deformation) that are mediated directly by these perinuclear emerin foci. A key experiment to begin untangling this would be to perform colocalization and binding analysis with F-actin filaments and emerin to see whether they are both found at sites of NE deformation.

Finally, I decided to focus on the effects of lamin A and found that silencing it alone in untreated cells lead to increases in the levels of several downstream markers typically seen on c-Myc activation at the same time points. This was in the form of increases to the levels of rRPA S33 (replication stress), DNA damage (pγH2AX S139) and the activation of the DNA damage response (pRPA S4/8). This again provided evidence that c-Myc induced lamin A silencing was a key contributor towards c-Myc induced early stage oncogenesis, through the resulting increases in DNA damage and GIN. Further work is needed to follow these lamin A silenced cells through for instance a colony formation assay to investigate their subsequent viability and proliferative potential. This would provide additional evidence of that reductions in lamin A levels represent an important step in early tumour cell transformation. n addition, several controls (vehicle only control and simultaneous RT-qPCR of *LMNA* mRNA transcript) are essential to validate that these phenotypic changes are due specifically to lamin A silencing and nothing else.

6.1.1 Chromatin contributions towards nuclear morphology and architecture.

As already discussed, nuclear morphology is the product of a complex interplay between three main determinants: the nuclear lamina, the cytoskeletal network and the underlying chromatin. Given the limited scope of my work, which focuses on c-Myc's effects specifically upon the nuclear lamina and the NE, it is important to note

the potential contributions of c-Myc induced alterations to chromatin organization towards nuclear shape.

Gross alterations to chromatin conformation, such as drug-induced increases in the proportion of euchromatin or heterochromatin can induce corresponding blebbing and large-scale changes to nuclear morphology and mechanics (Stephens et al., 2017, Stephens et al., 2018). This is thought to occur via large alterations to nuclear mechanics: increasing euchromatin in mouse embryonic fibroblasts (MEFs) led to softer nuclei that were more fragile and prone to blebbing (Stephens et al., 2019).

There is much evidence to suggest that c-Myc activity has widespread effects on global chromatin organization through its regulation of chromatin remodeling complexes. Early work first identified the HATs Gcn5-related N-acetyltransferase (GCN5) and tat-interactive protein 60 (Tip60) as key interacting partners with c-Myc (Frank et al., 2003, Knoepfler et al., 2006). It is now known that c-Myc interacts with a wide range of HATs that combine to mediate c-Myc's crucial role in the regulation and alteration of chromatin organization and subsequent nuclear morphology.

Whilst it would be tempting to speculate that a significant part of c-Myc's effect on nuclear morphology and mechanics is mediated by alterations to chromatin organization, further work is necessary to elucidate whether this is the case within our system. Firstly, it is necessary to demonstrate whether the activation of several of c-Myc's target chromatin remodeling complexes is sufficient by itself to induce similar nuclear morphology defects to c-Myc activation. It is also important to then demonstrate that these wide-scale changes to chromatin organization have significant downstream consequences in terms of increases to GIN to contextualise the process within early-stage oncogenesis. Given that c-Myc is involved in the regulation of a wide range of chromatin remodeling proteins, it is likely that the contribution of individual c-Myc activated HATs towards overall nuclear morphology is minor and less significant than its effects on elements of the nuclear lamina or cytoskeleton. Nevertheless, an investigation into c-Myc induced alterations to chromatin conformation is an intriguing line of inquiry. Overall, what is clear is that nuclear morphology is a complex and context-dependent phenomenon regulated by multiple elements and that it is important to isolate and evaluate the relative contributions of the three determinants (lamina, cytoskeleton and chromatin) within my studied system of induced early stage oncogenesis.

6.2 c-Myc silencing of lamin A is cell-cycle dependent and may be mediated by miR-9

Having established a set of robust nuclear phenotypes observed to occur on c-Myc activation, I decided to focus on investigating the mechanism of c-Myc's silencing of lamin A protein as the most significant contributor to both the aberrant nuclear morphologies and downstream increases in DNA damage and GIN that contribute towards tumorigenesis.

Whilst lamin A expression has been shown to vary considerably across cancers with both increases and decreases in levels seen, there is currently no evidence in the literature linking c-Myc activity with lamin A downregulation. An important additional experiment therefore would be the computational search of human cancer databases to see whether there is a correlation between c-Myc amplified tumours and lamin A silencing. However, it is important to note that the system used in my project only studies the initial stages of oncogenesis up to 48 hours after activation, which may not be relevant to the processes that occur or are seen in mature tumour tissue.

The c-Myc induced silencing of lamin A observed was both robust and challenging to explain. There were two questions to be addressed. Firstly, how c-Myc caused a reduction in expression levels of *LMNA* transcript (and subsequently lamin A protein). Secondly, whether c-Myc caused an increase in the degradation of existing lamin A protein within the nucleus. Given lamins are very stable proteins with long half-lives, it is likely that c-Myc caused both a reduction in lamin A expression and an increase in its degradation to produce the silencing observed just 24 hours after activation.

To address the question of increased degradation, I decided to investigate several well known post-translational modifications to the lamin A protein itself that affected its stability, to see whether c-Myc caused an increase in certain markers that resulted in an increased degradation of existing lamin A protein. However, I found that c-Myc does not cause increases in phosphorylation of S22 or direct cleavage by caspase-6. In addition, I have also found that there is no change in in Akt activity on c-Myc activation, which was an otherwise common mechanism by which lamin A is phosphorylated at S404 and targeted for degradation.

Further work is necessary to confirm these findings. Firstly, it is important to investigate lamin A half-life directly to verify whether there is indeed increased lamin A degradation on c-Myc activation. The simplest method would be a pulse-chase experiment, similar to one described in where cells would be transfected with a N-terminally tagged lamin A protein and incubated in media containing ^{35}S-methionine ("the pulse") before being grown in non-radioactive media for various timepoint (0, 4, 12 and 24 hours). Lysates could then be collected and levels of radioactive lamin A measured first by extracting the protein using anti-FLAG M2 affinity agarose gel and separated by SDS PAGE to measure the decline in levels of lamin A over time.

It is also important to further investigate the relationship between c-Myc and Akt activity, as well as directly assay levels of lamin A pS404. Given total Akt levels were not probed, there is a possibility that c-Myc induction does cause an increase in Akt activity which was not detected by probing for phosph-Akt levels alone. These findings also do not rule out the possibility of the induction of other, less well studied post-translational modifications such as SUMOylation being responsible for an increased degradation.

I next investigated the possible interplay between lamin A silencing and emerin upregulation. Given the two were binding partners, and that emerin relies on lamin A for localization at the NE (Vaughan et al., 2001), it was possible that c-Myc induced lamin A silencing was responsible for emerin upregulation, or vice versa. However, I found through RT-qPCR assays and imaging studies that there was little interaction between the two phenomena, with their generation appearing to constitute two separate and distinct downstream consequences of c-Myc activity. Whilst this did not reveal any causal link between the two phenomena, it did further underline the complex and pleiotropic nature of c-Myc activity, with the dysregulation of two proteins otherwise linked in the maintenance of nuclear morphology through apparently separate mechanisms.

I next investigated whether c-Myc induced silencing of lamin A was mediated by the production of micro-RNA molecules. Micro-RNA-9 (miR-9) was first identified as a regulator of neurogenesis (Krichevsky et al., 2006) and whose deregulation was since then implicated in tumour development. Work has showed that miR-9 was a c-Myc target (Ma et al., 2010), and that it was responsible for the degradation of lamin A in brain tissue (Jung et al., 2012). Unfortunately I found, through the use of an miR-9 inhibitor molecule that c-Myc induced lamin A silencing was not significantly rescued

by the inhibition of miR-9 activity, suggesting that further work is needed to determine whether c-Myc induced lamin A silencing was mediated in part by its production of miR-9.

In terms of follow-up experiments, firstly, an assay of mi-R9 levels on c-Myc induction within the inducible system would provide the most direct evidence of c-Myc induced miR-9 production. Chromatin immunoprecipitation (ChIP) assays would also be important at the miR-9 promoter to see whether c-Myc induces its upregulation through direct binding or via a more indirect mechanism.

Taken together, it is perhaps unsurprising that there was no single mechanism by which c-Myc induces lamin A silencing. The likelihood is that the silencing is the result of several pathways, both local and global that result in an overall lower level of transcript and protein. There is the possibility that lamin A and B1 levels are downregulated due to a global transcriptional effect of c-Myc; that is to say that their silencing is not by a specific mechanism but more a consequence of the demand that c-Myc activity places on the cell's transcriptional machinery that results in inadequate synthesis of proteins required in regular interphase. Another unexplored idea is that c-Myc activation causes changes to global and local chromatin structure, leading to certain genes and their promoters (such as *LMNA* and *LMNB1*) becoming less accessible to their transcription factors, resulting in lower expression levels overall.

Finally, I wanted to see whether c-Myc induced lamin A mislocalisation and resulting nuclear morphology defects were dependent on the cell cycle state of the cells themselves. I found, through the use of Cdk1 inhibitor RO-3306, that c-Myc induced nuclear morphology defects and lamin A mislocalisation were not present if c-Myc was activated in cells that were already arrested in G2 phase. This provides evidence for the idea that c-Myc activity does not lead to either the mislocalisation of lamin A or reductions in nuclear circularity until progress through the first mitosis after induction. This lends support to the idea that NE disassembly and reassembly is the main point at which morphology defects appear, during which the limited post-mitotic supply of available lamin proteins means that they are not adequately deposited within the two daughter nuclei, resulting in mislocalisation and subsequent irregularity in their nuclear morphologies.

If the abovementioned nuclear morphology defects and lamin A mislocalisation only appeared after the first mitosis, it would also suggest that c-Myc activity in cells

arrested in interphase would also not lead to irregular nuclei. Using a the Cdk4/6 inhibitor palbociclib, I found however that c-Myc activity in cells arrested in G1 phase still led to altered lamin A localization and nuclear morphology defects. This suggested therefore that c-Myc induced nuclear defects are only partially dependent on entry into mitosis. However, it is important to note that arresting cells in G1 phase, during which nuclei grow and lamins are synthesized and incorporated into the nuclear lamina, would affect lamin A dynamics through a separate process to c-Myc's effects in cycling cells. It is possible that c-Myc activity in cells arrested in G1 lead to abnormal lamin A mobility that affects its localization both at the lamina and within the nucleoplasm; this could then result in morphology defects through the altered nuclear mechanics that this causes. Further work is needed firstly to verify with a solvent only control that the effect on cell cycle profile and circularity and localisation are not partially due to DMSO, and secondly to understand the dynamics of lamin A synthesis and degradation during the cell cycle in untreated cells, and to see what parts of this process are deregulated on c-Myc activation.

6.3 The downstream consequences of c-Myc induced alterations to nuclear architecture and morphology.

Through my work I have seen that c-Myc induced changes to nuclear architecture and morphology are multifactorial and significant. Having focused on c-Myc induced lamin A silencing as a key mediator in the oncogenic process, I wanted to investigate the downstream consequences of this in terms of DNA damage and GIN. As already discussed, lamin A has a variety of roles that are deregulated within a cancer context, such as DNA repair, telomere localization and cell signaling. All of these are likely deregulated following c-Myc activation and present fruitful avenues of further research. However, I decided to focus on the process of NE rupture (NER), as it provides a well-established mechanism by which cells experienced increased levels of DNA damage GIN. It was also noteworthy that when first imaging c-Myc induced nuclei, there was an increased frequency of visible gaps in the nuclear lamina, the first step in the generation of a NER event. This hinted that c-Myc nuclei were more prone to NER due to the absence of regular lamin localization around the lamina, and I wanted to test whether this was true using live-cell imaging to visualize these events directly.

I found using a transient transfection approach of a plasmid containing GFP fused to a nuclear localization signal (NLS) that 24 hours of c-Myc activity did indeed lead to

an increased frequency of nuclei that underwent at least one NER event, and that this increased with longer c-Myc activity at 48 hours. This suggests that c-Myc induced lamin A (and B1) silencing leads both to mechanically fragile nuclei prone to deformation and an increased frequency of local gaps in the lamina, both of which facilitate the occurrence of NER events. This also provides evidence of the potential contribution of NER in the very first stages of oncogenesis and underlines the importance of studying NER within the context of tumour cell evolution.

6.3.1. The next steps within my model. Whilst encouraging, further work however is required in two main areas to support my model that c-Myc induced lamin A silencing results in increased NER events, that then result in increased DNA damage and GIN (Figure 5.5). Firstly, it is crucial to demonstrate that it is specifically c-Myc induced lamin A silencing that results on increased NER, and not a separate process that was not investigated. To do this, rescue experiments are necessary where c-Myc is induced in cells with lamin A expression restored to wild type levels, to see whether lamin A expression alone could result in a decreased frequency of both NER events and nuclear morphology defects even in the presence of c-Myc activity.

Secondly, it is important to verify whether these c-Myc induced increases in NER are actually causing increases in DNA damage and GIN within the nuclei themselves. To do this, a live-cell imaging approach can be used, to monitor nuclei that undergo NER events alongside markers of DNA damage, such as 53-BP1 or γH2AX foci. In addition, it would be necessary to elucidate by what mechanism(s) these NER events result in DNA damage or GIN; for instance through the prevention of DNA repair by the segregation of repair factors, or an increased generation of DSBs via direct exposure of chromatin to cytoplasmic nucleases.

A third angle by which to extend the breadth of insight of my work is to study the same phenomena of c-Myc's effects on nuclear morphology in an *in vivo* context. At present, *in vivo* studies that have employed the c-Myc-ER system in transgenic mice have not reported any similar phenomena to those seen in my work (nuclear atypia, nuclear lamina rearrangements, changes to levels of cytoskeletal proteins and an increase in NE rupture events). There are several potential reasons for this; firstly, the timescales of my work were on the order of 1-2 days post c-Myc activation, whereas *in vivo* work tracks tissue for at least 3-6 days before measuring any changes to phenotype (e.g., Murphy et al., 2008). It is possible that if I had followed my c-Myc-ER cells with sustained c-Myc activation for longer time periods any nuclear morphology defects

were resolved through compensatory mechanisms, such as selective apoptosis of nuclei exhibiting nuclear atypia (as c-Myc has been shown to induce apoptosis following sustained over-expression), with nuclei that displayed less overt morphological defects remaining; giving the appearance of no nuclear atypia. Another potential reason is that nuclei within *in vivo* contexts are in cells that grow in three dimensions, with an immediate environment of extracellular matrix. This is softer than the plastic that cells in culture are grown on, meaning the frequency of phenomena such as NE rupture may be exaggerated within this context due to increased mechanical stresses cells experience growing within culture.

It is therefore important to verify whether the phenomena I observed in cell culture occurs in a more complex (and physiologically relevant) tissue context. One initial follow-up could be to perform the same experiments using a transgenic mouse model with the same c-Myc-ER fusion protein to validate whether changes to nuclear morphology, the nuclear lamina, emerin and increased NER can be seen in tissue samples as well as in cell culture over the same timescales.

6.4 Summary

Overall, my work (summarized in Figure 5.5) has investigated the effects of c-Myc activity on regulators of nuclear morphology and architecture and has then looked into the contributions these effects have towards oncogenesis. Specifically, I have found that c-Myc activity induces an acute downregulation of both lamins A and B1 that result in their mislocalisation and abnormal nuclear morphologies. These then lead to nuclei that undergo an increased frequency of NER events that is a well-established way by which cells experience increases in DNA damage and GIN. Taken together, my work has important implications for understanding the process of tumour evolution. It provides evidence that oncogene induced alterations to nuclear morphology are important drivers of tumour cell transformation and links oncogene activity to an increase in NER events.

7. Bibliography

Alhudiri, I. M., Nolan, C. C., Ellis, I. O., Elzagheid, A., Rakha, E. A., Green, A. R., & Chapman, C. J. (2019). Expression of Lamin A/C in early-stage breast cancer and its prognostic value. *Breast cancer research and treatment*, *174*(3), 661–668.

Alisafaei, F., Jokhun, D. S., Shivashankar, G. V., & Shenoy, V. B. (2019). Regulation of nuclear architecture, mechanics, and nucleocytoplasmic shuttling of epigenetic factors by cell geometric constraints. *Proceedings of the National Academy of Sciences of the United States of America*, *116*(27), 13200–13209.

Alitalo, K., Ramsay, G., Bishop, J. M., Pfeifer, S. O., Colby, W. W., & Levinson, A. D. (1983). Identification of nuclear proteins encoded by viral and cellular myc oncogenes. *Nature*, *306*(5940), 274–277.

Aljada, A., Doria, J., Saleh, A. M., Al-Matar, S. H., AlGabbani, S., Shamsa, H. B., Al-Bawab, A., & Ahmed, A. A. (2016). Altered Lamin A/C splice variant expression as a possible diagnostic marker in breast cancer. *Cellular oncology (Dordrecht)*, *39*(2), 161–174.

Almeida, F. V., Walko, G., McMillan, J. R., McGrath, J. A., Wiche, G., Barber, A. H., & Connelly, J. T. (2015). The cytolinker plectin regulates nuclear mechanotransduction in keratinocytes. *Journal of cell science*, *128*(24), 4475–4486.

Amati, B., Brooks, M. W., Levy, N., Littlewood, T. D., Evan, G. I., & Land, H. (1993). Oncogenic activity of the c-Myc protein requires dimerization with Max. *Cell*, *72*(2), 233–245.

Antmen, E., Demirci, U., & Hasirci, V. (2019). Amplification of nuclear deformation of breast cancer cells by seeding on micropatterned surfaces to better distinguish their malignancies. *Colloids and surfaces. B, Biointerfaces*, *183*, 110402.

Beagan, J. A., & Phillips-Cremins, J. E. (2020). On the existence and functionality of topologically associating domains. *Nature genetics*, *52*(1), 8–16.

Bell, E. S., & Lammerding, J. (2016). Causes and consequences of nuclear envelope alterations in tumour progression. *European journal of cell biology*, *95*(11), 449–464.

Bell, E. S., Shah, P., Zuela-Sopilniak, N., Kim, D., Varlet, A. A., Morival, J. L. P., McGregor, A. L., Isermann, P., Davidson, P. M., Elacqua, J. J., Lakins, J. N., Vahdat, L., Weaver, V. M., Smolka, M. B., Span, P. N., & Lammerding, J. (2022). Low lamin A levels enhance confined cell migration and metastatic capacity in breast cancer. *Oncogene*, *41*(36), 4211–4230.

Belt, E. J., Fijneman, R. J., van den Berg, E. G., Bril, H., Delis-van Diemen, P. M., Tijssen, M., van Essen, H. F., de Lange-de Klerk, E. S., Beliën, J. A., Stockmann, H. B., Meijer, S., & Meijer, G. A. (2011). Loss of lamin A/C expression in stage II and III colon cancer is associated with disease recurrence. *European journal of cancer (Oxford, England : 1990)*, *47*(12), 1837–1845.

Bertacchini, J., Beretti, F., Cenni, V., Guida, M., Gibellini, F., Mediani, L., Marin, O., Maraldi, N. M., de Pol, A., Lattanzi, G., Cocco, L., & Marmiroli, S. (2013). The protein kinase Akt/PKB regulates both prelamin A degradation and Lmna gene

expression. *FASEB journal : official publication of the Federation of American Societies for Experimental Biology*, *27*(6), 2145–2155.

Bertoli, C., Herlihy, A.E., Pennycook, B.R., Kriston-Vizi, J., and de Bruin, R.A.M. (2016). Sustained E2F-Dependent Transcription Is a Key Mechanism to Prevent Replication- Stress-Induced DNA Damage. Cell Reports *15*, 1412–1422.

Bickmore, W. A., & van Steensel, B. (2013). Genome architecture: domain organization of interphase chromosomes. *Cell*, *152*(6), 1270–1284.

Blackwell, T. K., Huang, J., Ma, A., Kretzner, L., Alt, F. W., Eisenman, R. N., & Weintraub, H. (1993). Binding of myc proteins to canonical and noncanonical DNA sequences. *Molecular and cellular biology*, *13*(9), 5216–5224.

Boijja, A., Klein, I. A., Sabari, B. R., Dall'Agnese, A., Coffey, E. L., Zamudio, A. V., Li, C. H., Shrinivas, K., Manteiga, J. C., Hannett, N. M., Abraham, B. J., Afeyan, L. K., Guo, Y. E., Rimel, J. K., Fant, C. B., Schuijers, J., Lee, T. I., Taatjes, D. J., & Young, R. A. (2018). Transcription Factors Activate Genes through the Phase-Separation Capacity of Their Activation Domains. *Cell*, *175*(7), 1842–1855.e16.

Bolzer, A., Kreth, G., Solovei, I., Koehler, D., Saracoglu, K., Fauth, C., Müller, S., Eils, R., Cremer, C., Speicher, M. R., & Cremer, T. (2005). Three-dimensional maps of all chromosomes in human male fibroblast nuclei and prometaphase rosettes. *PLoS biology*, *3*(5), e157.

Bouzid, T., Kim, E., Riehl, B. D., Esfahani, A. M., Rosenbohm, J., Yang, R., Duan, B., & Lim, J. Y. (2019). The LINC complex, mechanotransduction, and mesenchymal stem cell function and fate. *Journal of biological engineering*, *13*, 68.

Boyd, J., Pienta, K. J., Getzenberg, R. H., Coffey, D. S., & Barrett, J. C. (1991). Preneoplastic alterations in nuclear morphology that accompany loss of tumor suppressor phenotype. *Journal of the National Cancer Institute*, *83*(12), 862–866.

Broers, J. L., Hutchison, C. J., & Ramaekers, F. C. (2004). Laminopathies. *The Journal of pathology*, *204*(4), 478–488.

Broers, J. L., Machiels, B. M., Kuijpers, H. J., Smedts, F., van den Kieboom, R., Raymond, Y., & Ramaekers, F. C. (1997). A- and B-type lamins are differentially expressed in normal human tissues. *Histochemistry and cell biology*, *107*(6), 505–517.

Bronstein, I., Israel, Y., Kepten, E., Mai, S., Shav-Tal, Y., Barkai, E., & Garini, Y. (2009). Transient anomalous diffusion of telomeres in the nucleus of mammalian cells. *Physical review letters*, *103*(1), 018102.

Bussolati, G., Maletta, F., Asioli, S., Annaratone, L., Sapino, A., & Marchiò, C. (2014). "To be or not to be in a good shape": diagnostic and clinical value of nuclear shape irregularities in thyroid and breast cancer. *Advances in experimental medicine and biology*, *773*, 101–121.

Butt, A. J., Sergio, C. M., Inman, C. K., Anderson, L. R., McNeil, C. M., Russell, A. J., Nousch, M., Preiss, T., Biankin, A. V., Sutherland, R. L., & Musgrove, E. A. (2008). The estrogen and c-Myc target gene HSPC111 is over-expressed in breast cancer and associated with poor patient outcome. *Breast cancer research : BCR*, *10*(2), R28.

Buxboim, A., Swift, J., Irianto, J., Spinler, K. R., Dingal, P. C., Athirasala, A., Kao, Y. R., Cho, S., Harada, T., Shin, J. W., & Discher, D. E. (2014). Matrix elasticity regulates lamin-A,C phosphorylation and turnover with feedback to actomyosin. *Current biology : CB*, *24*(16), 1909–1917.

Callan H. G., & Tomlin, S. G. (1950). Experimental studies on amphibian oocyte nuclei. I. Investigation of the structure of the nuclear membrane by means of the electron microscope. *Proceedings of the Royal Society of London. Series B, Biological sciences*, *137*(888), 367–378.

Carabet, L. A., Lallous, N., Leblanc, E., Ban, F., Morin, H., Lawn, S., Ghaidi, F., Lee, J., Mills, I. G., Gleave, M. E., Rennie, P. S., & Cherkasov, A. (2018). Computer-aided drug discovery of Myc-Max inhibitors as potential therapeutics for prostate cancer. *European journal of medicinal chemistry*, *160*, 108–119.

Cenni, V., Bertacchini, J., Beretti, F., Lattanzi, G., Bavelloni, A., Riccio, M., Ruzzene, M., Marin, O., Arrigoni, G., Parnaik, V., Wehnert, M., Maraldi, N. M., de Pol, A., Cocco, L., & Marmiroli, S. (2008). Lamin A Ser404 is a nuclear target of Akt phosphorylation in C2C12 cells. *Journal of proteome research*, *7*(11), 4727–4735.

Cerni, C., Mougneau, E., Zerlin, M., Julius, M., Marcu, K. B., & Cuzin, F. (1986). c-myc and functionally related oncogenes induce both high rates of sister chromatid exchange and abnormal karyotypes in rat fibroblasts. *Current topics in microbiology and immunology*, *132*, 193–201.

Chambliss, A. B., Khatau, S. B., Erdenberger, N., Robinson, D. K., Hodzic, D., Longmore, G. D., & Wirtz, D. (2013). The LINC-anchored actin cap connects the extracellular milieu to the nucleus for ultrafast mechanotransduction. *Scientific reports*, *3*, 1087.

Chang, W., Folker, E. S., Worman, H. J., & Gundersen, G. G. (2013). Emerin organizes actin flow for nuclear movement and centrosome orientation in migrating fibroblasts. *Molecular biology of the cell*, *24*(24), 3869–3880.

Chen, H., Liu, H., & Qing, G. (2018). Targeting oncogenic Myc as a strategy for cancer treatment. *Signal transduction and targeted therapy*, *3*, 5.

Chen, X., Chen, Y., Huang, H. M., Li, H. D., Bu, F. T., Pan, X. Y., Yang, Y., Li, W. X., Li, X. F., Huang, C., Meng, X. M., & Li, J. (2019). SUN2: A potential therapeutic target in cancer. *Oncology letters*, *17*(2), 1401–1408.

Cho, S., Irianto, J., & Discher, D. E. (2017). Mechanosensing by the nucleus: From pathways to scaling relationships. *The Journal of cell biology*, *216*(2), 305–315.

Ciampi, R., Giordano, T. J., Wikenheiser-Brokamp, K., Koenig, R. J., & Nikiforov, Y. E. (2007). HOOK3-RET: a novel type of RET/PTC rearrangement in papillary thyroid carcinoma. *Endocrine-related cancer*, *14*(2), 445–452.

Clements, L., Manilal, S., Love, D. R., & Morris, G. E. (2000). Direct interaction between emerin and lamin A. *Biochemical and biophysical research communications*, *267*(3), 709–714.

Coffinier, C., Jung, H. J., Nobumori, C., Chang, S., Tu, Y., Barnes, R. H., 2nd, Yoshinaga, Y., de Jong, P. J., Vergnes, L., Reue, K., Fong, L. G., & Young, S. G. (2011). Deficiencies in lamin B1 and lamin B2 cause neurodevelopmental defects and distinct nuclear shape abnormalities in neurons. *Molecular biology of the cell*, *22*(23), 4683–4693.

Coussens, L. M., Fingleton, B., & Matrisian, L. M. (2002). Matrix metalloproteinase inhibitors and cancer: trials and tribulations. *Science (New York, N.Y.)*, *295*(5564), 2387–2392.

Cremer, M., von Hase, J., Volm, T., Brero, A., Kreth, G., Walter, J., Fischer, C., Solovei, I., Cremer, C., & Cremer, T. (2001). Non-random radial higher-order chromatin arrangements in nuclei of diploid human cells. *Chromosome research : an international journal on the molecular, supramolecular and evolutionary aspects of chromosome biology*, *9*(7), 541–567.

Croci, O., De Fazio, S., Biagioni, F., Donato, E., Caganova, M., Curti, L., Doni, M., Sberna, S., Aldeghi, D., Biancotto, C., Verrecchia, A., Olivero, D., Amati, B., & Campaner, S. (2017). Transcriptional integration of mitogenic and mechanical signals by Myc and YAP. *Genes & development*, *31*(20), 2017–2022.

Crosetto, N., & Bienko, M. (2020). Radial Organization in the Mammalian Nucleus. *Frontiers in genetics*, *11*, 33.

Dang, C. V., O'Donnell, K. A., Zeller, K. I., Nguyen, T., Osthus, R. C., & Li, F. (2006). The c-Myc target gene network. *Seminars in cancer biology*, *16*(4), 253–264.

Danielian, P. S., White, R., Hoare, S. A., Fawell, S. E., & Parker, M. G. (1993). Identification of residues in the estrogen receptor that confer differential sensitivity to estrogen and hydroxytamoxifen. *Molecular endocrinology (Baltimore, Md.)*, *7*(2), 232–240.

Davidson, P. M., & Lammerding, J. (2014). Broken nuclei--lamins, nuclear mechanics, and disease. *Trends in cell biology*, *24*(4), 247–256.

de Leeuw, R., Gruenbaum, Y., & Medalia, O. (2018). Nuclear Lamins: Thin Filaments with Major Functions. *Trends in cell biology*, *28*(1), 34–45.

De Vos, W. H., Houben, F., Hoebe, R. A., Hennekam, R., van Engelen, B., Manders, E. M., Ramaekers, F. C., Broers, J. L., & Van Oostveldt, P. (2010). Increased plasticity of the nuclear envelope and hypermobility of telomeres due to the loss of A-type lamins. *Biochimica et biophysica acta*, *1800*(4), 448–458.

De Vos, W. H., Houben, F., Kamps, M., Malhas, A., Verheyen, F., Cox, J., Manders, E. M., Verstraeten, V. L., van Steensel, M. A., Marcelis, C. L., van den Wijngaard, A., Vaux, D. J., Ramaekers, F. C., & Broers, J. L. (2011). Repetitive disruptions of the nuclear envelope invoke temporary loss of cellular compartmentalization in laminopathies. *Human molecular genetics*, *20*(21), 4175–4186.

Dechat, T., Adam, S. A., & Goldman, R. D. (2009). Nuclear lamins and chromatin: when structure meets function. *Advances in enzyme regulation*, *49*(1), 157–166.

Dechat, T., Adam, S. A., Taimen, P., Shimi, T., & Goldman, R. D. (2010). Nuclear lamins. *Cold Spring Harbor perspectives in biology*, *2*(11), a000547.

Demma, M. J., Mapelli, C., Sun, A., Bodea, S., Ruprecht, B., Javaid, S., Wiswell, D., Muise, E., Chen, S., Zelina, J., Orvieto, F., Santoprete, A., Altezza, S., Tucci, F., Escandon, E., Hall, B., Ray, K., Walji, A., & O'Neil, J. (2019). Omomyc Reveals New Mechanisms To Inhibit the MYC Oncogene. *Molecular and cellular biology*, *39*(22), e00248-19.

Denais, C. M., Gilbert, R. M., Isermann, P., McGregor, A. L., te Lindert, M., Weigelin, B., Davidson, P. M., Friedl, P., Wolf, K., & Lammerding, J. (2016). Nuclear envelope rupture and repair during cancer cell migration. *Science (New York, N.Y.)*, *352*(6283), 353–358.

Devaiah, B. N., Mu, J., Akman, B., Uppal, S., Weissman, J. D., Cheng, D., Baranello, L., Nie, Z., Levens, D., & Singer, D. S. (2020). MYC protein stability is negatively regulated by BRD4. *Proceedings of the National Academy of Sciences of the United States of America*, *117*(24), 13457–13467.

Dupont, S., Morsut, L., Aragona, M., Enzo, E., Giulitti, S., Cordenonsi, M., Zanconato, F., Le Digabel, J., Forcato, M., Bicciato, S., Elvassore, N., & Piccolo, S. (2011). Role of YAP/TAZ in mechanotransduction. *Nature*, *474*(7350), 179–183.

Earle, A. J., Kirby, T. J., Fedorchak, G. R., Isermann, P., Patel, J., Iruvanti, S., Moore, S. A., Bonne, G., Wallrath, L. L., & Lammerding, J. (2020). Mutant lamins cause nuclear envelope rupture and DNA damage in skeletal muscle cells. *Nature materials*, *19*(4), 464–473.

Elosegui-Artola, A., Andreu, I., Beedle, A. E. M., Lezamiz, A., Uroz, M., Kosmalska, A. J., Oria, R., Kechagia, J. Z., Rico-Lastres, P., Le Roux, A. L., Shanahan, C. M., Trepat, X., Navajas, D., Garcia-Manyes, S., & Roca-Cusachs, P. (2017). Force Triggers YAP Nuclear Entry by Regulating Transport across Nuclear Pores. *Cell*, *171*(6), 1397–1410.e14.

Emerson, L. J., Holt, M. R., Wheeler, M. A., Wehnert, M., Parsons, M., & Ellis, J. A. (2009). Defects in cell spreading and ERK1/2 activation in fibroblasts with lamin A/C mutations. *Biochimica et biophysica acta*, *1792*(8), 810–821.

Evangelisti, C., Rusciano, I., Mongiorgi, S., Ramazzotti, G., Lattanzi, G., Manzoli, L., Cocco, L., & Ratti, S. (2022). The wide and growing range of lamin B-related diseases: from laminopathies to cancer. *Cellular and molecular life sciences : CMLS*, *79*(2), 126.

Fawcett D. W. (1966). On the occurrence of a fibrous lamina on the inner aspect of the nuclear envelope in certain cells of vertebrates. *The American journal of anatomy*, *119*(1), 129–145.

Ferrera, D., Canale, C., Marotta, R., Mazzaro, N., Gritti, M., Mazzanti, M., Capellari, S., Cortelli, P., & Gasparini, L. (2014). Lamin B1 overexpression increases nuclear rigidity in autosomal dominant leukodystrophy fibroblasts. *FASEB journal : official publication of the Federation of American Societies for Experimental Biology*, *28*(9), 3906–3918.

Filippova, G. N., Fagerlie, S., Klenova, E. M., Myers, C., Dehner, Y., Goodwin, G., Neiman, P. E., Collins, S. J., & Lobanenkov, V. V. (1996). An exceptionally conserved transcriptional repressor, CTCF, employs different combinations of zinc fingers to bind diverged promoter sequences of avian and mammalian c-myc oncogenes. *Molecular and cellular biology*, *16*(6), 2802–2813.

Finch, A. J., Soucek, L., Junttila, M. R., Swigart, L. B., & Evan, G. I. (2009). Acute overexpression of Myc in intestinal epithelium recapitulates some but not all the changes elicited by Wnt/beta-catenin pathway activation. *Molecular and cellular biology*, *29*(19), 5306–5315.

Finlan, L. E., Sproul, D., Thomson, I., Boyle, S., Kerr, E., Perry, P., Ylstra, B., Chubb, J. R., & Bickmore, W. A. (2008). Recruitment to the nuclear periphery can alter expression of genes in human cells. *PLoS genetics*, *4*(3), e1000039.

Fiore, M., Zanier, R., & Degrassi, F. (2002). Reversible G(1) arrest by dimethyl sulfoxide as a new method to synchronize Chinese hamster cells. *Mutagenesis*, *17*(5), 419–424.

Fischer A. H. (2014). The diagnostic pathology of the nuclear envelope in human cancers. *Advances in experimental medicine and biology*, *773*, 49–75.

Fischer E. G. (2020). Nuclear Morphology and the Biology of Cancer Cells. *Acta cytologica*, *64*(6), 511–519.

Fischer, A. H., Taysavang, P., & Jhiang, S. M. (2003). Nuclear envelope irregularity is induced by RET/PTC during interphase. *The American journal of pathology*, *163*(3), 1091–1100.

Frank, S. R., Parisi, T., Taubert, S., Fernandez, P., Fuchs, M., Chan, H. M., Livingston, D. M., & Amati, B. (2003). MYC recruits the TIP60 histone acetyltransferase complex to chromatin. *EMBO reports*, *4*(6), 575–580.

Fudenberg, G., Imakaev, M., Lu, C., Goloborodko, A., Abdennur, N., & Mirny, L. A. (2016). Formation of Chromosomal Domains by Loop Extrusion. *Cell reports*, *15*(9), 2038–2049.

Furusawa, T., Rochman, M., Taher, L., Dimitriadis, E. K., Nagashima, K., Anderson, S., & Bustin, M. (2015). Chromatin decompaction by the nucleosomal binding protein HMGN5 impairs nuclear sturdiness. *Nature communications*, *6*, 6138.

Gerace, L., & Burke, B. (1988). Functional organization of the nuclear envelope. *Annual review of cell biology*, *4*, 335–374.

Gerace, L., Comeau, C., & Benson, M. (1984). Organization and modulation of nuclear lamina structure. *Journal of cell science. Supplement*, *1*, 137–160.

Goldman, R. D., Gruenbaum, Y., Moir, R. D., Shumaker, D. K., & Spann, T. P. (2002). Nuclear lamins: building blocks of nuclear architecture. *Genes & development*, *16*(5), 533–547.

Goldman, R. D., Shumaker, D. K., Erdos, M. R., Eriksson, M., Goldman, A. E., Gordon, L. B., Gruenbaum, Y., Khuon, S., Mendez, M., Varga, R., & Collins, F. S. (2004). Accumulation of mutant lamin A causes progressive changes in nuclear architecture in Hutchinson-Gilford progeria syndrome. *Proceedings of the National Academy of Sciences of the United States of America*, *101*(24), 8963–8968.

Gong, G., Chen, P., Li, L., Tan, H., Zhou, J., Zhou, Y., Yang, X., & Wu, X. (2015). Loss of lamin A but not lamin C expression in epithelial ovarian cancer cells is associated with metastasis and poor prognosis. *Pathology, research and practice*, *211*(2), 175–182.

Gonzalez-Suarez, I., Redwood, A. B., & Gonzalo, S. (2009). Loss of A-type lamins and genomic instability. *Cell cycle (Georgetown, Tex.)*, *8*(23), 3860–3865.

Gonzalez-Suarez, I., Redwood, A. B., Grotsky, D. A., Neumann, M. A., Cheng, E. H., Stewart, C. L., Dusso, A., & Gonzalo, S. (2011). A new pathway that regulates 53BP1 stability implicates cathepsin L and vitamin D in DNA repair. *The EMBO journal*, *30*(16), 3383–3396.

Graziano, S., Kreienkamp, R., Coll-Bonfill, N., & Gonzalo, S. (2018). Causes and consequences of genomic instability in laminopathies: Replication stress and interferon response. *Nucleus (Austin, Tex.)*, *9*(1), 258–275.

Greenwald, W. W., Li, H., Benaglio, P., Jakubosky, D., Matsui, H., Schmitt, A., Selvaraj, S., D'Antonio, M., D'Antonio-Chronowska, A., Smith, E. N., & Frazer, K. A. (2019). Subtle changes in chromatin loop contact propensity are associated with differential gene regulation and expression. *Nature communications*, *10*(1), 1054.

Gruenbaum, Y., & Aebi, U. (2014). Intermediate filaments: a dynamic network that controls cell mechanics. *F1000prime reports*, *6*, 54.

Gruenbaum, Y., & Medalia, O. (2015). Lamins: the structure and protein complexes. *Current opinion in cell biology*, *32*, 7–12.

Guelen, L., Pagie, L., Brasset, E., Meuleman, W., Faza, M. B., Talhout, W., Eussen, B. H., de Klein, A., Wessels, L., de Laat, W., & van Steensel, B. (2008). Domain organization of human chromosomes revealed by mapping of nuclear lamina interactions. *Nature*, *453*(7197), 948–951.

Guilak, F., Sato, M., Stanford, C. M., & Brand, R. A. (2000). Cell mechanics. *Journal of biomechanics*, *33*(1), 1–2.

Guilluy, C., Osborne, L. D., Van Landeghem, L., Sharek, L., Superfine, R., Garcia-Mata, R., & Burridge, K. (2014). Isolated nuclei adapt to force and reveal a mechanotransduction pathway in the nucleus. *Nature cell biology*, *16*(4), 376–381.

Guinde, J., Benoit, A., Frankel, D., Robert, S., Ostacolo, K., Lévy, N., Astoul, P., Roll, P., & Kaspi, E. (2020). miR-9 Does Not Regulate Lamin A Expression in Metastatic Cells from Lung Adenocarcinoma. *International journal of molecular sciences*, *21*(5), 1599.

Halfmann, C. T., Sears, R. M., Katiyar, A., Busselman, B. W., Aman, L. K., Zhang, Q., O'Bryan, C. S., Angelini, T. E., Lele, T. P., & Roux, K. J. (2019). Repair of nuclear ruptures requires barrier-to-autointegration factor. *The Journal of cell biology*, *218*(7), 2136–2149.

Han, H., Jain, A. D., Truica, M. I., Izquierdo-Ferrer, J., Anker, J. F., Lysy, B., Sagar, V., Luan, Y., Chalmers, Z. R., Unno, K., Mok, H., Vatapalli, R., Yoo, Y. A., Rodriguez, Y., Kandela, I., Parker, J. B., Chakravarti, D., Mishra, R. K., Schiltz, G. E., & Abdulkadir, S. A. (2019). Small-Molecule MYC Inhibitors Suppress Tumor Growth and Enhance Immunotherapy. *Cancer cell*, *36*(5), 483–497.e15.

Haque, F., Lloyd, D. J., Smallwood, D. T., Dent, C. L., Shanahan, C. M., Fry, A. M., Trembath, R. C., & Shackleton, S. (2006). SUN1 interacts with nuclear lamin A and

cytoplasmic nesprins to provide a physical connection between the nuclear lamina and the cytoskeleton. *Molecular and cellular biology*, *26*(10), 3738–3751.

Harada, T., Swift, J., Irianto, J., Shin, J. W., Spinler, K. R., Athirasala, A., Diegmiller, R., Dingal, P. C., Ivanovska, I. L., & Discher, D. E. (2014). Nuclear lamin stiffness is a barrier to 3D migration, but softness can limit survival. *The Journal of cell biology*, *204*(5), 669–682.

Hatch, E. M., & Hetzer, M. W. (2016). Nuclear envelope rupture is induced by actin-based nucleus confinement. *The Journal of cell biology*, *215*(1), 27–36.

Hatch, E. M., Fischer, A. H., Deerinck, T. J., & Hetzer, M. W. (2013). Catastrophic nuclear envelope collapse in cancer cell micronuclei. *Cell*, *154*(1), 47–60.

Ho, C. Y., & Lammerding, J. (2012). Lamins at a glance. *Journal of cell science*, *125*(Pt 9), 2087–2093.

Ho, C. Y., Jaalouk, D. E., Vartiainen, M. K., & Lammerding, J. (2013). Lamin A/C and emerin regulate MKL1-SRF activity by modulating actin dynamics. *Nature*, *497*(7450), 507–511.

Holaska, J. M., & Wilson, K. L. (2007). An emerin "proteome": purification of distinct emerin-containing complexes from HeLa cells suggests molecular basis for diverse roles including gene regulation, mRNA splicing, signaling, mechanosensing, and nuclear architecture. *Biochemistry*, *46*(30), 8897–8908.

Holaska, J. M., Kowalski, A. K., & Wilson, K. L. (2004). Emerin caps the pointed end of actin filaments: evidence for an actin cortical network at the nuclear inner membrane. *PLoS biology*, *2*(9), E231.

Holt, I., Ostlund, C., Stewart, C. L., Man, N.t, Worman, H. J., & Morris, G. E. (2003). Effect of pathogenic mis-sense mutations in lamin A on its interaction with emerin in vivo. *Journal of cell science*, *116*(Pt 14), 3027–3035.

Horn, H. F., Brownstein, Z., Lenz, D. R., Shivatzki, S., Dror, A. A., Dagan-Rosenfeld, O., Friedman, L. M., Roux, K. J., Kozlov, S., Jeang, K. T., Frydman, M., Burke, B., Stewart, C. L., & Avraham, K. B. (2013). The LINC complex is essential for hearing. *The Journal of clinical investigation*, *123*(2), 740–750.

Hutchison C. J. (2011). The role of DNA damage in laminopathy progeroid syndromes. *Biochemical Society transactions*, *39*(6), 1715–1718.

Irianto, J., Pfeifer, C. R., Ivanovska, I. L., Swift, J., & Discher, D. E. (2016). Nuclear lamins in cancer. *Cellular and molecular bioengineering*, *9*(2), 258–267.

Isermann, P., & Lammerding, J. (2013). Nuclear mechanics and mechanotransduction in health and disease. *Current biology : CB*, *23*(24), R1113–R1121.

Isermann, P., & Lammerding, J. (2017). Consequences of a tight squeeze: Nuclear envelope rupture and repair. *Nucleus (Austin, Tex.)*, *8*(3), 268–274.

Jackson S. P. (2002). Sensing and repairing DNA double-strand breaks. *Carcinogenesis*, *23*(5), 687–696

Jamin, A., & Wiebe, M. S. (2015). Barrier to Autointegration Factor (BANF1): interwoven roles in nuclear structure, genome integrity, innate immunity, stress responses and progeria. *Current opinion in cell biology*, *34*, 61–68.

Janin, A., & Gache, V. (2018). Nesprins and Lamins in Health and Diseases of Cardiac and Skeletal Muscles. *Frontiers in physiology*, *9*, 1277.

Jevtić, P., & Levy, D. L. (2014). Mechanisms of nuclear size regulation in model systems and cancer. *Advances in experimental medicine and biology*, *773*, 537–569.

Jevtić, P., Edens, L. J., Vuković, L. D., & Levy, D. L. (2014). Sizing and shaping the nucleus: mechanisms and significance. *Current opinion in cell biology*, *28*, 16–27.

Jin, H., Zhang, C., Zwahlen, M., von Feilitzen, K., Karlsson, M., Shi, M., Yuan, M., Song, X., Li, X., Yang, H., Turkez, H., Fagerberg, L., Uhlén, M., & Mardinoglu, A. (2023). Systematic transcriptional analysis of human cell lines for gene expression landscape and tumor representation. *Nature communications*, *14*(1), 5417.

Johnson, B. R., Nitta, R. T., Frock, R. L., Mounkes, L., Barbie, D. A., Stewart, C. L., Harlow, E., & Kennedy, B. K. (2004). A-type lamins regulate retinoblastoma protein function by promoting subnuclear localization and preventing proteasomal degradation. *Proceedings of the National Academy of Sciences of the United States of America*, *101*(26), 9677–9682.

Jung, H. J., Coffinier, C., Choe, Y., Beigneux, A. P., Davies, B. S., Yang, S. H., Barnes, R. H., 2nd, Hong, J., Sun, T., Pleasure, S. J., Young, S. G., & Fong, L. G. (2012). Regulation of prelamin A but not lamin C by miR-9, a brain-specific microRNA. *Proceedings of the National Academy of Sciences of the United States of America*, *109*(7), E423–E431.

Kalukula, Y., Stephens, A. D., Lammerding, J., & Gabriele, S. (2022). Mechanics and functional consequences of nuclear deformations. *Nature reviews. Molecular cell biology*, *23*(9), 583–602.

Kamikawa, Y., Saito, A., & Imaizumi, K. (2022). Impact of Nuclear Envelope Stress on Physiological and Pathological Processes in Central Nervous System. *Neurochemical research*, *47*(9), 2478–2487.

Khatau, S. B., Hale, C. M., Stewart-Hutchinson, P. J., Patel, M. S., Stewart, C. L., Searson, P. C., Hodzic, D., & Wirtz, D. (2009). A perinuclear actin cap regulates nuclear shape. *Proceedings of the National Academy of Sciences of the United States of America*, *106*(45), 19017–19022.

Kim, J., Roh, M., & Abdulkadir, S. A. (2010). Pim1 promotes human prostate cancer cell tumorigenicity and c-MYC transcriptional activity. *BMC cancer*, *10*, 248.

Kim, J. K., Louhghalam, A., Lee, G., Schafer, B. W., Wirtz, D., & Kim, D. H. (2017). Nuclear lamin A/C harnesses the perinuclear apical actin cables to protect nuclear morphology. *Nature communications*, *8*(1), 2123.

Kim, Y., Zheng, X., & Zheng, Y. (2019). Role of lamins in 3D genome organization and global gene expression. *Nucleus (Austin, Tex.)*, *10*(1), 33–41.

Kind, J., Pagie, L., de Vries, S. S., Nahidiazar, L., Dey, S. S., Bienko, M., Zhan, Y., Lajoie, B., de Graaf, C. A., Amendola, M., Fudenberg, G., Imakaev, M., Mirny, L. A.,

Jalink, K., Dekker, J., van Oudenaarden, A., & van Steensel, B. (2015). Genome-wide maps of nuclear lamina interactions in single human cells. *Cell*, *163*(1), 134–147.

Knoepfler, P. S., Zhang, X. Y., Cheng, P. F., Gafken, P. R., McMahon, S. B., & Eisenman, R. N. (2006). Myc influences global chromatin structure. *The EMBO journal*, *25*(12), 2723–2734.

Kochin, V., Shimi, T., Torvaldson, E., Adam, S. A., Goldman, A., Pack, C. G., Melo-Cardenas, J., Imanishi, S. Y., Goldman, R. D., & Eriksson, J. E. (2014). Interphase phosphorylation of lamin A. *Journal of cell science*, *127*(Pt 12), 2683–2696.

Kong, L., Schäfer, G., Bu, H., Zhang, Y., Zhang, Y., & Klocker, H. (2012). Lamin A/C protein is overexpressed in tissue-invading prostate cancer and promotes prostate cancer cell growth, migration and invasion through the PI3K/AKT/PTEN pathway. *Carcinogenesis*, *33*(4), 751–759.

Krichevsky, A. M., Sonntag, K. C., Isacson, O., & Kosik, K. S. (2006). Specific microRNAs modulate embryonic stem cell-derived neurogenesis. *Stem cells (Dayton, Ohio)*, *24*(4), 857–864.

Lammerding, J., Fong, L. G., Ji, J. Y., Reue, K., Stewart, C. L., Young, S. G., & Lee, R. T. (2006). Lamins A and C but not lamin B1 regulate nuclear mechanics. *The Journal of biological chemistry*, *281*(35), 25768–25780.

Lammerding, J., Schulze, P. C., Takahashi, T., Kozlov, S., Sullivan, T., Kamm, R. D., Stewart, C. L., & Lee, R. T. (2004). Lamin A/C deficiency causes defective nuclear mechanics and mechanotransduction. *The Journal of clinical investigation*, *113*(3), 370–378.

Lawlor, E. R., Soucek, L., Brown-Swigart, L., Shchors, K., Bialucha, C. U., & Evan, G. I. (2006). Reversible kinetic analysis of Myc targets in vivo provides novel insights into Myc-mediated tumorigenesis. *Cancer research*, *66*(9), 4591–4601.

Lee, D. C., Welton, K. L., Smith, E. D., & Kennedy, B. K. (2009). A-type nuclear lamins act as transcriptional repressors when targeted to promoters. *Experimental cell research*, *315*(6), 996–1007.

Lee, Y. L., & Burke, B. (2018). LINC complexes and nuclear positioning. *Seminars in cell & developmental biology*, *82*, 67–76.

Lei, K., Zhang, X., Ding, X., Guo, X., Chen, M., Zhu, B., Xu, T., Zhuang, Y., Xu, R., & Han, M. (2009). SUN1 and SUN2 play critical but partially redundant roles in anchoring nuclei in skeletal muscle cells in mice. *Proceedings of the National Academy of Sciences of the United States of America*, *106*(25), 10207–10212.

Lei, K., Zhu, X., Xu, R., Shao, C., Xu, T., Zhuang, Y., & Han, M. (2012). Inner nuclear envelope proteins SUN1 and SUN2 play a prominent role in the DNA damage response. *Current biology : CB*, *22*(17), 1609–1615.

Lewinska, A., Klukowska-Rötzler, J., Deregowska, A., Adamczyk-Grochala, J., & Wnuk, M. (2019). c-Myc activation promotes cofilin-mediated F-actin cytoskeleton remodeling and telomere homeostasis as a response to oxidant-based DNA damage in medulloblastoma cells. *Redox biology*, *24*, 101163.

Lewis, P. W., Elsaesser, S. J., Noh, K. M., Stadler, S. C., & Allis, C. D. (2010). Daxx is an H3.3-specific histone chaperone and cooperates with ATRX in replication-independent chromatin assembly at telomeres. *Proceedings of the National Academy of Sciences of the United States of America*, *107*(32), 14075–14080.

Li, J., & Xu, X. (2016). DNA double-strand break repair: a tale of pathway choices. *Acta biochimica et biophysica Sinica*, *48*(7), 641–646.

Liddane, A. G., McNamara, C. A., Campbell, M. C., Mercier, I., & Holaska, J. M. (2021). Defects in Emerin-Nucleoskeleton Binding Disrupt Nuclear Structure and Promote Breast Cancer Cell Motility and Metastasis. *Molecular cancer research : MCR*, *19*(7), 1196–1207.

Lieberman-Aiden, E., van Berkum, N. L., Williams, L., Imakaev, M., Ragoczy, T., Telling, A., Amit, I., Lajoie, B. R., Sabo, P. J., Dorschner, M. O., Sandstrom, R., Bernstein, B., Bender, M. A., Groudine, M., Gnirke, A., Stamatoyannopoulos, J., Mirny, L. A., Lander, E. S., & Dekker, J. (2009). Comprehensive mapping of long-range interactions reveals folding principles of the human genome. *Science (New York, N.Y.)*, *326*(5950), 289–293.

Liu, B., Wang, J., Chan, K. M., Tjia, W. M., Deng, W., Guan, X., Huang, J. D., Li, K. M., Chau, P. Y., Chen, D. J., Pei, D., Pendas, A. M., Cadiñanos, J., López-Otín, C., Tse, H. F., Hutchison, C., Chen, J., Cao, Y., Cheah, K. S., Tryggvason, K., … Zhou, Z. (2005). Genomic instability in laminopathy-based premature aging. *Nature medicine*, *11*(7), 780–785.

Lomakin, A. J., Cattin, C. J., Cuvelier, D., Alraies, Z., Molina, M., Nader, G. P. F., Srivastava, N., Sáez, P. J., Garcia-Arcos, J. M., Zhitnyak, I. Y., Bhargava, A., Driscoll, M. K., Welf, E. S., Fiolka, R., Petrie, R. J., De Silva, N. S., González-Granado, J. M., Manel, N., Lennon-Duménil, A. M., Müller, D. J., … Piel, M. (2020). The nucleus acts as a ruler tailoring cell responses to spatial constraints. *Science (New York, N.Y.)*, *370*(6514), eaba2894.

Luger, K., Mäder, A. W., Richmond, R. K., Sargent, D. F., & Richmond, T. J. (1997). Crystal structure of the nucleosome core particle at 2.8 A resolution. *Nature*, *389*(6648), 251–260.

Lukášová, E., Kovarˇík, A., Bacˇíková, A., Falk, M., & Kozubek, S. (2017). Loss of lamin B receptor is necessary to induce cellular senescence. *The Biochemical journal*, *474*(2), 281–300.

Lund, E., Oldenburg, A. R., Delbarre, E., Freberg, C. T., Duband-Goulet, I., Eskeland, R., Buendia, B., & Collas, P. (2013). Lamin A/C-promoter interactions specify chromatin state-dependent transcription outcomes. *Genome research*, *23*(10), 1580–1589.

Ma, L., Young, J., Prabhala, H., Pan, E., Mestdagh, P., Muth, D., Teruya-Feldstein, J., Reinhardt, F., Onder, T. T., Valastyan, S., Westermann, F., Speleman, F., Vandesompele, J., & Weinberg, R. A. (2010). miR-9, a MYC/MYCN-activated microRNA, regulates E-cadherin and cancer metastasis. *Nature cell biology*, *12*(3), 247–256.

Maciejowski, J., & Hatch, E. M. (2020). Nuclear Membrane Rupture and Its Consequences. *Annual review of cell and developmental biology*, *36*, 85–114.

Magaña-Acosta, M., & Valadez-Graham, V. (2020). Chromatin Remodelers in the 3D Nuclear Compartment. *Frontiers in genetics*, *11*, 600615.

Mahajan, S., Thieme, D., Czugala, M., Kruse, F. E., & Fuchsluger, T. A. (2017). Lamin Cleavage: A Reliable Marker for Studying Staurosporine-Induced Apoptosis in Corneal Tissue. *Investigative ophthalmology & visual science*, *58*(13), 5802–5809.

Makarov, A. A., Zou, J., Houston, D. R., Spanos, C., Solovyova, A. S., Cardenal-Peralta, C., Rappsilber, J., & Schirmer, E. C. (2019). Lamin A molecular compression and sliding as mechanisms behind nucleoskeleton elasticity. *Nature communications*, *10*(1), 3056.

Massó-Vallés, D., Beaulieu, M. E., & Soucek, L. (2020). MYC, MYCL, and MYCN as therapeutic targets in lung cancer. *Expert opinion on therapeutic targets*, *24*(2), 101–114.

Matsumoto, A., Hieda, M., Yokoyama, Y., Nishioka, Y., Yoshidome, K., Tsujimoto, M., & Matsuura, N. (2015). Global loss of a nuclear lamina component, lamin A/C, and LINC complex components SUN1, SUN2, and nesprin-2 in breast cancer. *Cancer medicine*, *4*(10), 1547–1557.

Maurer, M., & Lammerding, J. (2019). The Driving Force: Nuclear Mechanotransduction in Cellular Function, Fate, and Disease. *Annual review of biomedical engineering*, *21*, 443–468.

Maynard, S., Keijzers, G., Akbari, M., Ezra, M. B., Hall, A., Morevati, M., Scheibye-Knudsen, M., Gonzalo, S., Bartek, J., & Bohr, V. A. (2019). Lamin A/C promotes DNA base excision repair. *Nucleic acids research*, *47*(22), 11709–11728.

McGregor, A. L., Hsia, C. R., & Lammerding, J. (2016). Squish and squeeze-the nucleus as a physical barrier during migration in confined environments. *Current opinion in cell biology*, *40*, 32–40.

Mellad, J. A., Warren, D. T., & Shanahan, C. M. (2011). Nesprins LINC the nucleus and cytoskeleton. *Current opinion in cell biology*, *23*(1), 47–54.

Merve, A., Zhang, X., Pomella, N., Acquati, S., Hoeck, J. D., Dumas, A., Rosser, G., Li, Y., Jeyapalan, J., Vicenzi, S., Fan, Q., Yang, Z. J., Sabò, A., Sheer, D., Behrens, A., & Marino, S. (2019). c-MYC overexpression induces choroid plexus papillomas through a T-cell mediated inflammatory mechanism. *Acta neuropathologica communications*, *7*(1), 95.

Meuleman, W., Peric-Hupkes, D., Kind, J., Beaudry, J. B., Pagie, L., Kellis, M., Reinders, M., Wessels, L., & van Steensel, B. (2013). Constitutive nuclear lamina-genome interactions are highly conserved and associated with A/T-rich sequence. *Genome research*, *23*(2), 270–280.

Moir, R. D., Spann, T. P., Lopez-Soler, R. I., Yoon, M., Goldman, A. E., Khuon, S., & Goldman, R. D. (2000). Review: the dynamics of the nuclear lamins during the cell cycle-- relationship between structure and function. *Journal of structural biology*, *129*(2-3), 324–334.

Moroishi, T., Hansen, C. G., & Guan, K. L. (2015). The emerging roles of YAP and TAZ in cancer. *Nature reviews. Cancer*, *15*(2), 73–79.

Morton, J. P., & Sansom, O. J. (2013). MYC-y mice: from tumour initiation to therapeutic targeting of endogenous MYC. *Molecular oncology*, *7*(2), 248–258.

Muchir, A., Pavlidis, P., Decostre, V., Herron, A. J., Arimura, T., Bonne, G., & Worman, H. J. (2007). Activation of MAPK pathways links LMNA mutations to cardiomyopathy in Emery-Dreifuss muscular dystrophy. *The Journal of clinical investigation*, *117*(5), 1282–1293.

Murphy, D. J., Swigart, L. B., Israel, M. A., & Evan, G. I. (2004). Id2 is dispensable for Myc-induced epidermal neoplasia. *Molecular and cellular biology*, *24*(5), 2083–2090.

Murphy, D. J., Junttila, M. R., Pouyet, L., Karnezis, A., Shchors, K., Bui, D. A., Brown-Swigart, L., Johnson, L., & Evan, G. I. (2008). Distinct thresholds govern Myc's biological output in vivo. *Cancer cell*, *14*(6), 447–457.

Nader, G. P. F., Agüera-Gonzalez, S., Routet, F., Gratia, M., Maurin, M., Cancila, V., Cadart, C., Palamidessi, A., Ramos, R. N., San Roman, M., Gentili, M., Yamada, A., Williart, A., Lodillinsky, C., Lagoutte, E., Villard, C., Viovy, J. L., Tripodo, C., Galon, J., Scita, G., … Piel, M. (2021). Compromised nuclear envelope integrity drives TREX1-dependent DNA damage and tumor cell invasion. *Cell*, *184*(20), 5230–5246.e22.

Nardella, M., Guglielmi, L., Musa, C., Iannetti, I., Maresca, G., Amendola, D., Porru, M., Carico, E., Sessa, G., Camerlingo, R., Dominici, C., Megiorni, F., Milan, M., Bearzi, C., Rizzi, R., Pirozzi, G., Leonetti, C., Bucci, B., Mercanti, D., Felsani, A., … D'Agnano, I. (2015). Down-regulation of the Lamin A/C in neuroblastoma triggers the expansion of tumor initiating cells. *Oncotarget*, *6*(32), 32821–32840.

Nava, M. M., Miroshnikova, Y. A., Biggs, L. C., Whitefield, D. B., Metge, F., Boucas, J., Vihinen, H., Jokitalo, E., Li, X., García Arcos, J. M., Hoffmann, B., Merkel, R., Niessen, C. M., Dahl, K. N., & Wickström, S. A. (2020). Heterochromatin-Driven Nuclear Softening Protects the Genome against Mechanical Stress-Induced Damage. *Cell*, *181*(4), 800–817.e22.

Nmezi, B., Xu, J., Fu, R., Armiger, T. J., Rodriguez-Bey, G., Powell, J. S., Ma, H., Sullivan, M., Tu, Y., Chen, N. Y., Young, S. G., Stolz, D. B., Dahl, K. N., Liu, Y., & Padiath, Q. S. (2019). Concentric organization of A- and B-type lamins predicts their distinct roles in the spatial organization and stability of the nuclear lamina. *Proceedings of the National Academy of Sciences of the United States of America*, *116*(10), 4307–4315.

Nowek, K., Wiemer, E. A. C., & Jongen-Lavrencic, M. (2018). The versatile nature of miR-9/9* in human cancer. *Oncotarget*, *9*(29), 20838–20854.

Okumura, K., Hosoe, Y., & Nakajima, N. (2004). c-Jun and Sp1 family are critical for retinoic acid induction of the lamin A/C retinoic acid-responsive element. *Biochemical and biophysical research communications*, *320*(2), 487–492.

Ortega, M. A., Fraile-Martínez, O., Asúnsolo, Á., Buján, J., García-Honduvilla, N., & Coca, S. (2020). Signal Transduction Pathways in Breast Cancer: The Important Role of PI3K/Akt/mTOR. *Journal of oncology*, *2020*, 9258396.

Osmanagic-Myers, S., Dechat, T., & Foisner, R. (2015). Lamins at the crossroads of mechanosignaling. *Genes & development*, *29*(3), 225–237.

Ostlund, C., Bonne, G., Schwartz, K., & Worman, H. J. (2001). Properties of lamin A mutants found in Emery-Dreifuss muscular dystrophy, cardiomyopathy and Dunnigan-type partial lipodystrophy. *Journal of cell science*, *114*(Pt 24), 4435–4445.

Pajerowski, J. D., Dahl, K. N., Zhong, F. L., Sammak, P. J., & Discher, D. E. (2007). Physical plasticity of the nucleus in stem cell differentiation. *Proceedings of the National Academy of Sciences of the United States of America*, *104*(40), 15619–15624.

Palacio, M., & Taatjes, D. J. (2022). Merging Established Mechanisms with New Insights: Condensates, Hubs, and the Regulation of RNA Polymerase II Transcription. *Journal of molecular biology*, *434*(1), 167216.

Pan, D., Estévez-Salmerón, L. D., Stroschein, S. L., Zhu, X., He, J., Zhou, S., & Luo, K. (2005). The integral inner nuclear membrane protein MAN1 physically interacts with the R-Smad proteins to repress signaling by the transforming growth factor-{beta} superfamily of cytokines. *The Journal of biological chemistry*, *280*(16), 15992–16001.

Pelengaris, S., Littlewood, T., Khan, M., Elia, G., & Evan, G. (1999). Reversible activation of c-Myc in skin: induction of a complex neoplastic phenotype by a single oncogenic lesion. *Molecular cell*, *3*(5), 565–577.

Pelengaris, S., Khan, M., & Evan, G. I. (2002). Suppression of Myc-induced apoptosis in beta cells exposes multiple oncogenic properties of Myc and triggers carcinogenic progression. *Cell*, *109*(3), 321–334.

Penfield, L., Wysolmerski, B., Mauro, M., Farhadifar, R., Martinez, M. A., Biggs, R., Wu, H. Y., Broberg, C., Needleman, D., & Bahmanyar, S. (2018). Dynein pulling forces counteract lamin-mediated nuclear stability during nuclear envelope repair. *Molecular biology of the cell*, *29*(7), 852–868.

Peric-Hupkes, D., & van Steensel, B. (2010). Role of the nuclear lamina in genome organization and gene expression. *Cold Spring Harbor symposia on quantitative biology*, *75*, 517–524.

Pfeifer, C. R., Vashisth, M., Xia, Y., & Discher, D. E. (2019). Nuclear failure, DNA damage, and cell cycle disruption after migration through small pores: a brief review. *Essays in biochemistry*, *63*(5), 569–577.

Prescott, J. D., & Zeiger, M. A. (2015). The RET oncogene in papillary thyroid carcinoma. *Cancer*, *121*(13), 2137–2146.

Raab, M., Gentili, M., de Belly, H., Thiam, H. R., Vargas, P., Jimenez, A. J., Lautenschlaeger, F., Voituriez, R., Lennon-Duménil, A. M., Manel, N., & Piel, M. (2016). ESCRT III repairs nuclear envelope ruptures during cell migration to limit DNA damage and cell death. *Science (New York, N.Y.)*, *352*(6283), 359–362.

Raeder, M. B., Birkeland, E., Trovik, J., Krakstad, C., Shehata, S., Schumacher, S., Zack, T. I., Krohn, A., Werner, H. M., Moody, S. E., Wik, E., Stefansson, I. M., Holst, F., Oyan, A. M., Tamayo, P., Mesirov, J. P., Kalland, K. H., Akslen, L. A., Simon, R., Beroukhim, R., … Salvesen, H. B. (2013). Integrated genomic analysis of the 8q24 amplification in endometrial cancers identifies ATAD2 as essential to MYC-dependent cancers. *PloS one*, *8*(2), e54873.

Rao, S. S., Huntley, M. H., Durand, N. C., Stamenova, E. K., Bochkov, I. D., Robinson, J. T., Sanborn, A. L., Machol, I., Omer, A. D., Lander, E. S., & Aiden, E. L. (2014). A 3D map of the human genome at kilobase resolution reveals principles of chromatin looping. *Cell*, *159*(7), 1665–1680.

Rapisarda, V., Malashchuk, I., Asamaowei, I. E., Poterlowicz, K., Fessing, M. Y., Sharov, A. A., Karakesisoglou, I., Botchkarev, V. A., & Mardaryev, A. (2017). p63 Transcription Factor Regulates Nuclear Shape and Expression of Nuclear Envelope-Associated Genes in Epidermal Keratinocytes. *The Journal of investigative dermatology*, *137*(10), 2157–2167.

Reddy, K. L., Zullo, J. M., Bertolino, E., & Singh, H. (2008). Transcriptional repression mediated by repositioning of genes to the nuclear lamina. *Nature*, *452*(7184), 243–247.

Reddy, S., & Comai, L. (2016). Recent advances in understanding the role of lamins in health and disease. *F1000Research*, *5*, 2536.

Redwood, A. B., Gonzalez-Suarez, I., & Gonzalo, S. (2011). Regulating the levels of key factors in cell cycle and DNA repair: new pathways revealed by lamins. *Cell cycle (Georgetown, Tex.)*, *10*(21), 3652–3657.

Redwood, A. B., Perkins, S. M., Vanderwaal, R. P., Feng, Z., Biehl, K. J., Gonzalez-Suarez, I., Morgado-Palacin, L., Shi, W., Sage, J., Roti-Roti, J. L., Stewart, C. L., Zhang, J., & Gonzalo, S. (2011). A dual role for A-type lamins in DNA double-strand break repair. *Cell cycle (Georgetown, Tex.)*, *10*(15), 2549–2560.

Reis-Sobreiro, M., Chen, J. F., Novitskaya, T., You, S., Morley, S., Steadman, K., Gill, N. K., Eskaros, A., Rotinen, M., Chu, C. Y., Chung, L. W. K., Tanaka, H., Yang, W., Knudsen, B. S., Tseng, H. R., Rowat, A. C., Posadas, E. M., Zijlstra, A., Di Vizio, D., & Freeman, M. R. (2018). Emerin Deregulation Links Nuclear Shape Instability to Metastatic Potential. *Cancer research*, *78*(21), 6086–6097.

Ricci, M. A., Manzo, C., García-Parajo, M. F., Lakadamyali, M., & Cosma, M. P. (2015). Chromatin fibers are formed by heterogeneous groups of nucleosomes in vivo. *Cell*, *160*(6), 1145–1158.

Röber, R. A., Weber, K., & Osborn, M. (1989). Differential timing of nuclear lamin A/C expression in the various organs of the mouse embryo and the young animal: a developmental study. *Development (Cambridge, England)*, *105*(2), 365–378.

Roux, K. J., Crisp, M. L., Liu, Q., Kim, D., Kozlov, S., Stewart, C. L., & Burke, B. (2009). Nesprin 4 is an outer nuclear membrane protein that can induce kinesin-mediated cell polarization. *Proceedings of the National Academy of Sciences of the United States of America*, *106*(7), 2194–2199.

Rowley, M. J., Nichols, M. H., Lyu, X., Ando-Kuri, M., Rivera, I. S. M., Hermetz, K., Wang, P., Ruan, Y., & Corces, V. G. (2017). Evolutionarily Conserved Principles Predict 3D Chromatin Organization. *Molecular cell*, *67*(5), 837–852.e7.

Ruchaud, S., Korfali, N., Villa, P., Kottke, T. J., Dingwall, C., Kaufmann, S. H., & Earnshaw, W. C. (2002). Caspase-6 gene disruption reveals a requirement for lamin A cleavage in apoptotic chromatin condensation. *The EMBO journal*, *21*(8), 1967–1977.

Ruggero D. (2009). The role of Myc-induced protein synthesis in cancer. *Cancer research*, *69*(23), 8839–8843.

Saarinen, I., Mirtti, T., Seikkula, H., Boström, P. J., & Taimen, P. (2015). Differential Predictive Roles of A- and B-Type Nuclear Lamins in Prostate Cancer Progression. *PloS one*, *10*(10), e0140671.

Sansom, O. J., Meniel, V. S., Muncan, V., Phesse, T. J., Wilkins, J. A., Reed, K. R., Vass, J. K., Athineos, D., Clevers, H., & Clarke, A. R. (2007). Myc deletion rescues Apc deficiency in the small intestine. *Nature*, *446*(7136), 676–679.
Sato, M., Liebau, R. C., Liu, Z., Liu, L., Rabadan, R., & Gautier, J. (2021). The UVSSA complex alleviates MYC-driven transcription stress. *The Journal of cell biology*, *220*(2), e201807163.

Sauzeau, V., Berenjeno, I. M., Citterio, C., & Bustelo, X. R. (2010). A transcriptional cross-talk between RhoA and c-Myc inhibits the RhoA/Rock-dependent cytoskeleton. *Oncogene*, *29*(26), 3781–3792.

Schöchlin, M., Weissinger, S. E., Brandes, A. R., Herrmann, M., Möller, P., & Lennerz, J. K. (2014). A nuclear circularity-based classifier for diagnostic distinction of desmoplastic from spindle cell melanoma in digitized histological images. *Journal of pathology informatics*, *5*(1), 40.

Schreiber, K. H., & Kennedy, B. K. (2013). When lamins go bad: nuclear structure and disease. *Cell*, *152*(6), 1365–1375.

Scott, S. J., Suvarna, K. S., & D'Avino, P. P. (2020). Synchronization of human retinal pigment epithelial-1 cells in mitosis. *Journal of cell science*, *133*(18), jcs247940.

Shah, P., Hobson, C. M., Cheng, S., Colville, M. J., Paszek, M. J., Superfine, R., & Lammerding, J. (2021). Nuclear Deformation Causes DNA Damage by Increasing Replication Stress. *Current biology: CB*, *31*(4), 753–765.e6.

Shah, P., Wolf, K., & Lammerding, J. (2017). Bursting the Bubble - Nuclear Envelope Rupture as a Path to Genomic Instability?. *Trends in cell biology*, *27*(8), 546–555.

Sheiness, D., Fanshier, L., & Bishop, J. M. (1978). Identification of nucleotide sequences which may encode the oncogenic capacity of avian retrovirus MC29. *Journal of virology*, *28*(2), 600–610.

Shimi, T., Kittisopikul, M., Tran, J., Goldman, A. E., Adam, S. A., Zheng, Y., Jaqaman, K., & Goldman, R. D. (2015). Structural organization of nuclear lamins A, C, B1, and B2 revealed by superresolution microscopy. *Molecular biology of the cell*, *26*(22), 4075–4086.

Simon, D. N., & Wilson, K. L. (2013). Partners and post-translational modifications of nuclear lamins. *Chromosoma*, *122*(1-2), 13–31.

Singh, M., Hunt, C. R., Pandita, R. K., Kumar, R., Yang, C. R., Horikoshi, N., Bachoo, R., Serag, S., Story, M. D., Shay, J. W., Powell, S. N., Gupta, A., Jeffery, J., Pandita, S., Chen, B. P., Deckbar, D., Löbrich, M., Yang, Q., Khanna, K. K., Worman, H. J., … Pandita, T. K. (2013). Lamin A/C depletion enhances DNA damage-induced stalled replication fork arrest. *Molecular and cellular biology*, *33*(6), 1210–1222.

Solovei, I., Wang, A. S., Thanisch, K., Schmidt, C. S., Krebs, S., Zwerger, M., Cohen, T. V., Devys, D., Foisner, R., Peichl, L., Herrmann, H., Blum, H., Engelkamp, D., Stewart, C. L., Leonhardt, H., & Joffe, B. (2013). LBR and lamin A/C sequentially tether peripheral heterochromatin and inversely regulate differentiation. *Cell*, *152*(3), 584–598.

Stearns, D., Chaudhry, A., Abel, T. W., Burger, P. C., Dang, C. V., & Eberhart, C. G. (2006). c-myc overexpression causes anaplasia in medulloblastoma. *Cancer research*, *66*(2), 673–681.

Stephens, A. D., Banigan, E. J., Adam, S. A., Goldman, R. D., & Marko, J. F. (2017). Chromatin and lamin A determine two different mechanical response regimes of the cell nucleus. *Molecular biology of the cell*, *28*(14), 1984–1996.

Stephens, A. D., Liu, P. Z., Banigan, E. J., Almassalha, L. M., Backman, V., Adam, S. A., Goldman, R. D., & Marko, J. F. (2018). Chromatin histone modifications and rigidity affect nuclear morphology independent of lamins. *Molecular biology of the cell*, *29*(2), 220–233.

Stewart, C., & Burke, B. (1987). Teratocarcinoma stem cells and early mouse embryos contain only a single major lamin polypeptide closely resembling lamin B. *Cell*, *51*(3), 383–392.

Stine, Z. E., Walton, Z. E., Altman, B. J., Hsieh, A. L., & Dang, C. V. (2015). MYC, Metabolism, and Cancer. *Cancer discovery*, *5*(10), 1024–1039.

Sullivan, T., Escalante-Alcalde, D., Bhatt, H., Anver, M., Bhat, N., Nagashima, K., Stewart, C. L., & Burke, B. (1999). Loss of A-type lamin expression compromises nuclear envelope integrity leading to muscular dystrophy. *The Journal of cell biology*, *147*(5), 913–920.

Suntharalingam, M., & Wente, S. R. (2003). Peering through the pore: nuclear pore complex structure, assembly, and function. *Developmental cell*, *4*(6), 775–789.

Sur-Erdem, I., Hussain, M. S., Asif, M., Pınarbası, N., Aksu, A. C., & Noegel, A. A. (2020). Nesprin-1 impact on tumorigenic cell phenotypes. *Molecular biology reports*, *47*(2), 921–934.

Sur, I., Neumann, S., & Noegel, A. A. (2014). Nesprin-1 role in DNA damage response. *Nucleus (Austin, Tex.)*, *5*(2), 173–191.

Swift, J., Ivanovska, I. L., Buxboim, A., Harada, T., Dingal, P. C., Pinter, J., Pajerowski, J. D., Spinler, K. R., Shin, J. W., Tewari, M., Rehfeldt, F., Speicher, D. W., & Discher, D. E. (2013). Nuclear lamin-A scales with tissue stiffness and enhances matrix-directed differentiation. *Science (New York, N.Y.)*, *341*(6149), 1240104.

Tajik, A., Zhang, Y., Wei, F., Sun, J., Jia, Q., Zhou, W., Singh, R., Khanna, N., Belmont, A. S., & Wang, N. (2016). Transcription upregulation via force-induced direct stretching of chromatin. *Nature materials*, *15*(12), 1287–1296.

Takaki, T., Montagner, M., Serres, M. P., Le Berre, M., Russell, M., Collinson, L., Szuhai, K., Howell, M., Boulton, S. J., Sahai, E., & Petronczki, M. (2017). Actomyosin drives cancer cell nuclear dysmorphia and threatens genome stability. *Nature communications*, *8*, 16013.

Tamashunas, A. C., Tocco, V. J., Matthews, J., Zhang, Q., Atanasova, K. R., Paschall, L., Pathak, S., Ratnayake, R., Stephens, A. D., Luesch, H., Licht, J. D., & Lele, T. P. (2020). High-throughput gene screen reveals modulators of nuclear shape. *Molecular biology of the cell*, *31*(13), 1392–1402.

Tapley, E. C., & Starr, D. A. (2013). Connecting the nucleus to the cytoskeleton by SUN-KASH bridges across the nuclear envelope. *Current opinion in cell biology*, *25*(1), 57–62.

Tilgner, K., Wojciechowicz, K., Jahoda, C., Hutchison, C., & Markiewicz, E. (2009). Dynamic complexes of A-type lamins and emerin influence adipogenic capacity of the cell via nucleocytoplasmic distribution of beta-catenin. *Journal of cell science*, *122*(Pt 3), 401–413.

Trappmann, B., Gautrot, J. E., Connelly, J. T., Strange, D. G., Li, Y., Oyen, M. L., Cohen Stuart, M. A., Boehm, H., Li, B., Vogel, V., Spatz, J. P., Watt, F. M., & Huck, W. T. (2012). Extracellular-matrix tethering regulates stem-cell fate. *Nature materials*, *11*(7), 642–649.

Travers, A., & Muskhelishvili, G. (2015). DNA structure and function. *The FEBS journal*, *282*(12), 2279–2295.

Trotter, E. W., & Hagan, I. M. (2020). Release from cell cycle arrest with Cdk4/6 inhibitors generates highly synchronized cell cycle progression in human cell culture. *Open biology*, *10*(10), 200200.

Tu, W. B., Helander, S., Pilstål, R., Hickman, K. A., Lourenco, C., Jurisica, I., Raught, B., Wallner, B., Sunnerhagen, M., & Penn, L. Z. (2015). Myc and its interactors take shape. *Biochimica et biophysica acta*, *1849*(5), 469–483.
Vafa, O., Wade, M., Kern, S., Beeche, M., Pandita, T. K., Hampton, G. M., & Wahl, G. M. (2002). c-Myc can induce DNA damage, increase reactive oxygen species, and mitigate p53 function: a mechanism for oncogene-induced genetic instability. *Molecular cell*, *9*(5), 1031–1044.

Tunçer, S., Gurbanov, R., Sheraj, I., Solel, E., Esenturk, O., & Banerjee, S. (2018). Low dose dimethyl sulfoxide driven gross molecular changes have the potential to interfere with various cellular processes. *Scientific reports*, *8*(1), 14828.

van Steensel, B., & Belmont, A. S. (2017). Lamina-Associated Domains: Links with Chromosome Architecture, Heterochromatin, and Gene Repression. *Cell*, *169*(5), 780–791.

Vargas, J. D., Hatch, E. M., Anderson, D. J., & Hetzer, M. W. (2012). Transient nuclear envelope rupturing during interphase in human cancer cells. *Nucleus (Austin, Tex.)*, *3*(1), 88–100.

Vassilev, L. T., Tovar, C., Chen, S., Knezevic, D., Zhao, X., Sun, H., Heimbrook, D. C., & Chen, L. (2006). Selective small-molecule inhibitor reveals critical mitotic functions of human CDK1. *Proceedings of the National Academy of Sciences of the United States of America*, *103*(28), 10660–10665.

Vaughan, A., Alvarez-Reyes, M., Bridger, J. M., Broers, J. L., Ramaekers, F. C., Wehnert, M., Morris, G. E., Whitfield WGF, & Hutchison, C. J. (2001). Both emerin and lamin C depend on lamin A for localization at the nuclear envelope. *Journal of cell science*, *114*(Pt 14), 2577–2590.

Venturini, V., Pezzano, F., Català Castro, F., Häkkinen, H. M., Jiménez-Delgado, S., Colomer-Rosell, M., Marro, M., Tolosa-Ramon, Q., Paz-López, S., Valverde, M. A., Weghuber, J., Loza-Alvarez, P., Krieg, M., Wieser, S., & Ruprecht, V. (2020). The nucleus measures shape changes for cellular proprioception to control dynamic cell behavior. *Science (New York, N.Y.)*, *370*(6514), eaba2644.

Vergnes, L., Péterfy, M., Bergo, M. O., Young, S. G., & Reue, K. (2004). Lamin B1 is required for mouse development and nuclear integrity. *Proceedings of the National Academy of Sciences of the United States of America*, *101*(28), 10428–10433.

Versaevel, M., Braquenier, J. B., Riaz, M., Grevesse, T., Lantoine, J., & Gabriele, S. (2014). Super-resolution microscopy reveals LINC complex recruitment at nuclear indentation sites. *Scientific reports*, *4*, 7362.

Vortmeyer-Krause, M. et al.(2020). Lamin B2 follows lamin A/C- mediated nuclear mechanics and cancer cell invasion efficacy. *bioRxiv*

Ward, I. M., Minn, K., Jorda, K. G., & Chen, J. (2003). Accumulation of checkpoint protein 53BP1 at DNA breaks involves its binding to phosphorylated histone H2AX. *The Journal of biological chemistry*, *278*(22), 19579–19582.

Watabe, S., Kobayashi, S., Hatori, M., Nishijima, Y., Inoue, N., Ikota, H., Iwase, A., Yokoo, H., & Saio, M. (2022). Role of Lamin A and emerin in maintaining nuclear morphology in different subtypes of ovarian epithelial cancer. *Oncology letters*, *23*(1), 9.

Weigelin, B., Bakker, G. J., & Friedl, P. (2012). Intravital third harmonic generation microscopy of collective melanoma cell invasion: Principles of interface guidance and microvesicle dynamics. *Intravital*, *1*(1), 32–43.

Wen, B., Wu, H., Shinkai, Y., Irizarry, R. A., & Feinberg, A. P. (2009). Large histone H3 lysine 9 dimethylated chromatin blocks distinguish differentiated from embryonic stem cells. *Nature genetics*, *41*(2), 246–250.

Wendt, K. S., Yoshida, K., Itoh, T., Bando, M., Koch, B., Schirghuber, E., Tsutsumi, S., Nagae, G., Ishihara, K., Mishiro, T., Yahata, K., Imamoto, F., Aburatani, H., Nakao, M., Imamoto, N., Maeshima, K., Shirahige, K., & Peters, J. M. (2008). Cohesin mediates transcriptional insulation by CCCTC-binding factor. *Nature*, *451*(7180), 796–801.

Whitfield, J., Littlewood, T., Evan, G. I., & Soucek, L. (2015). The estrogen receptor fusion system in mouse models: a reversible switch. *Cold Spring Harbor protocols*, *2015*(3), 227–234.

Willaume, S., Rass, E., Fontanilla-Ramirez, P., Moussa, A., Wanschoor, P., & Bertrand, P. (2021). A Link between Replicative Stress, Lamin Proteins, and Inflammation. *Genes*, *12*(4), 552.

Willis, N. D., Cox, T. R., Rahman-Casañs, S. F., Smits, K., Przyborski, S. A., van den Brandt, P., van Engeland, M., Weijenberg, M., Wilson, R. G., de Bruïne, A., & Hutchison, C. J. (2008). Lamin A/C is a risk biomarker in colorectal cancer. *PloS one*, *3*(8), e2988.

Wong, X., Loo, T. H., & Stewart, C. L. (2021). LINC complex regulation of genome organization and function. *Current opinion in genetics & development*, *67*, 130–141.
Wood, A. M., Rendtlew Danielsen, J. M., Lucas, C. A., Rice, E. L., Scalzo, D., Shimi, T., Goldman, R. D., Smith, E. D., Le Beau, M. M., & Kosak, S. T. (2014). TRF2 and lamin A/C interact to facilitate the functional organization of chromosome ends. *Nature communications*, *5*, 5467.

Worman, H. J., & Bonne, G. (2007). "Laminopathies": a wide spectrum of human diseases. *Experimental cell research*, *313*(10), 2121–2133.

Wu, Z., Wu, L., Weng, D., Xu, D., Geng, J., & Zhao, F. (2009). Reduced expression of lamin A/C correlates with poor histological differentiation and prognosis in primary gastric carcinoma. *Journal of experimental & clinical cancer research : CR*, *28*(1), 8.

Wutz, G., Várnai, C., Nagasaka, K., Cisneros, D. A., Stocsits, R. R., Tang, W., Schoenfelder, S., Jessberger, G., Muhar, M., Hossain, M. J., Walther, N., Koch, B., Kueblbeck, M., Ellenberg, J., Zuber, J., Fraser, P., & Peters, J. M. (2017). Topologically associating domains and chromatin loops depend on cohesin and are regulated by CTCF, WAPL, and PDS5 proteins. *The EMBO journal*, *36*(24), 3573–3599.

Xia, Y., Pfeifer, C. R., Zhu, K., Irianto, J., Liu, D., Pannell, K., Chen, E. J., Dooling, L. J., Tobin, M. P., Wang, M., Ivanovska, I. L., Smith, L. R., Greenberg, R. A., & Discher, D. E. (2019). Rescue of DNA damage after constricted migration reveals a mechano-regulated threshold for cell cycle. *The Journal of cell biology*, *218*(8), 2545–2563.

Xiao, W., Wang, J., Ou, C., Zhang, Y., Ma, L., Weng, W., Pan, Q., & Sun, F. (2013). Mutual interaction between YAP and c-Myc is critical for carcinogenesis in liver cancer. *Biochemical and biophysical research communications*, *439*(2), 167–172.

Xie, W., & Burke, B. (2016). Lamins. *Current biology : CB*, *26*(9), R348–R350.

Xing, X., Mroß, C., Hao, L., Munck, M., Herzog, A., Mohr, C., Unnikannan, C. P., Kelkar, P., Noegel, A. A., Eichinger, L., & Neumann, S. (2017). Nesprin-2 Interacts with Condensin Component SMC2. *International journal of cell biology*, *2017*, 8607532.

Yang, L., Guan, T., & Gerace, L. (1997). Lamin-binding fragment of LAP2 inhibits increase in nuclear volume during the cell cycle and progression into S phase. *The Journal of cell biology*, *139*(5), 1077–1087.

Yang, S. H., Jung, H. J., Coffinier, C., Fong, L. G., & Young, S. G. (2011). Are B-type lamins essential in all mammalian cells?. *Nucleus (Austin, Tex.)*, *2*(6), 562–569.

Yang, Z., Maciejowski, J., & de Lange, T. (2017). Nuclear Envelope Rupture Is Enhanced by Loss of p53 or Rb. *Molecular cancer research : MCR*, *15*(11), 1579–1586.

Zhang, J., Alisafaei, F., Nikolić, M., Nou, X. A., Kim, H., Shenoy, V. B., & Scarcelli, G. (2020). Nuclear Mechanics within Intact Cells Is Regulated by Cytoskeletal Network and Internal Nanostructures. *Small (Weinheim an der Bergstrasse, Germany)*, *16*(18), e1907688.

Zhironkina, O. A., Kurchashova, S. Y., Pozharskaia, V. A., Cherepanynets, V. D., Strelkova, O. S., Hozak, P., & Kireev, I. I. (2016). Mechanisms of nuclear lamina growth in interphase. *Histochemistry and cell biology*, *145*(4), 419–432.

Zimmerli, C. E., Allegretti, M., Rantos, V., Goetz, S. K., Obarska-Kosinska, A., Zagoriy, I., Halavatyi, A., Hummer, G., Mahamid, J., Kosinski, J., & Beck, M. (2021). Nuclear pores dilate and constrict in cellulo. *Science (New York, N.Y.)*, *374*(6573), eabd9776.

Zink, D., Fischer, A. H., & Nickerson, J. A. (2004). Nuclear structure in cancer cells. *Nature reviews. Cancer*, *4*(9), 677–687.

Zuo, B., Yang, J., Wang, F., Wang, L., Yin, Y., Dan, J., Liu, N., & Liu, L. (2012). Influences of lamin A levels on induction of pluripotent stem cells. *Biology open*, *1*(11), 1118–1127.

Zwerger, M., Jaalouk, D. E., Lombardi, M. L., Isermann, P., Mauermann, M., Dialynas, G., Herrmann, H., Wallrath, L. L., & Lammerding, J. (2013). Myopathic lamin mutations impair nuclear stability in cells and tissue and disrupt nucleo-cytoskeletal coupling. *Human molecular genetics*, *22*(12), 2335–2349.